การศึกษาตัวเร่งปฏิกิริยาฮาฟเมทัลโลซีนสำหรับพอลิเอทิลีนความหนาแน่นต่ำเชิงเส้น

นายเอกราชันย์ ไชยชนะ

วิทยานิพนธ์นี้เป็นส่วนหนึ่งของการศึกษาตามหลักสูตรปริญญาวิศวกรรมศาสตรดุษฎีบัณฑิต
สาขาวิชาวิศวกรรมเคมี ภาควิชาวิศวกรรมเคมี
คณะวิศวกรรมศาสตร์ จุฬาลงกรณ์มหาวิทยาลัย
ปีการศึกษา 2552

STUDY ON HALF-METALLOCENE CATALYST FOR LINEAR LOW DENSITY POLYETHYLENE

Mister Ekrachan Chaichana

A Dissertation Submitted in Partial Fulfillment of the Requirements
for the Degree of Doctor of Engineering Program in Chemical Engineering
Department of Chemical Engineering
Faculty of Engineering
Chulalongkorn University
Academic Year 2009

Thesis Title	STUDY ON HALF-METALLOCENE CATALYST FOR LINEAR LOW DENSITY POLYETHYLENE
By	Mister Ekrachan Chaichana
Field of Study	Chemical Engineering
Thesis Advisor	Associate Professor Bunjerd Jongsomjit,Ph.D.

Accepted by the Faculty of Engineering, Chulalongkorn University in Partial Fulfillment of the Requirements for the Doctoral Degree

..... Dean of the Faculty of Engineering
(Associate Professor Boonsom Lerdhirunwong, Dr.Ing.)

THESIS COMMITTEE

..... Chairman
(Assistant Professor Anongnat Somwangthanaroj, Ph.D.)

..... Thesis Advisor
(Associate Professor Bunjerd Jongsomjit, Ph.D.)

..... Examiner
(Associate Professor ML. Supakanok Thongyai, Ph.D.)

..... Examiner
(Assistant Professor Joongjai Panpranot, Ph.D.)

..... External Examiner
(Assistant Professor Sirirat Wacharawichanant, D.Eng.)

เอกราชันย์ ไชยชนะ : การศึกษาตัวเร่งปฏิกิริยาฮาฟเมทัลโลซีนสำหรับพอลิเอทิลีนความหนาแน่นต่ำเชิงเส้น. (STUDY ON HALF-METALLOCENE CATALYST FOR LINEAR LOW DENSITY POLYETHYLENE) อ. ที่ปรึกษาวิทยานิพนธ์หลัก : รองศาสตราจารย์ ดร. บรรเจิด จงสมจิตร,115 หน้า.

ในการศึกษาครั้งนี้ ตัวเร่งปฏิกิริยาฮาฟเมททัลโลซีนถูกสังเคราะห์ขึ้นและใช้ในโคพอลิเมอร์ไรเซชันของเอทิลีนกับหนึ่งเฮกซีน โดยใช้เมทิลอะลูมินอกเซนที่ได้รับการปรับปรุงแล้วเป็นตัวเร่งปฏิกิริยาร่วม จากการศึกษาพบว่าแม้จะใช้โคมอนอเมอร์ในปริมาณสูงก็ยังคงทำให้ระบบตัวเร่งปฏิกิริยาฮาฟเมทัลโลซีนว่องไวอยู่ได้ จากการศึกษาเปรียบเทียบการเตรียมพอลิเมอร์คอมโพสิท สามารถเตรียมพอลิเมอร์คอมโพสิทได้โดยใช้ระบบการเตรียมตัวเร่งปฏิกิริยาบนตัวรองรับแบบอินซิทู สำหรับระบบแบบวิวิธพันธ์นั้น พบว่าแกลเลี่ยมที่ทำหน้าที่ปรับปรุงตัวรองรับช่วยเพิ่มความว่องไวให้กับระบบการเร่งปฏิกิริยาและวิธีที่ดีที่สุดในการเตรียมตัวรองรับคือการยึดเกาะตัวเร่งปฏิกิริยากับตัวเร่งปฏิกิริยาร่วมที่ผสมกันอยู่แล้วบนตัวรองรับจะให้ค่าความว่องไวการเกิดปฏิกิริยาสูงที่สุด ตัวรองรับที่เหมาะสมที่สุดในระบบตัวเร่งปฏิกิริยาชนิดนี้คือ ตัวรองรับที่มีลักษณะกลม พื้นที่ผิวสูง จะให้ค่าความว่องไวการเกิดปฏิกิริยาสูงที่สุด จากข้อมูลการศึกษาทั้งหมดทำให้เรามีความเข้าใจในตัวเร่งปฏิกิริยาเมทัลโลซีนมากขึ้นและค้นพบวิธีการที่จะนำตัวเร่งปฏิกิริยาเมทัลโลซีนไปใช้ในได้อย่างมีประสิทธิภาพ

ภาควิชา วิศวกรรมเคมี ลายมือชื่อนิสิต .....

สาขาวิชา วิศวกรรมเคมี ลายมือชื่อ อ.ที่ปรึกษาวิทยานิพนธ์หลัก .....

ปีการศึกษา 2552

4971882821 : MAJOR CHEMICAL ENGINEERING
KEYWORDS : METALLOCENE / POLYMER COMPOSITES / SILICA
EKRACHAN CHAICHANA : STUDY ON HALF-METALLOCENE CATALYST FOR LINEAR LOW DENSITY POLYETHYLENE
THESIS ADVISOR : ASSOCIATE PROFESSOR BUNJERD JONGSOMJIT, Ph.D., 115 pp.

In this study, the half-metallocene was synthesized and then used in copolymerization of ethylene and 1-hexene with modified methyl aluminoxane as a cocatalyst. It was found from the investigation of comonomer effect that even thought the high amounts of comonomer were introduced into the half-metallocene catalytic systems, they were still in an active condition. From the comparative study on LLDPE/ silica composites synthesized by different copolymerization systems, it was found that the polymer composites can be efficiently produced by the half-metallocene catalytic systems especially combining with *in situ* impregnation methods. As regard the heterogeneous system, the support used can be modified by gallium to improve the activity for the system and the best method for preparation the supported catalysts was to mix between the catalyst and cocatalyst prior to immobilizing onto the support and then introducing it into the system. The most appropriate support for using in the catalytic system should have a spherical shape, a high surface area and a moderate pore diameter. Finally, from all the above investigations, a better understanding of the metallocene catalyst was achieved and the effective ways of using this catalyst in a certain condition were discovered.

Department : Chemical Engineering Student's Signature .....
Field of Study : Chemical Engineering Advisor's Signature .....
Academic Year : 2009

ACKNOWLEDGEMENTS

The author would like to give special recognition to Associate Professor Dr. Bunjerd Jongsomjit, my advisor, for his generosity in providing guidance and sharing his ideas on the interesting work. His advices are always worthwhile and without him this work could not be possible.

Sincere thanks are given to the graduate school and department of chemical engineering at Chulalongkorn University for the financial support of this work. And many thanks are given to PTT Chemical Public Company Limited for ethylene gas supply and MEKTEC Manufacturing Corporation (Thailand) Limited for NMR measurements.

CONTENTS

Page

ABSTRACT (IN THAI)……iv

ABSTRACT (IN ENGLISH)……v

ACKNOWLEDGEMENTS……vi

CONTENTS……vii

LIST OF TABLES……x

LIST OF FIGURES……xi

CHAPTER I INTRODUCTION ……1

CHAPTER II LITERATURE REVIEWS……4

2.1. Classification of Linear low density polyethylene (LLDPE)…… 4

2.2 Background on Metallocene Catalysts…… 5

2.2.1. Catalyst Structure…… 5

2.2.2 Derivatives of Metallocene…… 8

2.2.3 Polymerization Mechanism…… 9

2.2.4 Cocatalysts…… 13

2.3 Heterogeneous System…… 16

2.3.1. Catalyst Chemistry…… 16

2.3.2 Supporting Methods…… 19

2.4 Catalytic and specific properties…… 22

2.4.1 Effect of substituted ligand…… 22

2.4.2 Effect of comonomer…… 23

CHAPTER III EXPERIMENTAL……25

3.1 Research objectives…… 25

3.2 Research scopes…… 25

3.3 Experimental…… 26

3.3.1 Chemicals…… 26

3.3.2 Equipments…… 28

3.3.3 Characterizing Instruments…… 30

3.3.4 Procedures…… 32

3.3.5 Characterization of supports and catalyst…… 37

3.3.6 Characterization Method of Polymer…… 37

CHAPTER IV RESULTS AND DISCUSSIONS 39
4.1 Effect of comonomer on the half-metallocene catalytic systems *(Part 1)* 39
4.1.1 Reactivity of (co)monomer to catalyst 39
4.1.2 Effect of the amount of 1-hexene on catalytic activity 41
4.1.3 Effect of the amount of 1-hexene on microstructure 42
4.2 A Comparative study on LLDPE/ silica composites synthesized by different copolymerization systems *(Part 2)* 46
4.2.1 Catalytic activity 46
4.2.2 Characteristic of polymer 52
4.3 Modification of supports by gallium *(Part 3)* 55
4.3.1 Characterization of supports 55
4.3.2 Catalytic activity of copolymerization 55
4.3.2.1 Effect of pore size of silica supports 55
4.3.2.2 Effect of gallium modification of silica surface 56
4.3.3 Characterization of copolymers 57
4.3.3.1 Effect of pore size of silica supports 58
4.3.3.4 Effect of gallium modification of silica surface 58
4.4 Effect of method for preparation of supported catalysts *(Part 4)* 63
4.4.1 Characteristics of support 63
4.4.2 Characteristics of catalysts on the support 63
4.4.3 Catalytic activity 64
4.4.3.1 Effect of support modification 65
4.4.3.2 Effect of catalyst phase 66
4.4.3.3 Effect of preparation method 67
4.4.4 Characteristics of polymer 71
4.4.4.1 Morphology 71
4.4.4.2 Polymer structure and property 72
4.5 Effect of support texture on copolymerization (Part 5) 74
4.5.1 Characteristic of support 74
4.5.2 Characteristics of catalysts on the support 75
4.5.2.1 The amount of catalyst and/or MMAO on the supports 75

4.5.2.2 Interaction between catalyst and MMAO on the support 76
4.5.3 Characteristic activity 78
4.5.3.1 Effect of preparation methods 78
4.5.3.2 Effect of silica texture 79
4.5.4 Characteristic of polymer 82
4.5.4.1 Morphology 82
4.5.4.2 Polymer structure and property 83
CHAPTER V CONCLUSIONS & RECOMMENDATION 85
5.1 Conclusion 85
5.2 Recommendations 86
REFERENCES……..……87
APPENDICES……...…….96
APPENDIX A…….……...…….97
APPENDIX B……..……106
APPENDIX C……...109
VITAE……...…115

LIST OF TABLES

Page

Table 2.1 Comonomer Content and Density Ranges. 4
Table 2.2 Representative Examples of Metallocenes....6
Table 4.1 Activities of system with various monomer concentrations 39
Table 4.2 Comonomer incorporation and the reactivity ratios....42
Table 4.3 Triad distribution of copolymer obtained from ^{13}C-NMR....43
Table 4.4 Polymerization activities for different systems....48
Table 4.5 Temperature at a certain weight loss for various systems....50
Table 4.6 Binding energy and elemental distribution on the surface of polymer measured by XPS....51
Table 4.7 Characteristic of polymers from ^{13}C-NMR....52
Table 4.8 Catalytic activities in ethylene/1-hexene copolymerization with different supports. 56
Table 4.9 Properties of the obtained copolymers....57
Table 4.11 The amount of titanium (catalyst) and aluminium (MMAO) investigated by Inductive Coupling Plasma Spectroscopy (ICP)....64
Table 4.12 Activity of copolymerization using catalysts from various preparation methods....65
Table 4.13 Comparison of Ti-catalyst on various supports 66
Table 4.14 Activity of copolymerization using catalysts from various preparation methods (no addition of MMAO)....71
Table 4.15 ^{13}C-NMR and DSC analysis of polymer....72
Table 4.16 Physical properties of supports 74
Table 4.17 The amount of titanium (catalyst) and aluminium (MMAO) investigated by Inductive Coupling Plasma Spectroscopy (ICP)....76
Table 4.18 Activity of copolymerization using different supported-catalysts from various preparation methods....77
Table 4.19 ^{13}C-NMR and DSC analysis of polymers 84

LIST OF FIGURES

Page

Figure 2.1 Molecular structure of metallocene 5
Figure 2.2 Some of zirconocene catalysts structure 6
Figure 2.3 Scheme of the different metallocene complex structures 7
Figure 2.4 The general structure of half-metallocene(titanocene).....8
Figure 2.5 *Nonbridged* half-metallocene containing anionic donor ligand 8
Figure 2.6 Constrained geometry catalyst (CGC) 9
Figure 2.7 Cossee mechanism for Ziegler-Natta olefin polymerization 10
Figure 2.8 The propagation step according to the trigger mechanism.....11
Figure 2.9 Propagation mechanism in polymerization 11
Figure 2.11 Chain transfer via β-CH_3 elimination 12
Figure 2.12 Chain transfer to aluminum 12
Figure 2.13 Chain transfer to monomer.....13
Figure 2.14 Chain transfer to hydrogen 13
Figure 2.15 Early structure models for MAO.....14
Figure 2.16 Representation of MAO showing.....15
Figure 2.17 Structure of chemical groups on silica surface.....17
Figure 2.18 Species of aluminium on silica surface 18
Figure 2.19 Species of aluminium (TMAL) on silica surface 19
Figure 2.20 Various methods for immobilization.....20
Figure 2.21 Effect of substituted ligands in polymerization.....23
Figure 3.1 Inert gas supply system.....28
Figure 3.2 Schlenk tube 29
Figure 3.3 Schlenk line 29
Figure 3.4 Diagram of system in slurry phase polymerization. 30
Figure 4.1 Schematic representation of copolymerization mechanism 40
Figure 4.2 Activity profile with various 1-hexene concentrations.....41
Figure 4.3 ^{13}C-NMR spectra of copolymers 44
Figure 4.4 Digital photograph of copolymer with various 1-hexene contents.....46
Figure 4.5 Conceptual model indicating the position of species composites. 49
Figure 4.6 TGA curves of polymers for different systems. 50
Figure 4.7 Morphologies of the polymers obtained from the different systems 54

Figure 4.8 Comparison of active site dispersion on the different surface areas..... 58
Figure 4.9 Conceptual model for impact of pore blockage on supports 60
Figure 4.10 DSC endotherms of LLDPE synthesized with various SiO_2 61
Figure 4.10 Deactivation of catalyst on silica 68
Figure 4.11 Linkage between silica support and catalyst through MMAO 70
Figure 4.12 Structural model of catalyst and MMAO on the support..... 70
Figure 4.13 Morphologies of polymers obtained from different method..... 71
Figure 4.15 Weight losses as a function of temperature 77
Figure 4.16 Derivative weight losses as a function of temperature 78
Figure 4.17 Structural model indicating the position of silanol groups 80
Figure 4.18 Catalyst deactivation in different pores 81
Figure 4.19 Morphologies of polymers obtained from the various silicas..... 83
Figure A-1 ^{13}C NMR spectrum of ethylene/1-hexene copolymer at ratio 1:2 98
Figure A-2 ^{13}C NMR spectrum of ethylene/1-hexene copolymer at ratio 1:1 98
Figure A-3 ^{13}C NMR spectrum of ethylene/1-hexene copolymer at ratio 2:1 99
Figure A-4 ^{13}C NMR spectrum of ethylene/1-hexene copolymer obtained from..... the homogeneous system..... 99
Figure A-5 ^{13}C NMR spectrum of ethylene/1-hexene copolymer obtained from..... the heterogeneous system with SiO_2-*S* support..... 100
Figure A-6 ^{13}C NMR spectrum of ethylene/1-hexene copolymer obtained from..... the heterogeneous system with SiO_2-*L* support 100
Figure A-7 ^{13}C NMR spectrum of ethylene/1-hexene copolymer obtained from..... the heterogeneous system with SiO_2-Ga-*S* support..... 101
Figure A-8 ^{13}C NMR spectrum of ethylene/1-hexene copolymer obtained from the heterogeneous system with SiO_2-Ga-*S* support..... 101
Figure A-9 ^{13}C NMR spectrum of ethylene/1-hexene copolymer obtained from silica ES-70X prepared by method A2..... 102
Figure A-10 ^{13}C NMR spectrum of ethylene/1-hexene copolymer obtained from silica ES-70X prepared by method B2..... 102
Figure A-11 ^{13}C NMR spectrum of ethylene/1-hexene copolymer obtained from silica Q-50 prepared by method A2 103
Figure A-12 ^{13}C NMR spectrum of ethylene/1-hexene copolymer obtained from silica NN-15 prepared by method B2..... 103

Figure A-13 ^{13}C NMR spectrum of ethylene/1-hexene copolymer obtained from silica P-10 prepared by method A1 104
Figure A-14 ^{13}C NMR spectrum of ethylene/1-hexene copolymer obtained from silica P-10 prepared by method A2 104
Figure A-15 ^{13}C NMR spectrum of ethylene/1-hexene copolymer obtained from silica P-10 prepared by method B2 105
Figure C-1 DSC curve of ethylene/1-hexene copolymer obtained from silica ES-70X prepared by method A2 110
Figure C-2 DSC curve of ethylene/1-hexene copolymer obtained from silica ES-70X prepared by method B2 111
Figure C-3 DSC curve of ethylene/1-hexene copolymer obtained from silica Q-50 prepared by method A2 112
Figure C-4 DSC curve of ethylene/1-hexene copolymer obtained from silica Q-50 prepared by method B2 113
Figure C-5 DSC curve of ethylene/1-hexene copolymer obtained from silica NN-15 prepared by method B2 114

CHAPTER I

INTRODUCTION

First commercialize in the late 1970s by Union Carbide and Dow Chemical [1], linear low-density polyethylene (LLDPE) has continued a fast grow rate in usage from that time to the present day. For using LLDPE in an efficient way, the specific properties of LLDPE, such as molecular weight distribution, stereoregularity and comonomer content need to be considered carefully. A metallocene is one of the most widely used catalysts for control those properties, and thus, many studies have been conducted with this type of catalyst [2-4]. It is a compound with the general formula $(C_5H_5)_2M$ consisting of two cyclopentadienyl anions (Cp, which is $C_5H_5^-$) bound to a metal center (M) in the oxidation state II. Metallocenes are a subset of a broader class of organometallic compounds called sandwich compounds. The word "sandwich compound" is derived from its structure that looks like a sandwich with the central metal being between the two rings of cyclopentadienyl. However, there are some metallocenes that consist of only one cyclopentadienyl ring and then they are called a half-sandwich or half-metallocene. In addition, constrained geometry catalysts (CGCs) having the formula $R_2Si(C_5R'_4)(R''N)MX2$ ($CGCMX_2$; M = Ti, Zr, Hf; X = Cl, Me) are sometimes classified as a half-metallocene with the similar structures [5]. These metallocenes (half-metallocenes and/or CGCs) will posses the open structure due to having only one cyclopentadieny ring binding then leaving the opposite side of that ring large enough space for comonomer incorporation with less hindrance [6]. It is because of this reason that these metallocenes are appropriate for producing polymers with high comonomer content such as a plastomer (% comonomer ≈ 25 %). Plastomer is an example of commercial polymers that can be produced by metallocene catalyst in industrial practice.

However, the industrial application of metallocenes is usually processed in a gas or slurry phase (heterogeneous system) so therefore the development of supported-metallocenes is very important. Inorganic materials, such as SiO_2, Al_2O_3 and ZrO_2 were applied for the purpose of supported-metallocenes preparation. The consequences of combination between the metallocene and the supporting material then need to be considered carefully especially when conducting with the

metallocenes which have the distinctive properties such as the half-metallocene. Hence, in this study, the half-metallocene was synthesized and then used in copolymerization of ethylene and 1-hexene with modified methyl aluminoxane as a cocatalyst. It was performed in both the homogeneous system and the heterogeneous system. In the latter system, since it had to be dealt with the supporting materials, then the study of these material properties was also essential and conducted in parallel with the study of the half-metallocene.

This thesis consists of 5 parts of investigations as followed.

1) Effect of comonomer on the half-metallocene catalytic systems:

The differences of initial comonomer were introduced into the homogeneous systems to investigate their effects on the comonomer contents, the activity of the system and the properties of the obtained polymers.

2) A Comparative study on LLDPE/ silica composites synthesized by different copolymerization systems:

In one aspect, the polymer obtained from the heterogeneous system can be comparable to polymer composites, and then the study focusing on the composite's properties was also conducted.

3) Modification of supports by gallium:

To improve the supports for performing in the catalytic system, gallium was brought for this purpose. Gallium that affected directly the support properties also affects the activity of the system. Therefore, roles of gallium during the modification step and copolymerization were investigated here.

4) Effect of method for preparation of supported catalysts:

In preparation of supported catalyst, there are many important things to be concerned, for example to keep the efficiency of catalyst when it was immobilized onto the supports, to reduce the adverse effects of support in copolymerization. Therefore, a variety of methods for preparation of supported catalyst were conducted to examine their effects on the copolymerization.

5) Effect of support texture:

To choose the appropriate supports for using in the system is another parameter that should be concerned as the textures of the supports can affect the system in many behaviors, ranging from the activities during polymerization to the properties of the obtained polymers. Therefore, a variety of supports were brought to use in this investigation.

In all the investigations, the properties of supports both before and after preparation steps, and the properties of the obtained polymers were determined by many techniques. The activities of the polymerizations were collected and were further analyzed along with the above properties. Finally, a better understanding of the metallocene catalyst was achieved and the effective ways of using this catalyst in a certain condition were discovered.

CHAPTER II

LITERATURE REVIEWS

2.1. Classification of Linear low density polyethylene (LLDPE)

Linear low density polyethylene (LLDPE) was first commercialized in the late 1970s by Union Carbide and Dow Chemical [1]. Since that first introduction, LLDPE has seen the fastest growth rate in usage of the three major polyethylene families low density polyethylene (LDPE), LLDPE, and high density polyethylene (HDPE) and now comprises approximately 25% of the annual production of polyethylene around the world, approaching 13 million metric tons. Conventional LLDPE differs from LDPE by having a narrower molecular weight distribution and by not containing long-chain branching. LLDPE is made by the copolymerization of ethylene and alpha-olefins.

Conventional LLDPE basically covers the density range of 0.915–0.940. Within that density range, and also lower density ranges, there are common product family subsets. **Table 2.1** shows comonomer content and subsequent density ranges for commercial LLDPE.

Table 2.1 Comonomer Content and Density Ranges for Commercial LLDPE Resins [1].

Family	Common name	Comonomer, mol%	Crystallinity, %	Density, g/cm^3
Medium density	MDPE	1–2	55–45	0.940–0.926
Low density	LLDPE	2.5–3.5	45–30	0.925–0.915
Very low/ultra low density	VLDPE/ ULDPE	> 4	< 30	< 0.915
Very low density (single-site catalyzed)	Plastomer	≤25	0–30	≤ 0.912

Whereas LDPE contains a mixture of long-chain branching and short-chain branching, LLDPE contains only short-chain branching, but that branching is not uniformly distributed through the molecular weight. LLDPE made using Ziegler–

Natta catalysts tends to have more comonomer in the lower molecular weight fraction and less in the high molecular weight fraction [7]. The first commercially available single-site-catalyzed polyethylenes were very low density resins called plastomers [8], which had high levels of comonomer and were very homogeneous. Later, commercial commodity grade mLLDPEs (produced by metallocene catalyst) were not quite as homogeneous as the plastomers, but were still more homogeneous than LLDPE [9].

2.2 Background on Metallocene Catalysts

Polyolefins can be produced with free radical initiators, Phillips type catalysts, Ziegler-Natta catalysts and metallocene catalysts. Ziegler-Natta catalysts have been most widely used because of their broad range of application. However, Ziegler-Natta catalyst provides polymers having broad molecular weight distribution (MWD) and composition distribution due to multiple active sites formed [10].

Metallocene catalysts have been used to polymerize ethylene and α-olefins commercially. The structural change of metallocene catalysts can control composition distribution, incorporation of various comonomers, MWD and stereoregularity [11].

2.2.1. Catalyst Structure

Metallocene is a class of compounds in which cyclopentadienyl or substituted cyclopentadienyl ligands are π-bonded to the metal atom. The stereochemistry of biscyclopentadienyl (or substituted cyclopentadienyl)-metal bis (unibidentate ligand) complexes can be most simply described as distorted tetrahedral, with each η^5-L group (L = ligand) occupying a single co-ordination position, as in **Figure 2.1** [12].

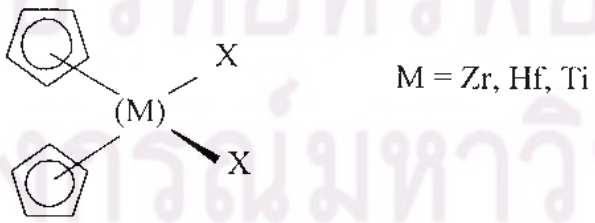

Figure 2.1 Molecular structure of metallocene [12]

Representative examples of each category of metallocenes and some of zirconocene catalysts are shown in **Table 2.2** and **Figure 2.2**, respectively.

Table 2.2 Representative Examples of Metallocenes [12]

Category of metallocenes	Metallocene Catalysts
[A] Nonstereorigid metallocenes	1) Cp_2MCl_2 (M = Ti, Zr, Hf) 2) Cp_2ZrR_2 (M = Me, Ph, CH_2Ph, CH_2SiMe_3) 3) $(Ind)_2ZrMe_2$
[B] Nonstereorigid ring-substituted metallocenes	1) $(Me_5C_5)_2MCl_2$ (M = Ti, Zr, Hf) 2) $(Me_3SiCp)_2ZrCl_2$
[C] Stereorigid metallocenes	1) $Et(Ind)_2ZrCl_2$ 2) $Et(Ind)_2ZrMe_2$ 3) $Et(IndH_4)_2ZrCl_2$
[D] Cationic metallocenes	1) $Cp_2MR(L)^+[BPh_4]^-$ (M = Ti, Zr) 2) $[Et(Ind)_2ZrMe]^+[B(C_6F_5)_4]^-$ 3) $[Cp_2ZrMe]^+[(C_2B_9H_{11})_2M]^-$ (M = Co)
[E] Supported metallocenes	1) Al_2O_3-$Et(IndH_4)_2ZrCl_2$ 2) $MgCl_2$-Cp_2ZrCl_2 3) SiO_2-$Et(Ind)_2ZrCl_2$

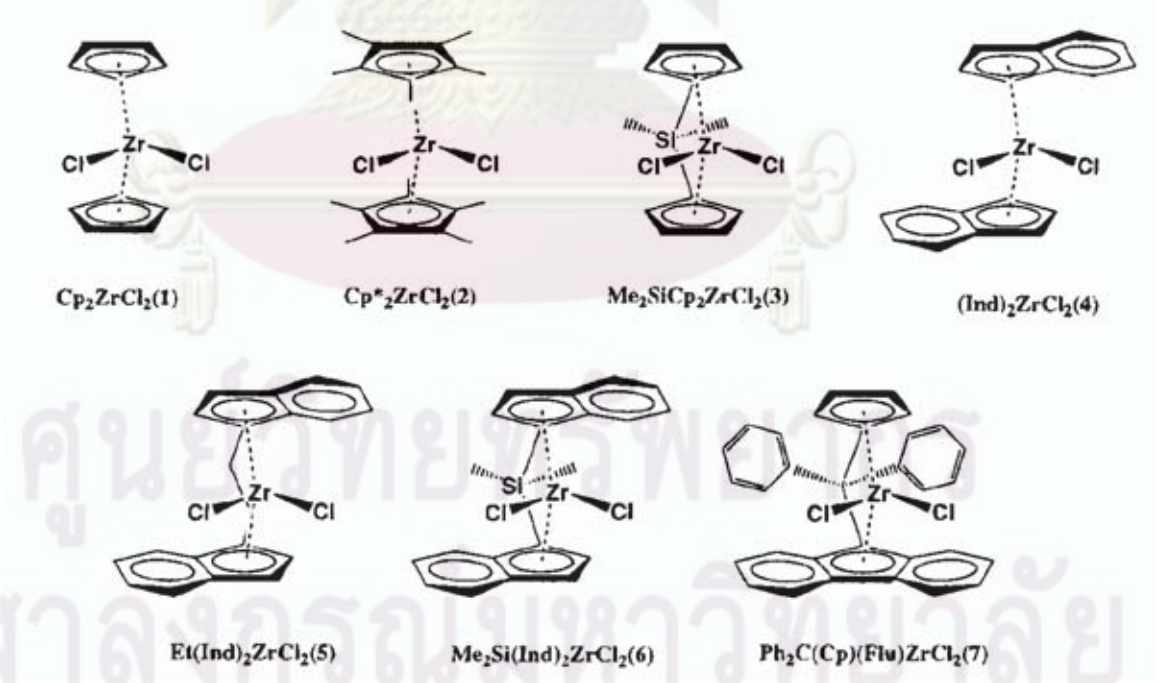

Figure 2.2 Some of zirconocene catalysts structure [13]

Composition and types of metallocene have several varieties. When the two cyclopentadienyl (Cp) rings on either side of the transition metal are unbridged, the metallocene is nonstereorigid and it is characterized by C_{2v} symmetry. The Cp_2M (M = metal) fragment is bent back with the centroid-metal-centroid angle θ about 140° due to an interaction with the other two σ bonding ligands [14]. When the Cp rings are bridged (two Cp rings arranged in a chiral array and connected together with chemical bonds by a bridging group), the stereorigid metallocene, so-called ansa-metallocene, could be characterized by either a C_1, C_2, or C_s symmetry depending upon the substituents on two Cp rings and the structure of the bridging unit as schematically illustrated in **Figure 2.3** [12].

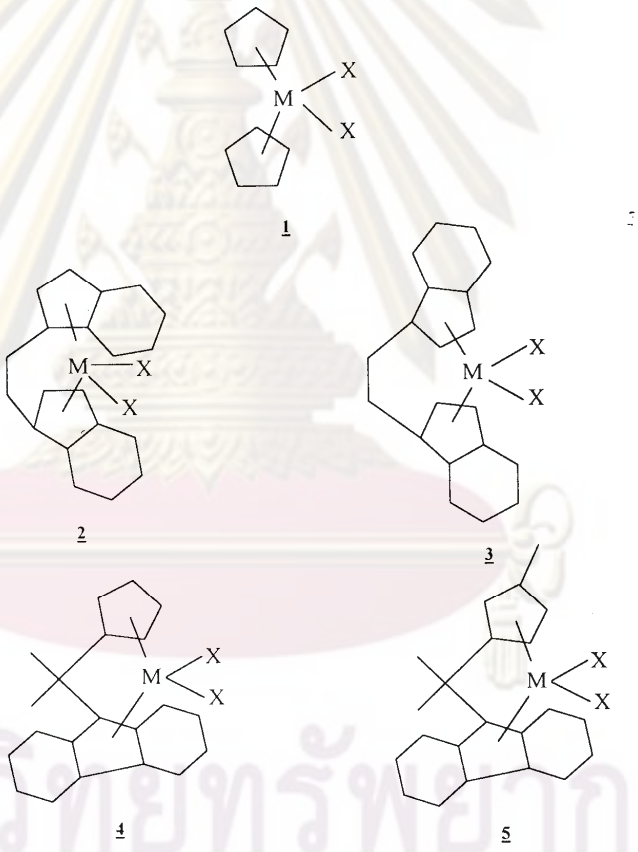

Figure 2.3 Scheme of the different metallocene complex structures [12]. Type 1 is C_{2v}-symmetric; Type 2 is C_2-symmetric; Type 3 is C_s-symmetric; Type 4 is C_s-symmetric; Type 5 is C_1-symmetric.

2.2.2 Derivatives of Metallocene

Metallocenes including just one facially-bound planar organic ligand instead of two gives rise to a still larger family of half sandwich compounds (also called half-metallocene). The general structure of half-metallocene is shown in **Figure 2.4**.

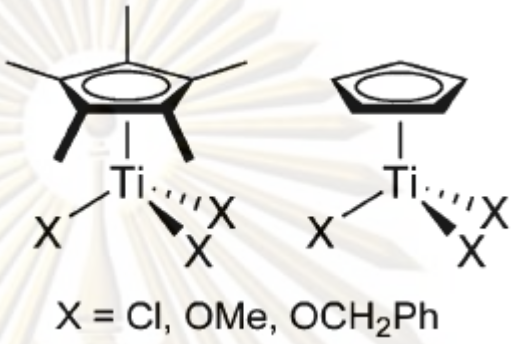

Figure 2.4 The general structure of half-metallocene(titanocene)[15]

Recently, *nonbridged* half-metallocene type group 4 transition metal complexes of the type, Cp'M(L)X_2 (Cp' =cyclopentadienyl group; M= Ti, Zr, Hf; L = anionic ligand such as OAr, NR_2, N CR_2, N PR_3, etc.; X= halogen, alkyl etc., **Figure 2.5**), become one of the promising candidates for new efficient catalysts for precise olefin polymerization [18-20]. This is because, as described below, that this type of complex catalyst has exhibited unique characteristics especially for ethylene (co)polymerizations affording new polymers that have never been prepared by conventional Zigler–Natta catalysts and by ordinary metallocene type [21-24].

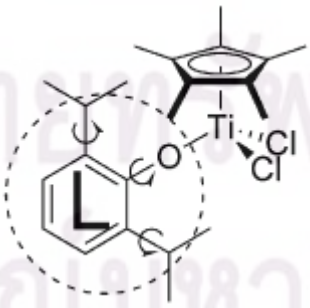

Figure 2.5 *Nonbridged* half-metallocene containing anionic donor ligand [15]

Another kind of well-known metallocene is the linked amido-cyclopentadienyl titanium complex catalysts, so called "constrained geometry catalyst (CGC)". It

showed efficient comonomer incorporation (**Figure 2.6**) [16-18]. This complex was designed according to the analogous scandium complex reported by Bercaw et al. [19], and the reason for better comonomer incorporation has been explained as that the bridge constrains more open Cp-Ti-N bond angle offering better comonomer incorporation by allowing improved accessibility for (rather) bulky alpha-olefin comonomers [16,18].

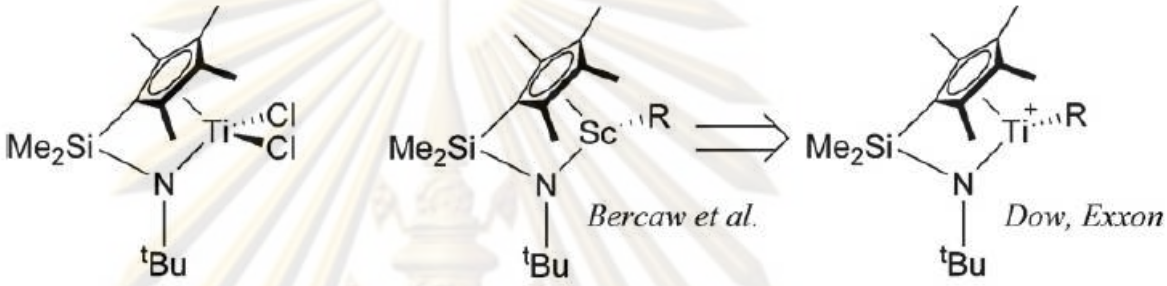

Figure 2.6 Constrained geometry catalyst (CGC) [16]

2.2.3 Polymerization Mechanism

The mechanism of catalyst activation is not clearly understood. However, alkylation and reduction of the metal site by a cocatalyst (generally alkyl aluminum or alkyl aluminoxane) is believed to generate the cationic active catalyst species.

First, in the polymerization, the initial mechanism started with formation of cationic species catalyst that is shown below.

Initiation

$$Et(Ind)_2ZrCl_2 + Al(CH_3)_3 \longrightarrow Et(Ind)_2ZrClMe + Al(CH_3)_2Cl$$

Propagation proceeds by coordination and insertion of new monomer unit in the metal carbon bond. Cossee mechanism is still one of the most generally acceptedpolymerization mechanism (**Figure 2.7**) [20]. In the first step, monomer forms a complex with the vacant coordination site at the active catalyst center. Then through a four-centered transition state, bond between monomer and metal center and

between monomer and polymer chain are formed, increasing the length of the polymer chain by one monomer unit and generating another vacant site.

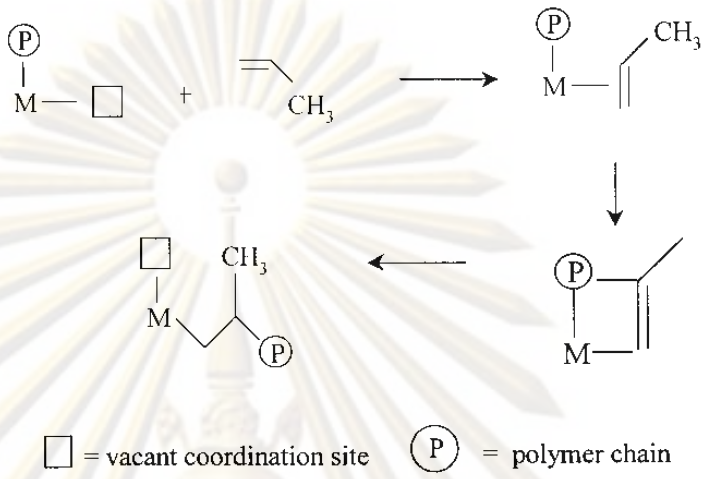

Figure 2.7 Cossee mechanism for Ziegler-Natta olefin polymerization [20].

The trigger mechanism has been proposed for the polymerization of α-olefin with Ziegler-Natta catalysts [21] (**Figure 2.8**). In this mechanism, two monomers interact with one active catalytic center in the transition state. A second monomer is required to form a new complex with the existing catalyst-monomer complex, thus trigger a chain propagation step. No vacant site is involved in this model. The trigger mechanism has been used to explain the rate enhancement effect observed when ethylene is copolymerized with α-olefins.

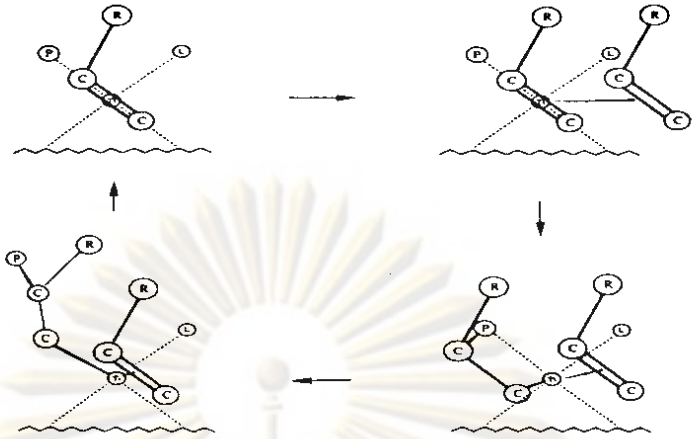

Figure 2.8 The propagation step according to the trigger mechanism [21].

After that, the propagation mechanism in polymerization shows in **Figure 2.9**.

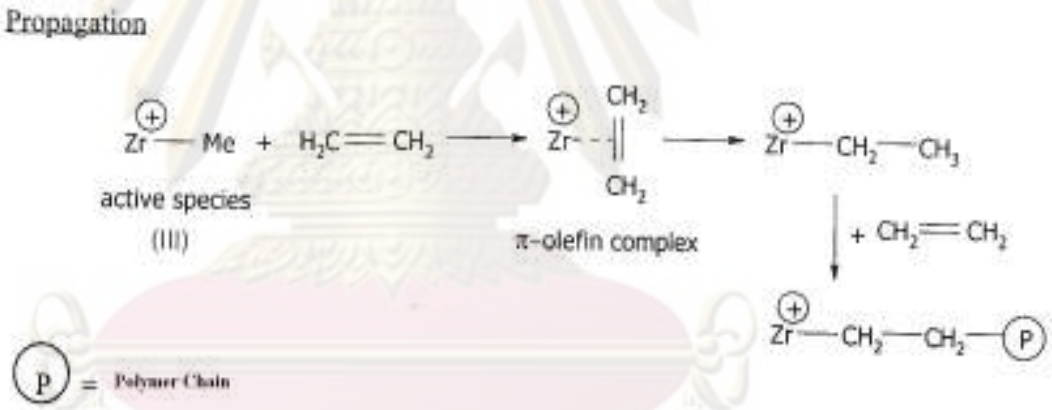

Figure 2.9 Propagation mechanism in polymerization [21]

Finally, the termination of polymer chains can be formed by 1) chain transfer via β-H elimination, 2) chain transfer via β-Me elimination, 3) chain transfer to aluminum, 4) chain transfer to monomer, and 5) chain transfer to hydrogen (**Figure 2.10-2.14**)[12]. The first two transfer reactions form the polymer chains containing terminal double bonds.

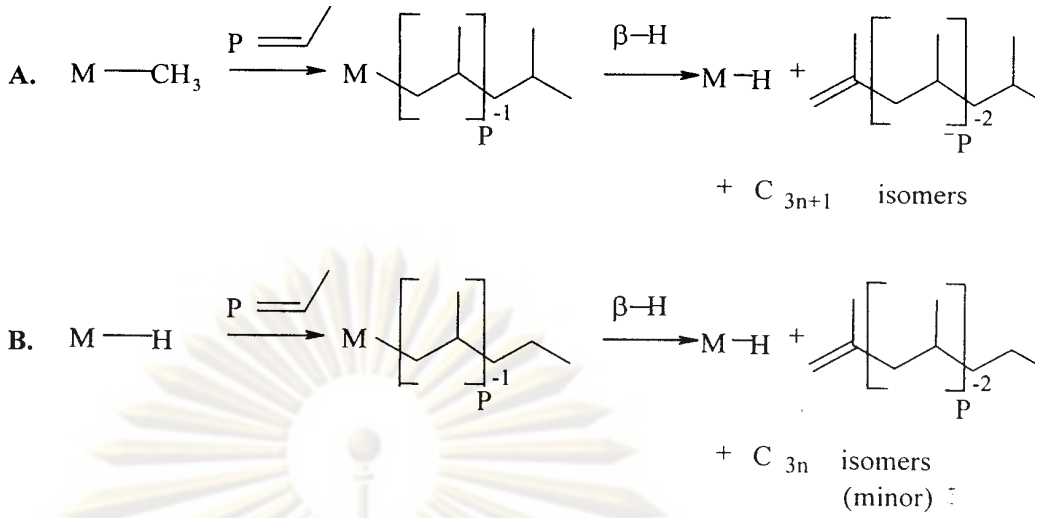

Figure 2.10 Chain transfer via β-H elimination [12]

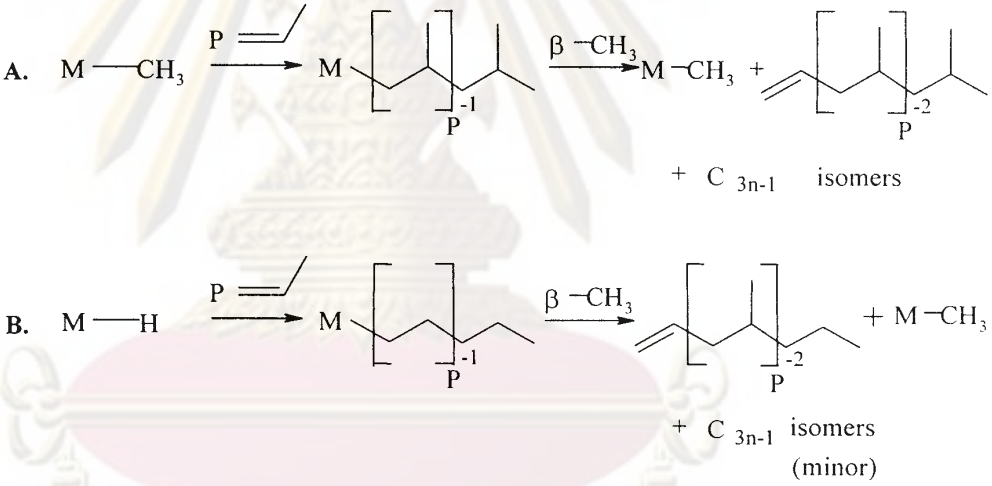

Figure 2.11 Chain transfer via β-CH_3 elimination [12]

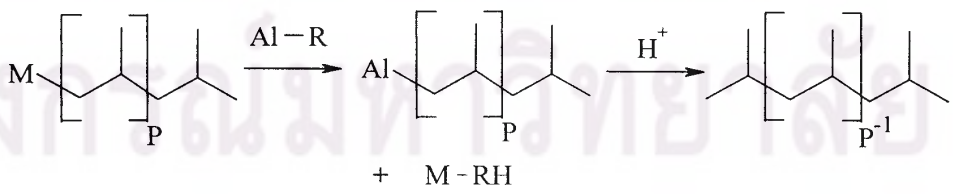

Figure 2.12 Chain transfer to aluminum [12]

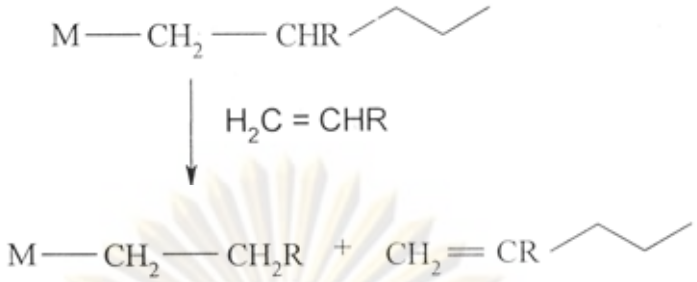

Figure 2.13 Chain transfer to monomer [12]

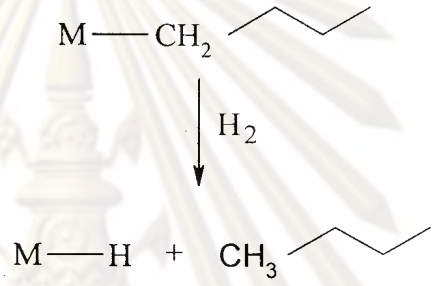

Figure 2.14 Chain transfer to hydrogen [12]

2.2.4 Cocatalysts

Metallocene catalysts have to be activated by a cocatalyst. The most common types of cocatalysts are alkylaluminums including methylaluminoxane (MAO), trimethylaluminum (TMA), triethylaluminum (TEA), triisobutylaluminum (TIBA) and cation forming agents such as $(C_6H_5)_3C^+(C_6F_5)_4B^-$ and $B(C_6F_5)_3$ [22].

Among these, MAO is a very effective cocatalyst for metallocene. However, due to the difficulties and costs involved in the synthesis of MAO, there has been considerable effort done to reduce or elimination the use of MAO. Due to difficulties in separation, most commercially available MAO contains a significant fraction of TMA (about 10-30%) [23]. This TMA in MAO could be substantially eliminated by toluene-evaporation at 25^{o}C.

Indeed, the difficulties encountered to better understand the important factors for an efficient activation are mainly due to the poor knowledge of the MAO composition and structure. Several types of macromolecular arrangements, involving linear chains, monocycles and/or various three-dimensional structures have been

successively postulated. These are shown in **Figure 2.15**. In recent work, a more detailed image of MAO was proposed as a cage molecule, with a general formula $Me_{6m}Al_{4m}O_{3m}$ (m equal to 3 or 4) [24].

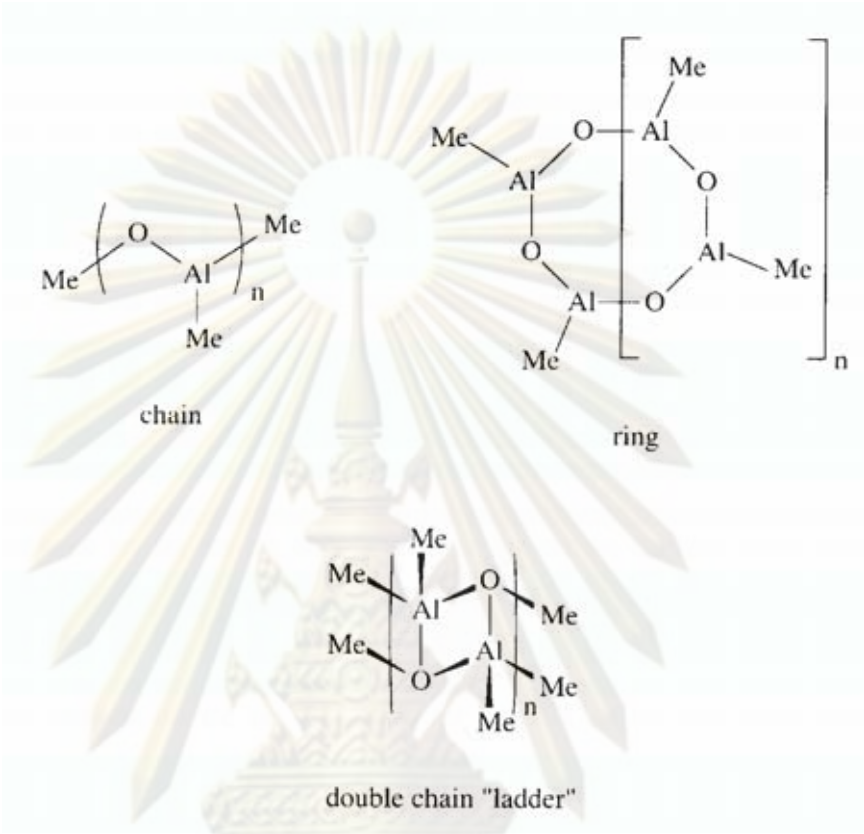

Figure 2.15 Early structure models for MAO [24]

In the case of rac-Et(Ind)$_2$ZrMe$_2$ as precursor, the extracted methyl ligands do not yield any modification in the structure and reactivity of the MAO counter-anion, thus allowing zirconium coordination site available for olefin that presented in **Figure 2.16** [25].

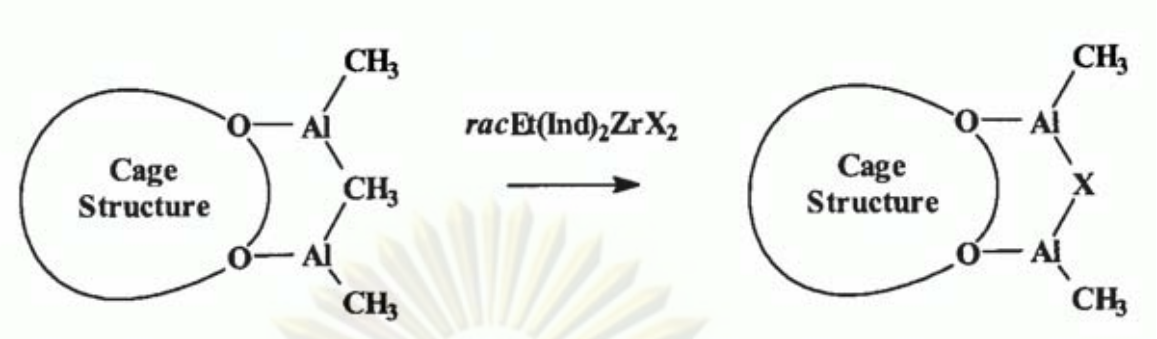

Figure 2.16 Representation of MAO showing the substitution of one bridging methyl group by X ligand extracted from racEt(Ind)$_2$ZrCl$_2$ (X = Cl, NMe$_2$, CH$_2$Ph) [25].

Cam and Giannini [26] investigated the role of TMA present in MAO by a direct analysis of Cp_2ZrCl_2/MAO solution in toluene-d_8 using ^{1}H-NMR. Their observation indicated that TMA might be the major alkylating agent and that MAO acted mainly as a polarization agent. However, in general it is believed that MAO is the key cocatalyst in polymerizations involving metallocene catalysts. The role of MAO included 1) alkylation of metallocene, thus forming catalyst active species, 2) scavenging impurities, 3) stabilizing the cationic center by ion-pair interaction and 4) preventing bimetallic deactivation of the active species.

The homogeneous metallocene catalyst cannot be activated by common trialkylaluminum only. However, Soga *et al.*[27] were able to produce polyethylene with modified homogeneous Cp_2ZrCl_2 activated by common trialkylaluminum in the presence of $Si(CH_3)_3OH$. Their results show that for an "optimum" yield aging of the catalyst and $Si(CH_3)_3OH$ mixture for four hours is required. However, MWD of the produced polymers is bimodal although the polymers obtained in the presence of MAO have narrow MWD.

Ethylene/α-olefins copolymers with bimodal CCD were produced with homogeneous Cp_2ZrCl_2 with different cocatalysts such as MAO and mixture of TEA/borate or TIBA/borate [28]. It seemed that the active species generated with different cocatalysts have different activities and produce polymers with different molecular weights.

2.3 Heterogeneous System

The new metallocene/MAO systems offer more possibilities in olefin polymerization compared to conventional Ziegler-Natta catalysts, such as narrow stereoregularity, molecular weight and chemical composition distributions (CCDs) through ligand design. However, only heterogeneous catalysts can be practically used for the existing gas phase and slurry polymerization processes. Without using a heterogeneous system, high bulk density and narrow size distribution of polymer particles cannot be achieved. The advantages of supporting catalysts include improved morphology, less reactor fouling, lower Al/metal mole ratios required to obtain the maximum activities in some cases the elimination of the use of MAO, and improved stability of the catalyst due to much slower deactivation by bimolecular catalyst interactions. Therefore, developing heterogeneous metallocene catalysts, that still have all the advantages of homogeneous systems, became one of the main research objectives of applied metallocene catalysis.

Steinmetz *et al*. [29] examined the particle growth of polypropylene made with a supported metallocene catalyst using scanning electron microscopy (SEM). They noticed formation of a polymer layer only on the outer surface of catalyst particles during the initial induction period. As the polymerization continued, the whole particle was filled with polymer. Particle fragmentation pattern depended on the type of supported metallocene.

2.3.1. Catalyst Chemistry

The nature of the active sites affects the polymer morphology, catalyst stability and activity, and the characteristics of the polymer produced. However, structure and chemistry of the active sites in supported catalysts are not clearly understood. Catalytic activities for supported metallocene are usually much lower than that of their counterpart homogeneous system. Formation of different active species, deactivation of catalyst during supporting procedure, and mass transfer resistance may contribute to decreased catalyst activity.

Tait *et al.* [30] reported general effects of support type, treatment, supporting procedure, and type of diluents on reaction kinetics and physical properties of polymer produced although the activities of supported catalysts are much lower compared to homogeneous systems. The activity of catalysts increased slightly when o-dichlorobenzene was introduced in toluene

The catalytic activities of supported catalyst depended on the percentage of the incorporated metallocene was reported by Quijada *et al*. [31]. However, in the case of metallocenes supported on MAO pretreated silica, depending on how the surface bound MAO complex with the catalyst, the activity can be as high as that of homogeneous system. According to the experiment by Chein *et al*. [32], if a single MAO is attached to silica, it would complex with zirconocene and lowers its activity. On the other hand, if multiple MAOs are attached to the surface silanol, the supported zirconocene will not be further complexed with MAO and have activity.

Interaction between MAO and silica surface

One has to be concerned in preparation of supported catalyst is the interactions between species fixed on the surface (catalyst and/or MAO) and the surface because their structures and strengths also affect an activity of the catalytic system into which they are introduced.

Silica or silicon dioxide is the natural compound forming with silicon and oxygen. In general, there are three different hydroxyl groups on the silica surface as shown in **Figure 2.17**. They are (**I**) isolated, (**II**) geminal and (**III**) vicinal. Besides these types, when silica is heated to higher 180 °C, the vicinals will be formed to surface siloxane (or siliyl ether, **Figure 2.17-IV**)

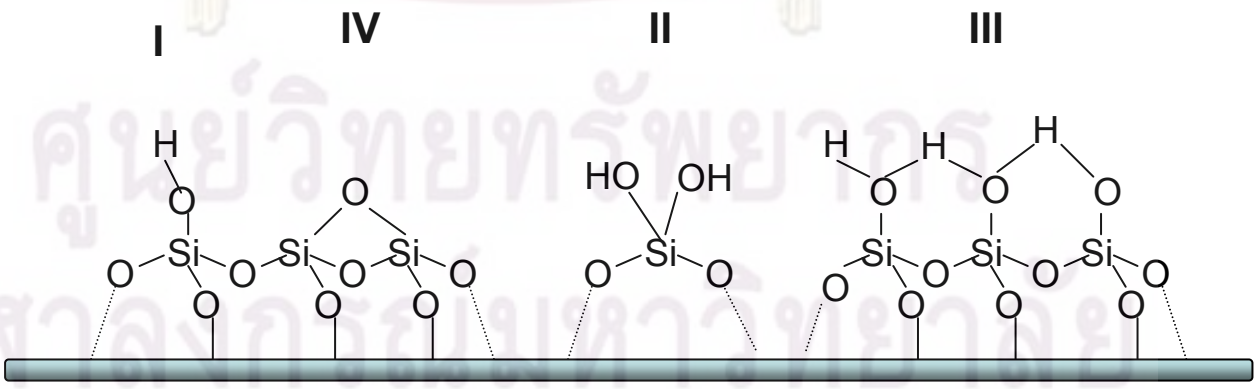

Figure 2.17 Structure of chemical groups on silica surface [33]

The variation of functional groups also affects reaction of silica. When silica is brought to use as a support in a heterogeneous reaction system, it has to improve some properties prior to using. In general, it was calcinated in an air or an inert atmosphere or sometimes in vacuum in order to evacuate water and reduce the amount of hydroxyl groups on the surface in addition this can improve some physical properties such as pore sizes, pore volume and strength. However, the hydroxyl groups also exist on the surface no matter how high temperature it was heated to. They are about 1-5 groups per nanometer square [34], so therefore interactions of silica through hydroxyl groups need to be considered.

Bartram et al. [35] proposed the model of interaction between MAO and silica as shown in **Figure 2.18**. This figure indicates three species of aluminium bonded with 3-coordinations indicated to highly reactive Lewis acids which has the ability to draw substitution group out of the catalyst then providing the active sites suitable for polymerization.

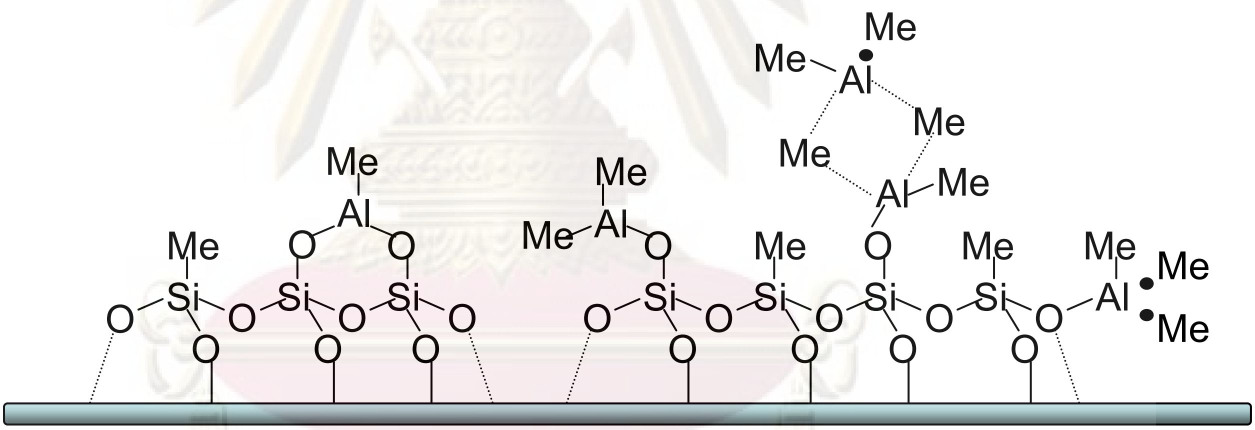

Figure 2.18 Species of aluminium on silica surface [33]

Scott et al. [36] proposed the model of 4-coordinations as **Figure 2.19**. These coordinations are generated by trimethyl aluminum (TMAL) composed in MAO.

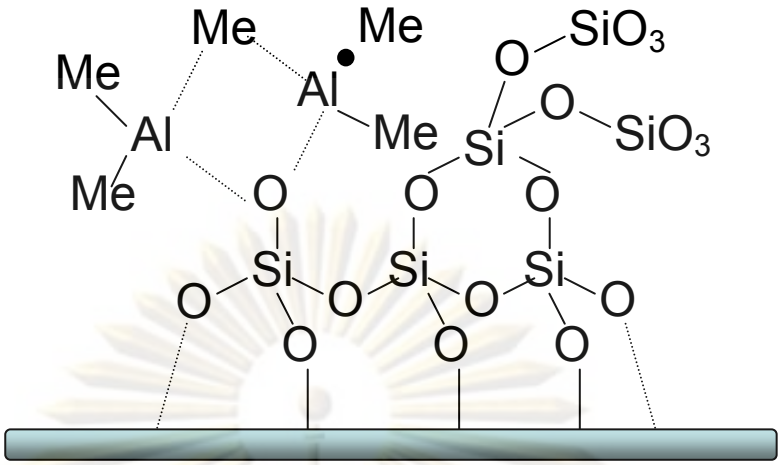

Figure 2.19 Species of aluminium (TMAL) on silica surface [33]

2.3.2 Supporting Methods

Preparation of supported catalyst

There are about 3 different methods used in preparation (immobilization) the supported catalyst for polymerization as shown in **Figure 2.20**.

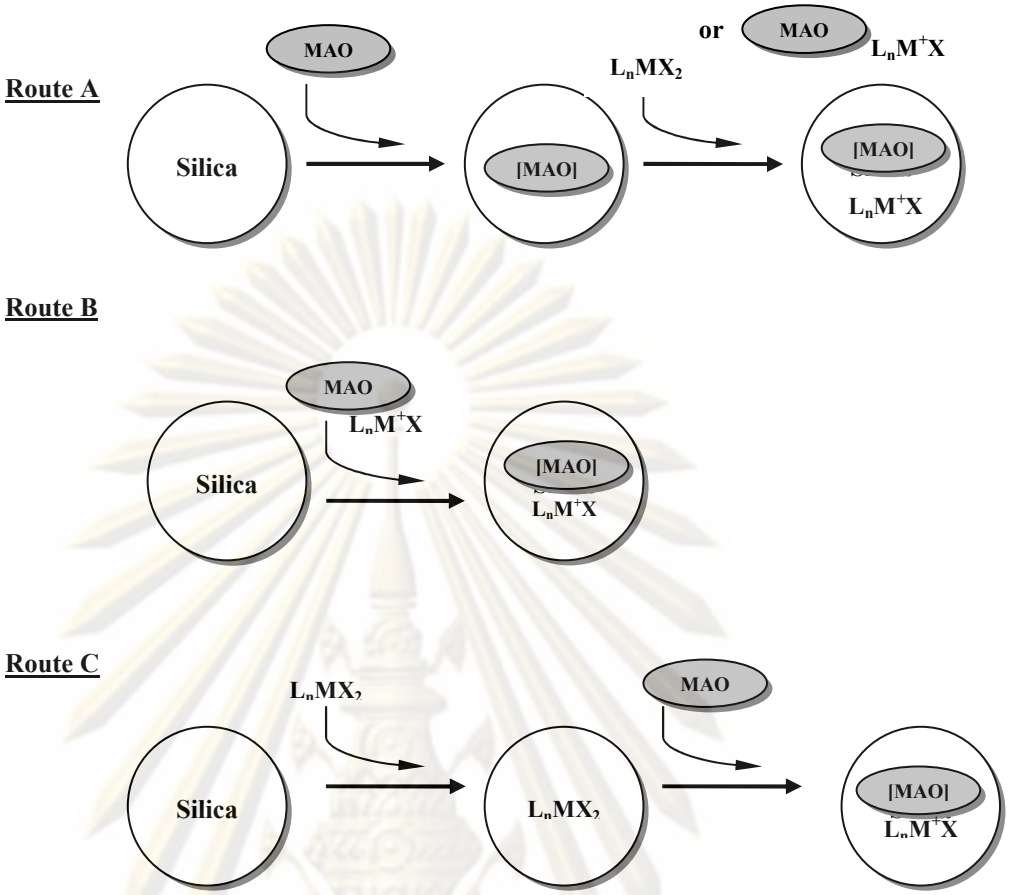

Figure 2.20 Various methods for immobilization [33]

It is the application of catalyst that decides which method is suitable for using. All methods, according to the literature, were studied by many researchers as described below.

Method A

Welborn [37] and Takahashi [38] found that contacting silica with MAO and then drying prior to reacting with dichloride- or daialkylmetallocene in copolymerization provided high efficiency to the system and produced polymers with high comomer insertion.

Razavi [39] and Gautheir [40] found that when reflux silica and MAO in a suspension of toluene prior to contacting to metallicene can improve stereoselectivity, activity and yield, and also found that the efficiency of catalyst related with temperatures used in immobilization step.

Jacobsen et al. [41] studied immobilization of MAO onto silica by contacting silica with MAO which had been dried in vacuum prior to heating to 100-200 °C for 2

h, and then washing and drying. It was found that the high amount of MAO existed on the silica.

Method B

Burkhardt et al. [42] brought MAO solvent to mix with metallocene before heating it up and then introduced it into copolymerization of ethylene and propylene. It was found that the obtained copolymer having a narrow molecular weight distribution and a uniformity of particle sizes. There was an effort to bring this method performing in a heterogeneous system with some metallocenes that is only reactive for a homogeneous system such as Me_2(2-Me-4-PhInd)$_2ZrCl_2$ and Me_2(2-Me-4-(Napth)Ind)$_2ZrCl_2$ [43] , but it was not successful.

Fraajie et al. [44] suggest the solution to this drawback by extension the contacting time up to 1 day without exposing to light. It was found that the activity increased two times compared with the conventional method in addition this method can perform with the complex structure metallocene.

Method C

As directing contact catalyst onto silica surface, the studies of this method then often involved the modification of surface for help silica suitable for reacting with the complicated structure of metallocene. Mostly, the modifications are performed in order to:

1) Reduce hydroxyl group on the surface
2) Provide the surface with uniform species
3) Add functional group into silica
4) Change the electronic properties of silica

Santos et al. [45] modified silica by variation of heating temperature from room temperature to 450 °C and then contacting with [nBuCp$_2$]$ZrCl_2$ after that introducing into polymerization. It was found that a high temperature decreased the amount of metallocene in silica compared with a low temperature but when using this support in ethylene polymerization, it gave higher activity and a higher molecular weight. They also discovered that structures of catalysts also influenced the activity of this system with the central metal atoms increasing the activity as followed Ti < Hf < Zr whereas the ligand group not significantly influencing the activity of the ethylene

polymerization. However, effect of ligand group was observed in copolymerization of ethylene and 1-hexene [46].

Modification of silica by silane

Besides non-uniformity of silica created by a variety of functional groups on the surface, the hydrophilic property (water attraction) is also one of the advantages to silica. This is because if silica is conducted with catalysts which can be decomposed by water, the remained water on the surface will cause the damage of catalyst. Therefore, treating the surface with hydrophobic functional groups such as aryl alkyl and silane can overcome this problem [47].

Silane is one of the compound of silicon which is the main element of silica. Therefore, with the composition like silica ,the silane modification is very favor to many researchers.

Jongsomjit et al. [55,56] used tetrachlorosilane ($SiCl_4$) in silica modification. It was found that it can enhance the activity of copolymerization between ethylene and 1-hexene but give molecular weights of the obtained polymers similar to those of the homogeneous system.

Schrekker et al. [47] used tetrachlorosilane ($SiCl_4$) trimethylaluminum ($AlMe_3$) and trichloroborane (BCl_3) in the modification in order to conduct in polymerization of ethylene. It was found that the activities of all modified silicas were higher than that of the unmodified one and there was no reactor fouling in the system because the catalyst linked to the silica through the covalent bond of silane (-$SiCl_3$, -$AlMe_2$ and BCl_2) then not leaching during polymerization.

2.4 Catalytic and specific properties

2.4.1 Effect of substituted ligand

It has been known that the ligand modification is very important in order for metal catalyzed olefin polymerization to proceed with remarkable catalytic activities [15]. For example, as shown in **Figure 2.21**, both substituents on cyclopentadienyl and aryloxo groups affected the catalytic activity for ethylene polymerization [48,49].

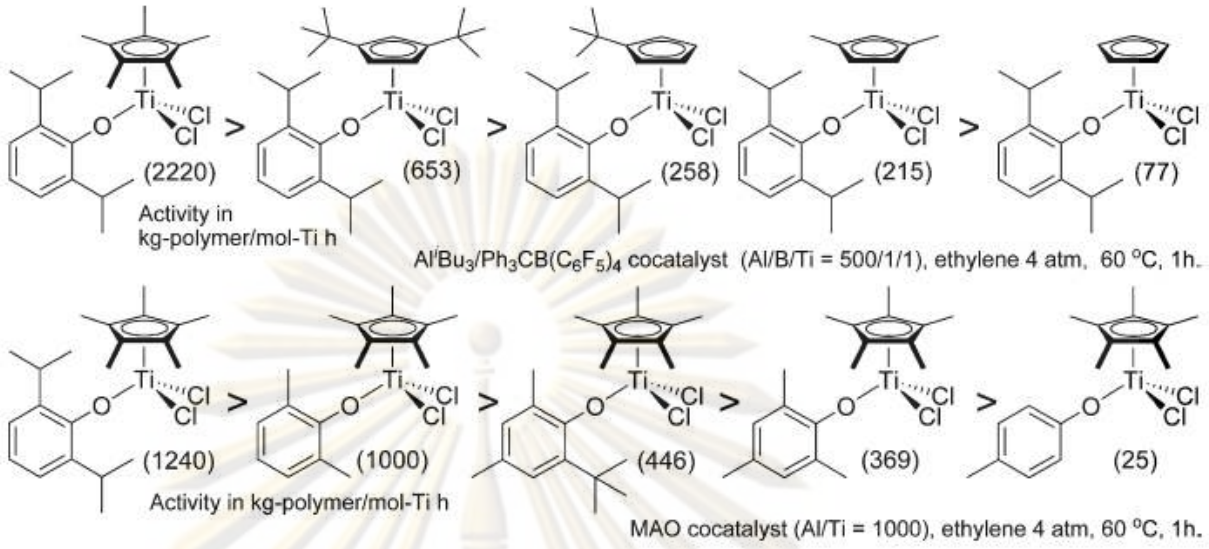

Figure 2.21 Effect of substituted ligands in polymerization [15].

. Cp*TiCl$_2$(O-2,6-*i*Pr$_2$C$_6$H$_3$) exhibited notable activities, and the activity by Cp'TiCl2(O-2,6-*i*Pr$_2$C$_6$H$_3$) increased in the order: Cp' =Cp* >>1,3-*t*Bu$_2$C$_5$H$_3$ > 1,3-Me$_2$C$_5$H$_3$, ^{t}BuC$_5$H$_4$>>Cp. This seems the similar observation for syndiospecific styrene polymerization using a series of Cp_Ti(OMe)$_3$ complexes [50] , and the similar explanation that the stabilization of the active site by more electron-donating substituents is important for the high activity can be thus assumed. On the other hand, as also shown in Scheme 8, the steric bulk of phenoxy ligand containing substituents in the 2,6-position should be very important for exhibiting the high activity. We assumed that the steric bulk of aryloxo ligand stabilized the catalytically active species under the polymerization conditions in the presence of cocatalyst (to protect the probable accompanied reaction with Al alkyls, dissociation of the aryloxide) [48,49].

2.4.2 Effect of comonomer

In copolymerization, one particular aspect in which should be considered is the incorporation of comonomer into the obtained polymer. The comonomer contents can determine directly the polymer properties and also involve the term of catalytic properties.

Al-Malaika and Peng [51] have found that the amount of comonomer have a significant influence on the polymer melt thermo-oxidative behaviour. At low to intermediate processing temperatures, all m-LLDPE polymers exhibited similar

behaviour with crosslinking reactions dominating their thermal oxidation. By contrast, at higher processing temperatures, the behaviour of the metallocene polymers changed depending on the level of comonomer content: higher SCB gave rise to predominantly chain scission reactions whereas polymers with lower level of SCB continued to be dominated by crosslinking.

Van Grieken et al. [52] studied the catalytic system $(nBuCp)_2ZrCl_2$/MAO immobilized over SiO_2-Al_2O_3 has been tested in ethylene-1-hexene copolymerizations using different amounts of comonomer. The catalytic activity shows a positive comonomer effect up to 1-hexene concentration of 0.724 mol/L since larger amounts of 1-hexene lead to a decrease in the activity. Copolymer properties analyzed by ^{13}C NMR, GPC, CRYSTAF and DSC point to the presence of important amorphous regions in the growing polymer chains as the 1-hexene concentration increases.

Hong et al.[53] examined the effects of comonomer (type and concentration) to copolymerization and physical properties of LLDPE resins. CGC metallocene technology, under high temperature and high pressure (industrial reaction condition), was used to prepare three types of well-defined LLDPE copolymers containing 1-hexene, 1-octene, and 1-decene units. They show high molecular weight with narrow molecular weight and composition distributions, comparative catalyst activities, and similar comonomer effects.

For investigating how comonomer affect the system of copolymerization , Biatek and Czaja [54] compared between homogeneous and supported systems in copolymerisation of ethylene with 1-hexene over metallocene catalysts L_2ZrCl_2/ MAO (L = Cp, n-BuCp, t-BuCp, i-PrCp, Me_5Cp). They found that metallocene structure also determined comonomer incorporation, both for homogeneous and supported catalytic systems. When a catalyst is anchored on a support, it becomes less effective at incorporating a comonomer into the polyethylene chain, and the type of the support material has no influence on that process.

CHAPTER III

EXPERIMENTAL

3.1 Research objectives

1) To synthesize half-metallocene catalyst (Ti-complex) and use in the copolymerization of ethylene and 1-hexene.
2) To investigate the effect of comonomer on catalytic activity and properties of LLDPE.
3) To compare the catalytic performance under homogeneous and heterogeneous systems.
4) To investigate the effect of preparation methods and texture of supports on catalytic activity and properties of LLDPE.

3.2 Research scopes

A half-metallocene catalyst was prepared and characterized by nuclear magnetic resonance (NMR) technique. It was then brought to synthesize LLDPE by copolymerization of ethylene and 1- hexene with MMAO as a cocatalyst. The study of this catalyst was divided into 5 parts consisting of**:**

- Effect of comonomer on the half-metallocene catalytic systems
- A Comparative study on LLDPE/ silica composites synthesized by different copolymerization systems
- Modification of supports by gallium
- Effect of method for preparation of supported catalysts
- Effect of support texture

The supports used together with the catalysts to become the supported catalyst was characterized by N_2 physisorption, X-ray diffraction (XRD), Scanning electron microscopy (SEM) Inductive couple plasma-optical emission spectroscopy (ICP-OES) and Thermogravimetric analysis (TGA). The obtained LLDPE was characterized by Differential scanning calorimetry (DSC), ^{13}C NMR spectroscopy (^{13}C NMR) and X-ray photoelectron spectroscopy (XPS).

3.2 Research methodology

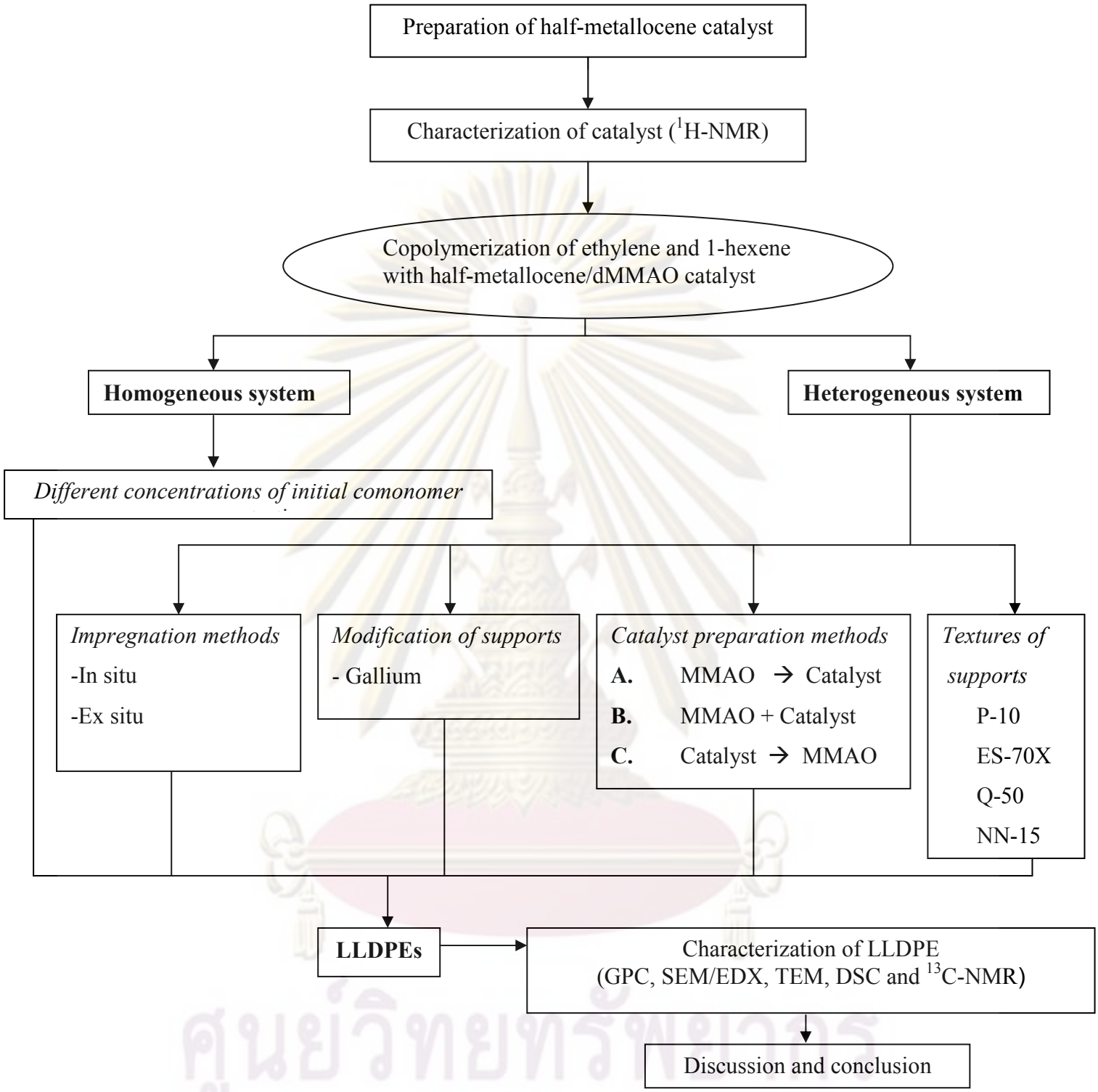

Figure 4.1 Flow diagram of research methodology

3.3 Experimental

3.3.1 Chemicals

The chemicals will be used in these experiments are analytical grade, but only major materials are specified as follows:

- Ethylene gas (99.96%) was devoted from National Petrochemical Co., Ltd., Thailand and used as received.
- 1-hexene (99+%) was purchased from Aldrich Chemical Company, Inc. and purified by distilling over sodium under argon atmosphere before use.
- 1-octene (98%) was purchased from Aldrich Chemical Company, Inc. and purified by distilling over sodium under argon atmosphere before use.
- 1-decene (≥ 97%) was purchased from Fluka Chemie A.G. Switzerland. and purified by distilling over sodium under argon atmosphere before use.
- Hexane (95%) was donated from Shell (Public) Company, Inc. and purified by distilling over sodium under argon atmosphere before use.
- Toluene was devoted from EXXON Chemical Ltd., Thailand. This solvent was dried over dehydrated $CaCl_2$ and distilled over sodium/benzophenone under argon atmosphere before use.
- Modified methylaluminoxane (MMAO) 1.86 M in toluene was donated from Tosoh Akso, Japan and used without further purification.
- Trimethylaluminum (TMA) 2.0 M in toluene was supplied from Nippon aluminum Alkyls Ltd., Japan and used without further purification.
- Hydrochloric acid (Fuming 36.7%) was supplied from Sigma and used as received.
- Methanol (Commercial grade) was purchased from SR lab and used as received.
- Sodium (99%) was purchased from Aldrich Chemical Company, Inc. and used as received.
- Benzophenone (99%) was purchased from Fluka Chemie A.G. Switzerland and used as received.
- Calciumhydride (99%) was purchased from Fluka Chemie A.G. Switzerland and used as received.
- Ultra high purity argon gas (99.999%) was purchased from Thai Industrial Gas Co., Ltd., and further purified by passing through columns packed with molecular sieve 3A, BASF Catalyst R3-11G, sodium hydroxide (NaOH) and phosphorus pentaoxide (P_2O_5) to remove traces of oxygen and moisture.

3.3.2 Equipments

Because of the metallocene system is extremely sensitive to the oxygen and moisture. Therefore, the special equipments will be required to handle while the preparation and polymerization process. For example, glove box: equipped with the oxygen and moisture protection system will be used to produce the inert atmosphere. Schlenk techniques (Vacuum and Purge with inert gas) are the others set of the equipment will be used to handle air-sensitive product.

- **Inert gas supply**

The inert gas (argon) will be passed through columns of BASF catalyst R3-11G as oxygen scavenger, molecular sieve 3×10^{-10} m to remove moisture. The BASF catalyst will be regenerated by treatment with hydrogen at 300 °C overnight before flowing the argon gas through all the above columns.

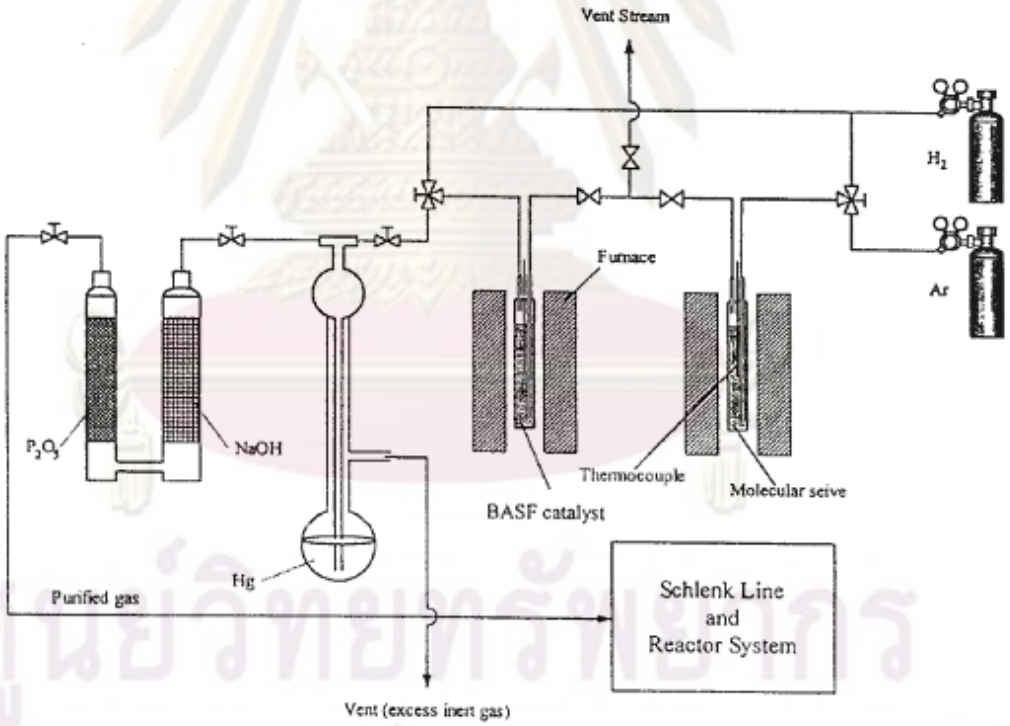

Figure 3.1 Inert gas supply system

- **Cooling system**

The cooling system is in the solvent distillation in order to condense the freshly evaporated solvent.

- **Schlenk tube**

A tube with a ground glass joint and side arm, which is three-way glass valve. Sizes of Schlenk tubes are 50, 100 and 200 ml. will be used to prepare catalyst and store materials which are sensitive to oxygen and moisture.

Figure 3.2 Schlenk tube

- **Schlenk line**

Schlenk line consists of vacuum and argon lines. The vacuum line will be equipped with the solvent trap and vacuum pump, respectively. The argon line will be connected with the trap and the mercury bubbler that is a manometer tube and contains enough mercury to provide a seal from the atmosphere when argon line will be evacuated.

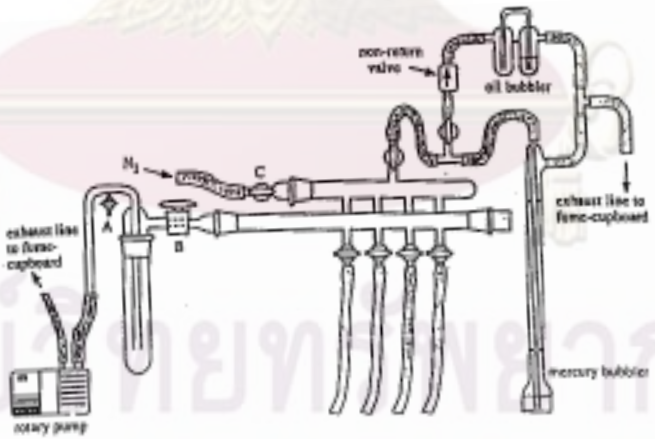

Figure 3.3 Schlenk line

- **Magnetic stirrer and heater**

The magnetic stirrer and heater model RTC basis from IKA Labortechnik will be used.

- **Reactor**

A 100 ml glass flask will be connected with 3-ways valve will be used as the copolymerization reactor for atmospheric pressure system and a 100 ml stainless steel autoclave will be used as the copolymerization reactor for high pressure systems.

- **Vacuum pump**

The vacuum pump model 195 from Labconco Corporation will be used. A pressure of 10-1 to 10-3 mmHg is adequate for the vacuum supply to the vacuum line in the Schlenk line.

- **Polymerization line**

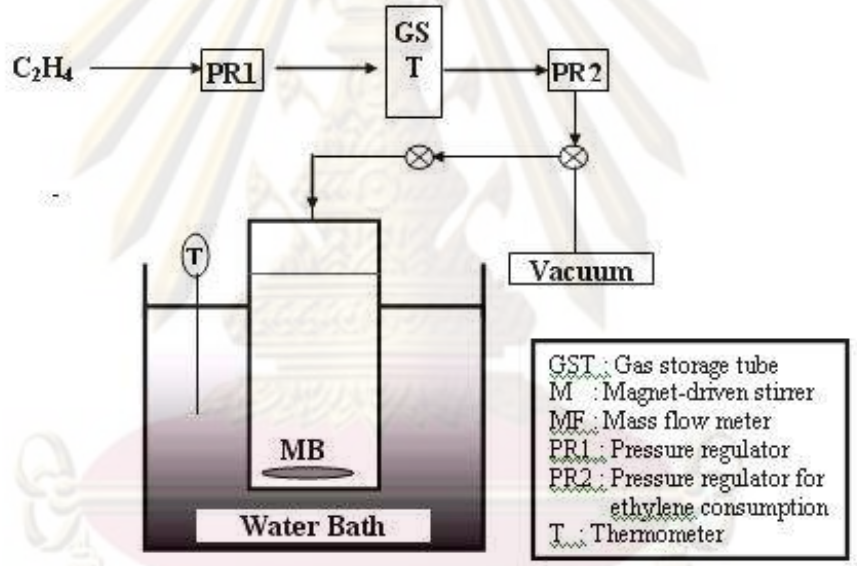

Figure 3.4 Diagram of system in slurry phase polymerization.

3.3.3 Characterizing Instruments

- **Scanning electron microscopy (SEM) and energy dispersive X-ray spectroscopy (EDX)**

SEM observation with a JSM-5800 LV Scanning Microscope, Microspec WDX at Scientific Technological Research Equipment Center, Chulalongkorn University will be employed to investigate the morphology of catalyst precursor and polymer. The polymer samples for SEM analysis will be coated with gold particles

by ion sputtering device to provide electrical contact to the specimen. EDX will be performed using Link Isis series 300 program.

- **Nuclear magnetic resonance (NMR)**

With 2 modes of operating, NMR can be performed for examination both catalyst and the obtained polymer. The first one, ^{1}H-NMR will be used to determine the structure of synthesized catalyst. And the second mode, ^{13}C-NMR will be used to investigate the amount of comonomer content in polymer. ^{13}C-NMR spectra will be recorded at 100 °C using JEOL JNM-A500 operating at 125 MHz. Copolymer solutions will be prepared using 1,2-dichlorobenzene as solvent and benzene-d_6 for internal lock.

- **Differential Scanning Calorimetry (DSC)**

The melting temperature of ethylene/1-hexene copolymer products will be determined with a Perkin-Elmer diamond DSC from MEKTEC, at the Center of Excellence on Catalysis and Catalytic Reaction Engineering, Department of Chemical Engineering, Chulalongkorn University. The analyses will be performed at the heating rate of 20 °C/ minutes in the temperature range of 50-150 °C. The heating cycle will run twice. In the first scan, samples will be heated and the cooled to room temperature. In the second, samples will be reheated at the same rate, but only the results of the second scan will be reported because the first scan will be influenced by the mechanical and thermal history of samples.

- **Gel Permeation Chromatography (GPC)**

Molecular weight and molecular weight distribution of the produced ethylene/1-hexene copolymer will be measured at 150 °C using *o*-dichlorobenzene as solvent by a gel permeation chromatography at Thai Petrochemical Industry Public Company Limited. The GPC instrument will be equipped with a PL-GPC 220 Differential refractometer (DRI), PL-BV 400 capillary bridge viscometer (Visc) and 2xPLgel 10 um MIXED-B (300x7.5mm) with PLgel 10 um guard (50 x 7.5 mm). The columns will be calibrated with standard narrow molar mass distribution polystyrenes and linear low density polyethylene and polystyrene.

- **Transmission electron microscopy (TEM)**

TEM will be used to determine the shape and size of the obtained polymer. The sample will be dispersed in ethanol before using TEM (JEOL JEM-2010) at Scientific Technological Research Equipment Center, Chulalongkorn University for microstructural characterization.

3.3.4 Procedures

- Preparation of catalyst

Half-metallocene catalysts (or constraint geometry catalyst) was prepared according to the method of Hakihara [55]. All the syntheses were carried out under Ar_2 by using standard Schlenk techniques. To a solution of t-BuNHSi$Me_2C_{13}H_9$ (4.51 g, 15.3 mmol) in hexane (40 mL) was added n-BuLi (23.5 mL of a 1.55M solution in hexane) by syringe at -78 °C. After warming to room temperature, the mixture was stirred for 3 h and then the solvent was removed to obtain Li_2[t-BuNSiMe_2Flu]. A solution of the dilithium salt in THF (60 mL) was added to a suspension of $TiCl_3$.3THF (5.38 g, 14.5 mmol) in THF (60 mL) at -78 °C. The mixture was stirred for one night and warmed to room temperature spontaneously. To the mixture was added solid $PbCl_2$ (4.25 g, 15.3 mmol), and the resulting mixture was stirred for 2 h.12 The solvent was removed, and the residue was extracted with toluene (3 x 50 mL). Then the extract was filtered, and the toluene was evaporated to give a crude product. The crude product was extracted with pentane (3 x 100 mL). The extract was then filtered and evaporated to give [t-BuNSiMe_2Flu]$TiCl_2$ as a dark red solid.

- Preparation of catalyst precursor

There were 5 different parts of investigation in this study, then the preparation of catalyst precursor (immobilization) following them as below:

Part 1: Effect of comonomer on the half-metallocene catalytic systems.

The catalyst was introduced into the system in liquid form and therefore no immobilization method was needed.

Part 2: A Comparative study on LLDPE/ silica composites synthesized by different copolymerization systems.

Two immobilization (impregnation) methods were used.

1) *In situ* impregnation method: silica (0.1 g) was allowed in contact with 4 mmol of MMAO for at least 2 h in a reactor with magnetic stirring, and then the slurry of MMAO/ support was obtained [56].

2) *Ex situ* impregnation: the support was reacted with the desired amount of MMAO in 20 ml of toluene at room temperature for 30 min. The solvent was then removed from the mixture by evacuation. This procedure was done only once with toluene (20 ml x 1) and three times with hexane (20 ml x 3). Then, the solid part was dried under vacuum at room temperature. The white powder of supported cocatalyst (MMAO/support) was then obtained.

Part 3: Modification of supports by gallium.

Supports used in this part were modified by gallium. Therefore, there were two steps in preparation consisting of;

1) Preparation of Ga-modified Silica Support

The Ga modification of the silica support was prepared by the conventional incipient-wetness impregnation method according to the procedure described previously [57]. The Ga source in the present case was $Ga(NO_3)$. Ga was impregnated onto silica gel (Cariact Q-50 and P-10) by 1.0 wt% of Ga. The support was dried in oven at 110 ºC for 12 h and then calcined in air at 400 ºC for 2 h.

2) Preparation of supported MMAO

The *in situ* impregnation was used as in part 1.

Part 4: Effect of method for preparation of supported catalysts**.**

Firstly, the supports were treated by $SiCl_4$ as already known that this can improve some surface properties. The procedure was conducted as followed:

- calcinated silica at 400 °C
- 1 g of silica suspended in 20 ml of toluene
- added 0.328 g of $SiCl_4$.

- stirred for 1 h
- removed solvent
- washed by toluene 3 times and 1 time with pentane
- dried under vacuum
- then brought to immobilization method.

There are 5 different methods (**A1, A2**, **B2, C1** and **C2**) to immobilize both metallocene and/or MMAO onto the supports as a diagram below:

Method **A1**

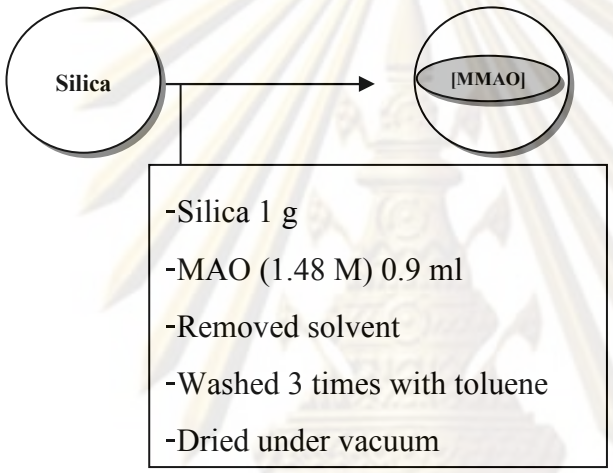

Method **A2**

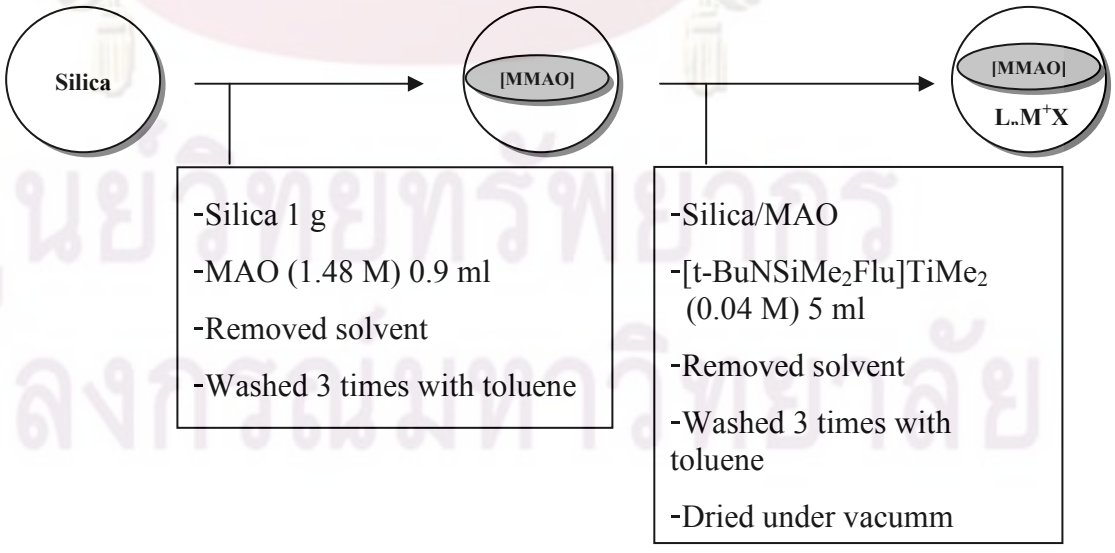

-

Method **B2**

-MAO (1.48 M) 0.9 ml + [t-BuNSiMe$_2$Flu]TiMe$_2$ (0.04 M) 5 ml
- Added 1 g of silica
- Removed solvent

-Washed 3 times with toluene

-Dried under vacuum

Method **C1**

-Silica

-[t-BuNSiMe$_2$Flu]TiMe$_2$ (0.04 M) 5 ml

-Removed solvent

-Washed 3 times with toluene

-Dried under vacuum

Method **C2**

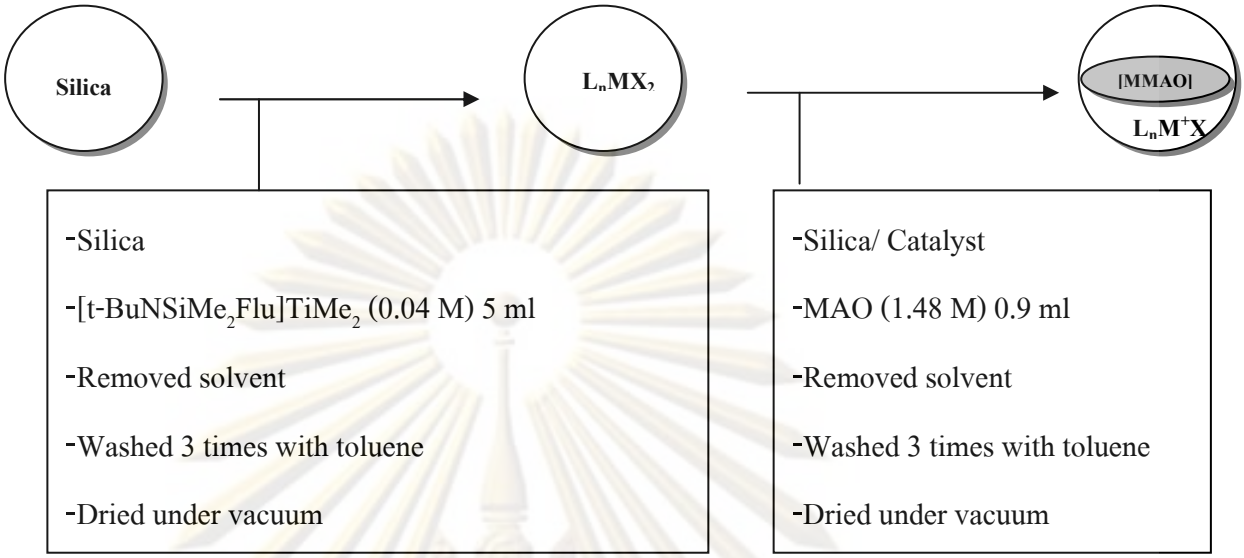

Part 5: Effect of support texture.

The immobilization methods used in part 5 was as the same as those in part 4.

- Copolymerization

The ethylene and 1-hexene copolymerization reaction was carried out in a 100 ml semi-batch stainless steel autoclave reactor equipped with magnetic stirrer. The autoclave and magnetic bar will be dried in oven at 110 ^{o}C for 30 minutes and will be purged with argon 5 times in glove box before use in copolymerization of ethylene and 1-olefin. At first, the desired amount of MMAO (or supported MMAO in the heterogeneous system) and 0.018 (0.009, 0.036) mole of 1-hexene along with toluene to make the total volume of 30 ml will be put into the reactor. The desired amount of half-metallocene catalyst (or supported catalyst in the heterogeneous system) was put into the reactor. The reactor will be frozen in liquid nitrogen to stop reaction for 15 minutes and then the reactor will be evacuated to remove argon. The reactor will be heated up to polymerization temperature (70°C). To start reaction, 0.018 mole of ethylene was fed into the reactor containing the comonomer and catalyst mixtures. After all ethylene will be consumed, the reaction will be terminated by addition of acidic methanol (10% HCl in methanol) and stirred for 30 minutes. After filtration, the obtained copolymer (white powder) will be washed with methanol and dried at room temperature.

3.3.5 Characterization of supports and catalyst

^{1}H-NMR spectroscopy

^{1}H NMR spectroscopy was used to determine chemical structure of the obtained catalyst. The spectra were recorded in C_6D_6 at 25 °C using BRUKER A400.

N_2 physisorption

Measurement of BET surface area, average pore diameter and pore size distribution of silica support were determined by N_2 physisorption using a Micromeritics ASAP 2000 automated system.

X-ray diffraction (XRD)

XRD was performed to determine the bulk crystalline phases of sample. It was conducted using a SIEMENS D-5000 X-ray diffractometer with CuK_{α}(λ = 1.54439×10^{-10} m). The spectra were scanned at a rate 2.4 degree/min in the range 2θ = 20-80 degrees.

Scanning electron microscopy (SEM)

SEM was used to determine the morphologies. The SEM of JEOL mode JSM-6400 was applied.

Thermogravimetric analysis (TGA)

TGA was performed to determine the interaction force of the supported dMMAO. It was conducted using TA Instruments SDT Q 600 analyzer. The samples of 10-20 mg and a temperature ramping from 25 to 600°C at 2 °C /min were used in the operation. The carrier gas was N_2 UHP.

3.3.6 Characterization Method of Polymer

Differential scanning calorimetry (DSC)

The melting temperature of polymer products was determined with thermal analysis measurement. It was performed using a Perkin-Elmer DSC P7 calorimeter. The DSC measurements reported here were recorded during the second heating/cooling cycle with the rate of 20°C min^{-1}. This procedure ensured that the

previous thermal history was erased and provided comparable conditions for all samples. Approximately 10 mg of sample was used for each DSC measurement.

^{13}C NMR spectroscopy (^{13}C NMR)

^{13}C NMR spectroscopy was used to determine the α-olefin incorporation and copolymer microstructure. Chemical shift were referenced internally to the benzene-d6 and calculated according to the method described by Randall. Sample solution was prepared by dissolving 50 mg of copolymer in 1,2,4-trichlorobenzene and benzene-d6. ^{13}C NMR spectra were taken at 60°C using BRUKER A400 operating at 100 MHz with an acquisition time of 1.5 s and a delay time of 4 s.

X-ray photoelectron spectroscopy (XPS)

XPS analysis was performed using an AMICUS photoelectron spectrometer equipped with a MgKa X-ray as a primary excitation and a KRATOS VISION2 software. XPS elemental spectra were acquired with 0.1 eV energy step at a pass energy of 75 eV.

Inductive couple plasma-optical emission spectroscopy (ICP-OES)

ICP-OES was performed using Perkin Elmer model PLASMA-1000 to determine the amount of MMAO (Al) on the support. About 50 μg of a sample was digested by sulfuric acid and then made the volume to 50 ml by ionized water.

Benefits

- LLDPE will be possibly synthesized with an good activity in the system of half-metallocene/d-MMAO catalyst.
- The insertion of a comonomer will be improved.
- Use this information as a reference for polymer industries.
- Produce international articles based on this research.

CHAPTER IV

RESULTS AND DISCUSSIONS

4.1 Effect of comonomer on the half-metallocene catalytic systems *(Part 1)*

The differences of initial comonomer were introduced into the homogeneous systems to investigate their effects on the comonomer contents, the activity of the system and the properties of the obtained polymers.

4.1.1 Reactivity of (co)monomer to catalyst

The catalytic activities based on polymer product are shown in **Table 4.1**. It can be seen that there is no catalytic activity for system conducted with only 1-hexene as monomer (entry 1). The opposite occurred on entry 2 for the system that used only ethylene as monomer. It suggests that this half-metallocene catalyst ([t-$BuNSiMe_2Flu]TiMe_2$) is active for ethylene polymerization, but not for 1-hexene polymerization. This result agreed with the finding of Intaragamjon et al. [58], who reported that this catalyst cannot proceed 1-hexene polymerization under the specified condition. It has been known that ethylene is the most reactive olefin [33], so it can react with itself for polymerization in the absence of any comonomer. Although 1-hexene was not reactive in its homopolymerization, it can be reacted in the system of copolymerization with ethylene (entry 3–5). Thus, this should be clarified in this finding that why 1-hexene was not active unless ethylene was introduced together in the system, even with the small amount of ethylene as seen for entry 5.

Table 4.1 Activities of system with various monomer concentrations

Entry	**Ethylene**[a] [mol/l]	**1-Hexene** [mol/l]	**Time** [s]	**Weight** [g]	**Activity**[b] (kg.polymer/ mol Ti .h)
1	0.0	0.6	475	–	–
2	0.6	0.0	475	0.2468	187
3	0.6	0.3	500	1.0596	763
4	0.6	0.6	248	1.4030	2037
5	0.6	1.2	326	1.9241	2125

[a]Ethylene addition into the system

[b]Copolymerization condition: Ti = 10 ⌈mol, Al/Ti = 400, temperature = 343 K, 349 kPa (50 psi) of ethylene pressure was applied

The mechanism of polymerization by metallocene catalyst system is reviewed here to explain the result. There are three main steps for completing the copolymerization (excluding chain transfer step), as shown in **Figure 4.1** [33]. The first step is the 'activation' of metallocene catalyst typically achieving via contact with an appropriate cocatalyst species (MMAO in this case). The second is the 'initiation' of the polymerization occurring as a result of the displacement of the anion and coordination of the monomer in the primary complex. In our study, this step seems to be a problem for obtaining the 1-hexene polymerization, since the ion-pairs still stay in their coordinated tightly. Therefore, only the strong reactive monomer like ethylene is able to insert in this coordination, and consequently displace the anion and make coordination with catalyst active site. This step can generate an available coordination site on the metal center, which provides high enough space for a large molecule, such as 1-hexene to coordinate with it in the next step. As the result, the final step that is the 'propagation' step will be the open competition between ethylene monomer and 1-hexene comonemer for insertion into the growing chain of polymer.

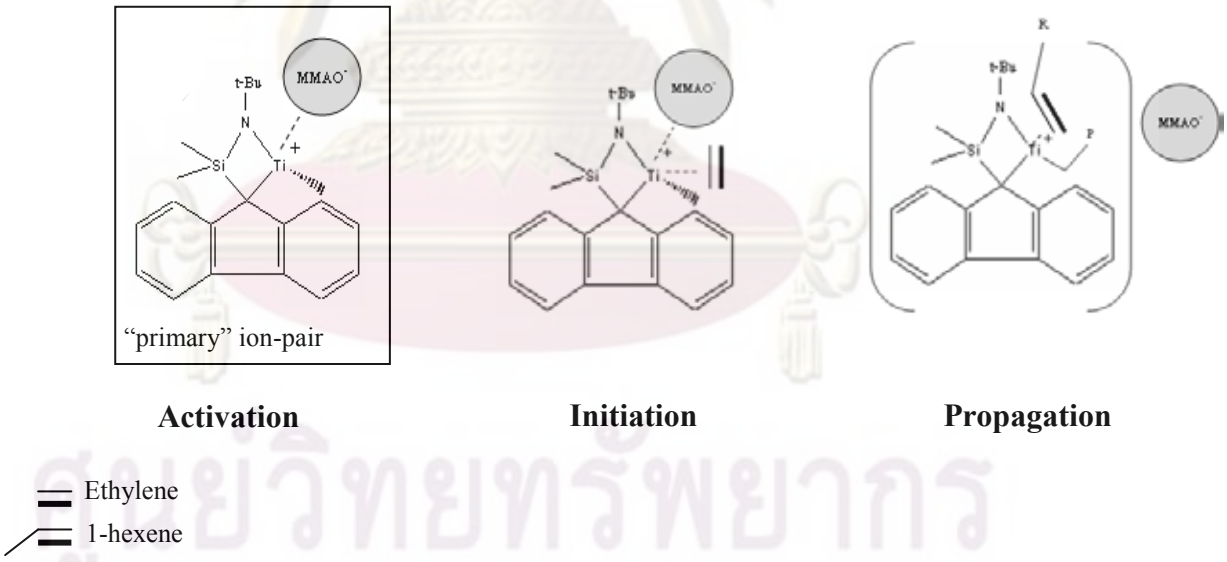

Figure 4.1 Schematic representation of copolymerization mechanism

As describe above, for this catalytic system, if ethylene was not introduced into the system first, 1-hexene would not be reactive for this half-metallocene catalyst even open structure. However, in many cases, 1-hexene can perform polymerization

by itself with some metallocenes such as iPr(Cp)(Flu)$ZrCl_2$ and En(Ind)$_2ZrCl_2$ [59] indicating that reactivities of α-olefin also depend on the catalyst structure [60].

4.1.2 Effect of the amount of 1-hexene on catalytic activity

In entry 3–5, introducing of 1-hexene into copolymerization enhanced catalytic activity higher than that of system without 1-hexene (entry 2). When the amounts of 1-hexene were increased, the catalytic activities were also increased. They increased pronouncedly when the amount of 1-hexene was raised from 0.3 to 0.6 mol/l. However, they gradually increased when the amount of 1-hexene was raised two times again from 0.6 to 1.2 mol/l. A comparison of activities is also shown in **Figure 4.2**.

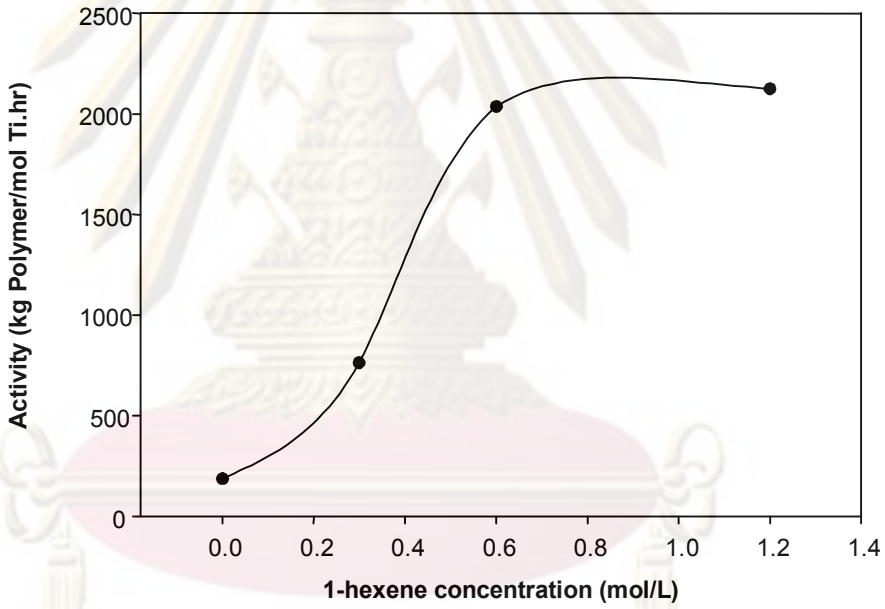

Figure 4.2 Activity profile with various 1-hexene concentrations.

It can be explained that the first range of increasing is because of comonomer effect in copolymerization behavior [61]. The chain structure of 1-hexene can increase the gap between the cationic active species and counter anion more separately in propagation step (**Figure 4.1**). Then, the propagation rate of polymerization can be raised leading to enhancing the activity of copolymerization. However, at 1.2 mol/l of 1-hexene concentration (entry 5), the anticipated activity can not be attained. This is because high excess of 1-hexene obstructed active sites of catalyst from reacting with ethylene monomer, and consequently reduce rate of ethylene insertion into the chain

of growing polymer. The explanation can be supported by polymerization time of entry 5, which was longer than that of entry 4. The longer polymerization time suggests that, in entry 5, the rate of ethylene consumption for polymerization was slower than that of entry 4. Although the rate of ethylene consumption in entry 4 was faster, activity or productivity of entry 5 was higher. This is because initial concentration of 1-hexene of entry 5 was higher then it can produce more product than entry 4 did resulting in high catalytic activity for the system.

4.1.3 Effect of the amount of 1-hexene on microstructure of copolymers

As seen in **Table 4.2**, the comonomer incorporations apparently increased with increasing the amount of 1-hexene in copolymerization. In this copolymerization process, which fixed the amount of ethylene addition and kept ethylene pressure constant during copolymerization, the incorporation of 1-hexene can be increased by two primary reasons. One is that enhancing the reactivity of 1-hexene or two, diminishing the reactivity of ethylene. It can be seen from **Table 4.2** that reactivities of ethylene decreased dramatically with increasing the concentration of 1-hexene in the system while reactivities of 1-hexene just slightly increased. So, it can be concluded that the initial concentrations of 1-hexene in the system have more effect on the reactivity of ethylene than itself. The increase of 1-hexene reactivity enables it to still incorporate continuously into the growing chain even at high concentration. The open structure of half-metallocene catalyst is one of the important factors that retains high reactivity of 1-hexene and encourages high comonomer incorporation. As compared with the works done by our group previously with normal metallocene, it has been found that with the same initial comonomer concentration in copolymerization, the obtained copolymer from those studies exhibited much lower comonomer incorporation than in this study [62,63].

Table 4.2 Comonomer incorporation and the reactivity ratios

Entry	Ethylene [mol/l]	1-Hexene [mol/l]	Incorporation		Reactivity[b]		
			E [mol%]	H [mol%]	r_E	r_H	$r_E r_H$
3	0.6	0.3	68.4	31.6	1.121	0.658	0.737
4	0.6	0.6	43.7	56.3	0.797	0.738	0.588
5	0.6	1.2	23.0	77.0	0.621	0.784	0.487

[a]Relative comonomer reactivities (rE for ethylene and rH for 1-hexene)

On account of the fact that the uniform comonomer incorporation is the key feature for producing lowdensity plastomer, which exhibited plastic and elastomeric behavior [64], the distribution of comonomer in the copolymers needs to be concerned in order to obtain plastomers with desired specification. The triad distribution for all copolymers obtained from ^{13}C-NMR is shown in **Table 4.3** Triad block of comonomer (HHH) was detected in samples having 1-hexene incorporation above 31.6% (entry 4, 5). It was also noticed from **Figure 4.3**, which showed 13C-NMR spectrum of the copolymers that the peaks between 39.5 and 42 ppm (proportional to the HHH triad) occurred obviously in the copolymer from entry 4 and 5. Nevertheless, the number of HHH triad was not converted directly from the area under these peaks. There are other peaks, which are more pronounced in the calculation. Therefore, the larger area of these peaks of entry 4 than entry 5 did not mean that entry 4 had more HHH triad than entry 5.

Table 4.3 Triad distribution of copolymer obtained from ^{13}C-NMR

Entry	**Ethylene** [mol/l]	**1-Hexene** [mol/l]	**EEE**	**EEH**	**HEH**	**EHE**	**EHH**	**HHH**
3	0.6	0.3	0.345	0.292	0.048	0.172	0.144	0.000
4	0.6	0.6	0.091	0.270	0.076	0.185	0.339	0.039
5	0.6	1.2	0.015	0.130	0.085	0.154	0.424	0.192

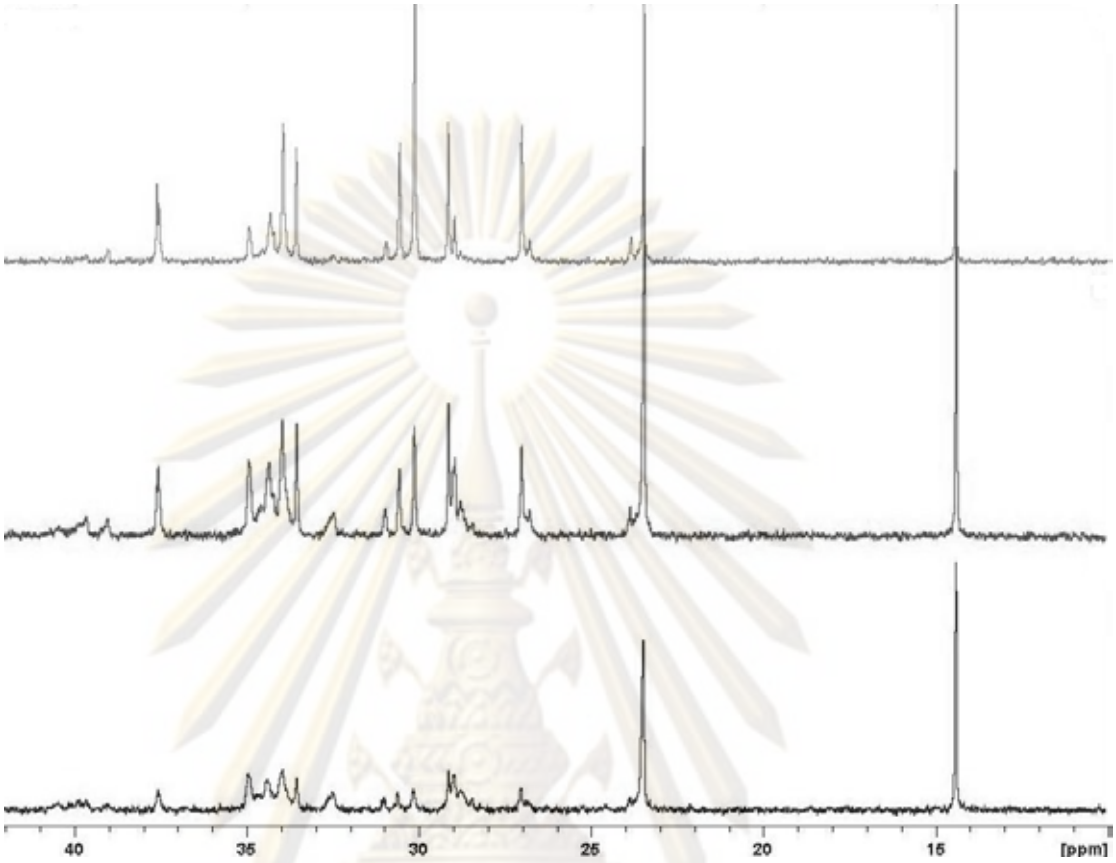

Figure 4.3 ^{13}C-NMR spectra of copolymers

The presence of HHH triad can imply that the good distribution of comonomer throughout the copolymer chain was interrupted at high incorporation of comonomer. Although the copolymers with high 1-hexene incorporation contain the block of comonomer, they are still not the block copolymer. It can be observed from the product of reactivity ratio (rErH), which is one of the parameters that can identify types of copolymer. A value rErH > 1 indicates a block copolymer structure and rErH < 1 reveals an alternating copolymer structure. Therefore, all the obtained copolymers are alternating copolymers having the rErH value being lower than 1. Once the alternating copolymers were obtained, it means the comonomers in their chain are distributed moderately well along the backbone, then shortening the average backbone sequence length for crystallization and therefore low crystallinity, including low density, would be gained. Thus, with these properties, the obtained copolymers are in closing proximately to be low-density plastomer. However, these copolymers

might not meet all properties required for the use in plastic industry because they probably lost completely the thermal properties.

As a result of the fact that disadvantages of alternating copolymer, which have been found by Hung et al. [65] that the polymer with a highly alternating sequence distribution did not exhibit any melting behavior. Based on the result, when the incorporations of comonomers increased, the obtained polymer tended to exhibit more highly alternating copolymer structure ($rErH < 1$). Therefore, they might lose the melting behavior at high level of 1-hexene incorporation. To prove that, melting temperatures of the obtained polymers were investigated by differential scanning calorimetry (DSC). From the investigation, it was found that only the sample from entry 2, which is the polyethylene sample, has the melting temperature (130°C) and the remaining samples cannot be found the melting temperatures. Thus, the losses of thermal properties existed in all obtained copolymers even the one that had low comonomer content (entry 3, 31.6%).

Copolymers were formed the gel-like structure as seen in **Figure 4.4** when the 1-hexene was introduced into the system, especially at the high level of incorporation. With this structure, it is obviously shown the character of amorphous material. Therefore, it accords with the results from ^{13}C-NMR and DSC that the obtained copolymers should not have the melting temperature.

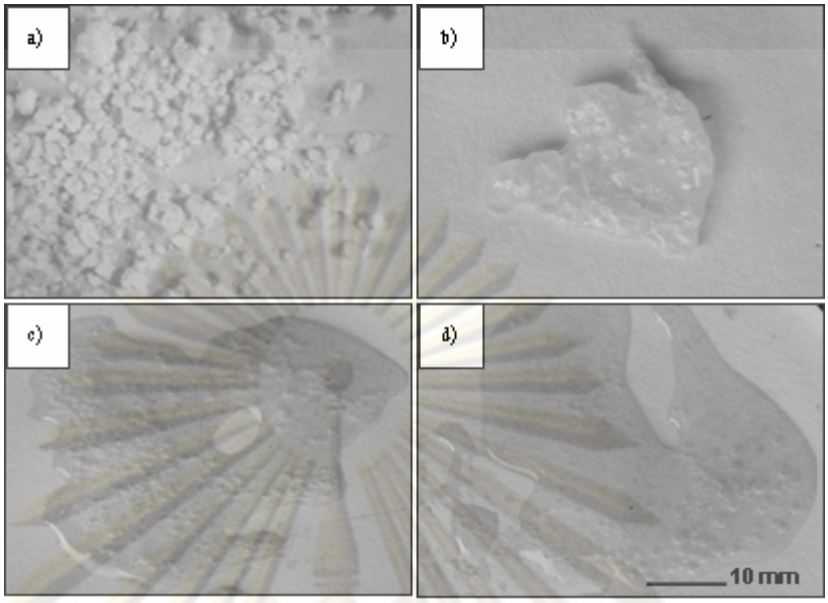

Figure 4.4 Digital photograph of copolymer with various 1-hexene contents a) 0%, b) 31.6%, c) 56.3% and d) 77.0%

4.2 A Comparative study on LLDPE/ silica composites synthesized by different copolymerization systems *(Part 2)*

In one aspect, the polymer obtained from the heterogeneous system can be comparable to polymer composites, and then the study focusing on the composite's properties was also conducted.

4.2.1 Catalytic activity

There were 3 copolymerization systems used for obtaining LLDPE in this comparison. The first was the homogeneous system (**HOMO**), where all materials: catalyst, MMAO, comonomer and solvent were in liquid phase (excluding ethylene introduced in gas phase). The second and the third (**HTRO-*ex*** and **HTRO-*in***) are the heterogeneous systems, which besides the materials used in the homogeneous system, silica in solid phase was also introduced into the system as a support. The different between **HTRO-*ex*** system and **HTRO-*in*** system is that, in **HTRO-*ex*** system, the *ex situ* impregnation method was used in preparation of support while in **HTRO-*in*** system the *in situ* impregnation was used instead. The *ex situ* was performed by impregnating MMAO onto silica, and then, washing and drying for 3 times before introducing it into the system during copolymerization. The *in situ* was performed simply by impregnating MMAO onto silica for a certain time after that introducing it

into the system during copolymerization without washing and drying. To ensure that that all MMAO used in the *in situ* impregnation was completely impregnated onto the support, a pretest for finding the proper amount of MMAO and the proper time in impregnation was performed as the method described by Wannaborworn [56].

It has already been known that for metallocene catalytic system, the heterogeneous reaction usually results in a low activity compared to the homogeneous reaction arising from one main reason that is the generation of active sites with lower propagation rates due to interactions with the support surface [66]. The problem of the probably strong interactions of species (catalyst or MMAO) on the support surface may be sorted out by introducing that species in liquid form into the system during reaction to compensate the one that was immobilized on the support surface with strong reaction. Then, the heterogeneous system along with *ex situ* impregnation (**HTRO-*ex***) conducted in this study had been added by the liquid MMAO during copolymerization to make the ratio of MMAO to metallocene catalyst (Al/Ti) about 400 equaling to the ratio used in the homogeneous system. To detect the amount of aluminium species in the silica support, ICP-OES technique was used. In **HTRO-*in*** system, the ratio of Al/Ti had already been fixed at 400 because, in this method, MMAO will never lose during immobilization process like *ex situ* impregnation, then the ratio of Al/Ti being constant until the time of copolymerization. The additional liquid MMAO is needless for this method.

Catalytic activities of all the systems with a titanocene catalyst were investigated during copolymerization of ethylene and 1-hexene, and then listed in **Table 4.4**. From this table, it can be seen that all activities are roughly similar at about 800 $kg_{pol}/(mol_{Ti}/hr)$. This means that the heterogeneous systems, which usually give a low activity, had been improved by addition of liquid MMAO as expected (**HTRO-*ex***). A little increase in activities of the heterogeneous systems compared with the homogeneous system may be come from some advantages of support when introducing it into the system, including decrease in reactor fouling and improvement in stability of the catalyst [67]. When comparing between both of the heterogeneous systems with different impregnation methods, it was found that the system with *in situ* impregnation (**HTRO-*in***) gave a slightly higher activity than the system with *ex situ* impregnation (**HTRO-*ex***). The differences between two impregnation methods are the amount of MMAO on the surface of silica supports during copolymerization and

the strength of interaction between MMAO and the silica surface. Hence, these two factors should be concerned in order to clarify the results.

Table 4.4 Polymerization activities for different systems

System	Reaction	Impregnation	Yields (g)	Activity [a] $kg_{pol}/(mol_{Ti}/h)$
HOMO	Homogeneous	-	1.261	**757**
HTRO-*ex*	Heterogeneous	Ex situ	1.311	**786**
HTRO-*in*		In situ	1.474	**885**

[a]Copolymerization condition: Ti = 10 μmol, Al/Ti = 400, temperature = 343 K, 50 psi of ethylene pressure was applied

As mentioned earlier that one disadvantage of the heterogeneous system is that the species on the support surface will generate active sites with a low propagation rate. Therefore, with the same amount of the overall active sites, which system has more active sites on the support surface than in liquid phase will give a lower activity than the others. However, for these two impregnation methods, it was the *in situ* impregnation method (**HTRO-*in***) that should posses more active species on the surface because there were no washing and drying in this method. Therefore, it reduced in the loss of MMAO during preparation and then, providing the higher amount of active species on the support surface. Whereas the *ex sit*u impregnation method (**HTRO-*ex***) which at first the support in the system was contacted with the same amount of MMAO, gave the finished support exhibited only about 60% of MMAO on it as investigated by ICP-OES technique.

The result that *in situ* impregnation provides better activity than *ex situ* impregnation contrasts with the presumption that the more the active species on the support surface, the less the activity for the system. Moreover, *in situ* impregnation even did not have liquid MMAO added into the system. Thus, the other difference between both impregnation systems that is the interaction of MMAO and the support surface should substitute for the first one to further explain about the deviation.

The stronger interaction of MMAO and support will cause lower activity for the system because with this strong interaction, MMAO is susceptible not to react

with metallocene catalyst during an activation step [68] (the position of each species can be seen in **Figure 4.5**). This interaction would occur more in *ex situ* impregnation as a result of the fact that with this method, MMAO bound to the support had to involve in washing and drying processes that making some lose during these processes, and then only some with sufficiently strong interaction to the support could exist until the end of the processes.

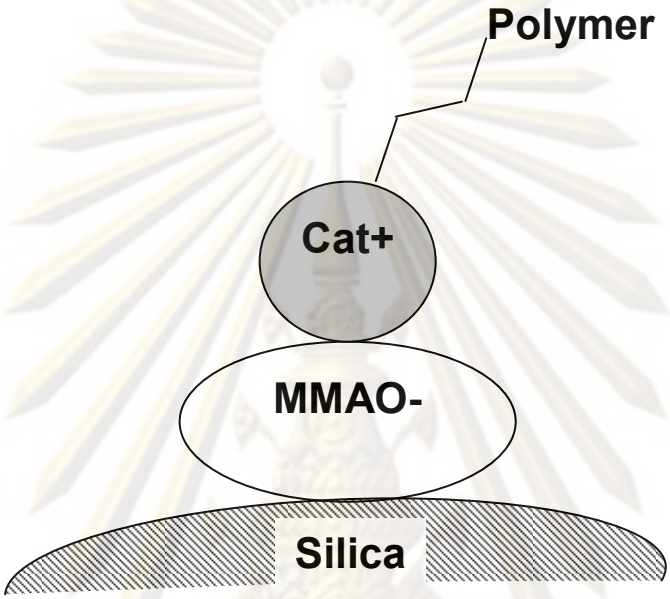

Figure 4.5 Conceptual model indicating the position of species in polymer composites.

To prove this hypothesis, some parameters obtained from TGA measurement, which normally indicate thermal stability, can also be used to indicate the degree of interaction in polymers and then used to trace back to the interaction of MMAO and support. **Figure 4.6** shows the weight loss profiles of the polymers obtained from different systems. From this, all three profiles were similar indicating to the normal profile of LLDPE. The temperatures at 5% and 10 % weight loss are shown in **Table 4.5**. The highest temperatures at 5% and 10% weight loss were observed in the polymer obtained from **HTRO-*ex*** system while **HTRO-*in*** system exhibited those temperatures nearly to the homogeneous system (**HOMO**). This suggests that, even polymers with the same type of filler (support) and also with nearly the same amount (about 7 %w) could differ in thermal stability due to the variation of internal interactions. The better thermal stability may derive from the support particles

interacting to polymer stronger through a tighten bond of MMAO and silica. Therefore, the polymer obtained from **HTRO-*ex*** system showed the better thermal stability than **HTRO-*in*** system because the first one has stronger interaction between silica and MMAO.

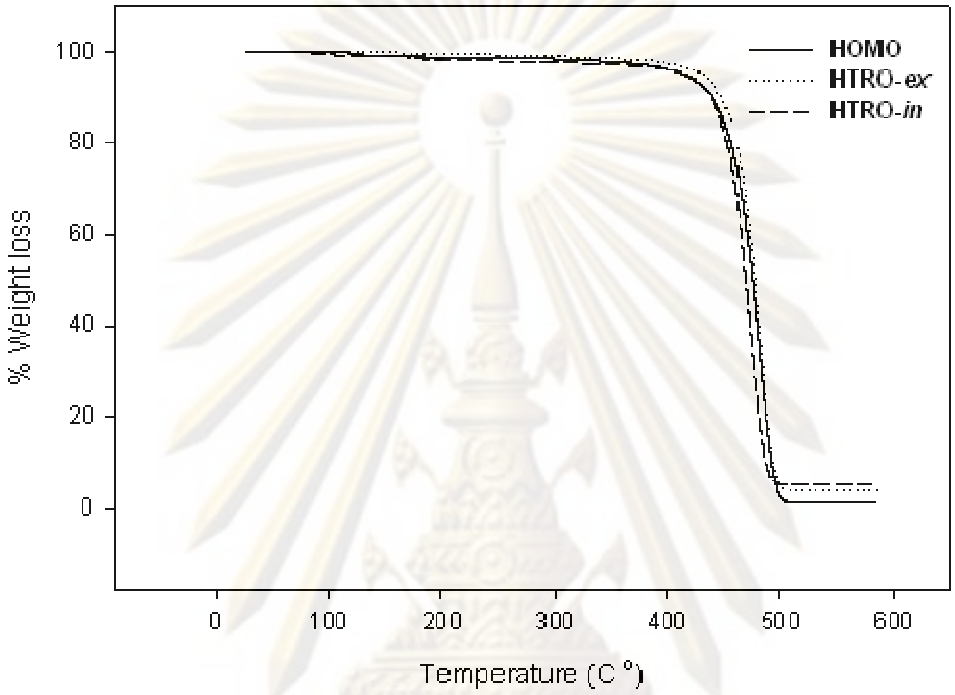

Figure 4.6 TGA curves of polymers for different systems.

Table 4.5 Temperature at a certain weight loss for various systems.

System	Temperature at weight loss (°C)	
	5%	**10%**
HOMO	414.6	439.6
HTRO-*ex*	433.6	451.7
HTRO-*in*	416.3	438.1

An XPS characterization is one of the methods that can reveal the chemical linkage between the support particles and the polymers [69], so it can be used to further investigate the interaction being discussed. With regard to binding energy values of Si in **Table 4.6** among two heterogeneous systems**,** the strong interaction would belong to **HTRO-*ex*** system due to the higher binding energy (B.E.) of Si. As a matter of fact, Si will decrease the binding energy when bound with the electron donating group because the density of the electron cloud around Si becomes lower (shielding effect). MMAO compound has been found that it presents some relatively Lewis acidity (electron withdrawing) when forming interaction [70]. On the other hand, it could increase the binding energy of Si when it interacts with Si through Si–O–MMAO bond. The stronger interaction between Si and MMAO in **HTRO-*ex*** system as presumption tends to draw MMAO closer to Si than in **HTRO-*in*** system. Therefore, MMAO more affected binding energy of Si in **HTRO-*ex*** system than in **HTRO-*in*** system and then caused binding energy of Si lower. The binding energies of O and C were also different among all the samples due to the variation of the chemical environment.

Table 4.6 Binding energy and elemental distribution on the surface of polymer measured by XPS

System	B.E. (eV)[a]			% atom content			C/O	C/Si
	Si	O	C	Si	O	C		
HOMO	0.0	532.4	285.0	0.0	9.6	90.4	9.4	-
HTRO-*ex*	103.1	534.0	286.5	0.8	2.3	96.9	41.6	129.2
HTRO-*in*	102.3	532.3	285.0	1.2	11.3	87.5	7.8	71.7

[a] Binding energy

In addition, **Table 4.6** also shows the amount of some elements in the polymer consisting of Si, O and C. The ratios of C to Si and O are also shown and will be used to explain the reasons for the previous results. The differences of C/O ratio among the systems can reflect the differences of mechanisms for producing the obtained polymer. The close C/O ratios of **HOMO** and **HTRO-*ex*** system indicated that two systems had the similar mechanism for growing polymer which differed considerably from that of

HTRO-*in* system observed from a huge difference of C/O ratio. This appears reasonable because the additional MMAO in **HTRO-*ex*** system may behaved like in **HOMO** system then, driving the heterogeneous system vaguely resembling the homogeneous system. When considering C/Si ratios, it was found that **HTRO-*ex*** system exhibited higher ratio than **HTRO-*in*** system almost two times. The reason is from the above mention that, in **HTRO-*in*** system, MMAO should cover the surface of silica with the higher amount than in **HTRO-*ex*** system. Therefore, the bare silica particles without polymer formed over them would have more in **HTRO-*ex*** system and consequently, lower ratio of C/Si was presented especially on the surface of polymer which has been detected by XPS technique.

4.2.2 Characteristic of polymer

Comonomer contents (1-hexene incorporations) and sequence distributions of each obtained polymer, which can influence on many properties of polymer can be investigated by ^{13}C-NMR technique. From **Table 4.7**, it was found that the 1-hexene incorporations of both heterogeneous systems (**HTRO-*ex*** and **HTRO-*in***) were significantly higher than that of the homogeneous system. This is due to good distribution of active sites influenced by the silica particles enhancing 1-hexene accessibility and depression in the reactivity of monomer in supported system [71].

Table 4.7 Characteristic of polymers from ^{13}C-NMR

Entry	Triad distribution[a]						Reactivity[b]			H[c]	T_m[d]
	EEE	EEH	HEH	EHE	EHH	HHH	r_E	r_C	$r_E r_C$	(%mol)	(°C)
1	0.611	0.229	0.034	0.126	0.000	0.000	*1.323*	*0.000*	*0.000*	**12.6**	112
2	0.533	0.173	0.036	0.154	0.103	0.002	*0.946*	*1.311*	*1.240*	**27.0**	126
3	0.452	0.230	0.048	0.159	0.108	0.003	*0.754*	*1.208*	*0.910*	**25.6**	122

[a] Examined by ^{13}C-NMR

[b] Relative comonomer reactivities (*rE* for ethylene and r*H* for 1-hexene)

[c] 1-hexene incorporation

[d] Melting temperature

The ethylene reactivities showed in **Table 4.7** agree with the suggestion as seen that these values of both heterogeneous systems were less than that of the homogeneous system. The product of reactivity ratio ($r_E r_H$) is one of the parameters which can identify types of copolymer with: a value *rErH* > 1 indicating a block copolymer structure, *rErH* < 1 indicating an alternating copolymer structure and *rErH* = 1 indicating a random copolymer structure. Therefore, the obtained polymers from the heterogeneous systems exhibited block copolymer properties whereas the one from homogeneous system exhibited highly alternating copolymer properties. Melting temperatures (T_m) of polymer obtained from both of the heterogeneous systems were roughly equal but higher than that obtained from the homogeneous system even higher 1-hexene incorporations. This is because the silica particles acted as a nucleating agent during polymerization; consequently, they increase the crystallinity of polymer, and then raising the melting temperature of polymer [61,72] for both of the heterogeneous systems. Thus, it can be concluded from these results that synthesis of LLDPE with the various phase reaction systems affect the 1-hexene incorporation, the molecular structure and melting temperature of the obtained polymer whereas the different impregnation methods do not.

Images of polymer morphologies created from scanning electron microscope (SEM) are shown in **Figure 4.7**. It can be observed that the polymer obtained from **HOMO** system look totally different from both of the heterogeneous systems. However, the polymers obtained from the heterogeneous systems are also exhibited a small difference in morphology. This is may be due to the different interaction of the silica particles and polymer inside the polymer matrix. The little more agglomeration of particles is found in the polymer obtained from **HTRO-*in*** system. The low interaction between MMAO (polymer part) and silica particles in **HTRO-*in*** system should take this responsibility because silica particles have a more chance of agglomeration when they have less interaction with some other molecules else.

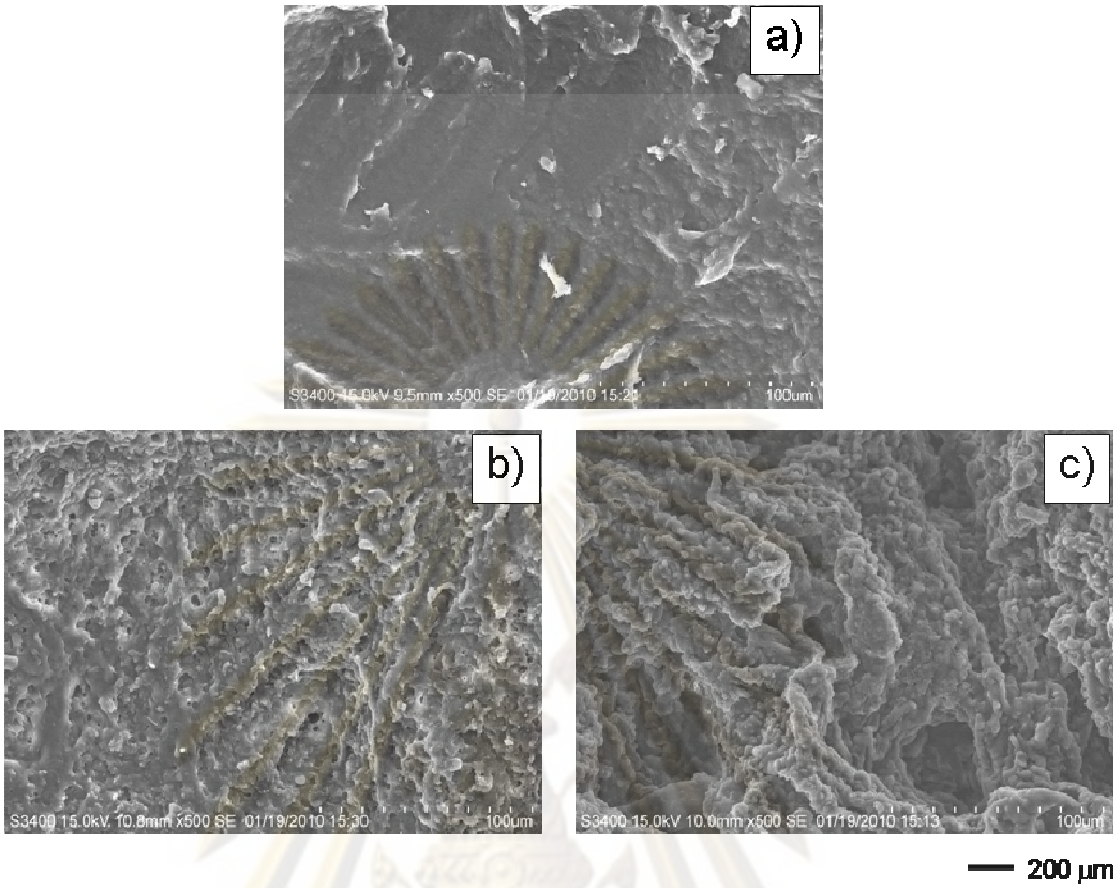

Figure 4.7 Morphologies of the polymers obtained from the different systems a): **HOMO**, b): **HTRO-ex** and c): **HTRO-in**

4.3 Modification of supports by gallium *(Part 3)*

To improve the supports for performing in the catalytic system, gallium was brought for this purpose. Gallium that affected directly the support properties also affects the activity of the system. Therefore, roles of gallium during the modification step and copolymerization were investigated here.

4.3.1 Characterization of supports

In this study, two kinds of silica with different pore diameters were used as a supporting material in copolymerization. By investigating their porous properties with N_2 physisorption, they were classified according to the size of pores. Large pores (LP) denote Q-50 silica which had an average pore diameter of 380 Å and small pores (SP) denote P-10 silica which had an average pore diameter of 170 Å. Besides using both silicas in pristine condition, they were modified by gallium for improving some specific properties prior to use. Thus, there were four kinds of supports used in copolymerization. The specific surfaces of them were 70.9, 216.8, 68.8 and 169.7 m^2/g for LP, SP, LP-Ga, and SP-Ga, respectively. The XRD patterns (not shown) for all supports were similar exhibited only a board peak between 20^o and 30^o, as seen typically for the conventional amorphous silica. No XRD peaks of gallium were observed after impregnation due to its highly dispersed form.

4.3.2 Catalytic activity of copolymerization

4.3.2.1 Effect of pore size of silica supports

In **Table 4.8, Entry 1** and **entry 2** were conducted to investigate the effect of support pore size on catalytic activity of copolymerization. It can be seen that the large pore silica (**entry 2**) exhibited higher catalytic activity than that of the small pore silica (**entry 1**). Although most MMAO is presumed located mostly at the external surface [56], some is located at the internal surface too. This can be observed from the effect of pore size of the silica support which still existed in this comparison. To grasp the effect of pore size, the internal diffusion resistance needs to be considered. In general, the supports with small pore size result in poor intra-pellet diffusion efficiency and slow transportation of reactants and products due to strong diffusion resistance [73], contrasting with the supports with large pore size which are able to diminish the diffusion resistance by their large pores. Then, copolymerization conducted along with large pore size support can give higher catalytic activity than

that with small pore size support. Another parameter, which provides compelling evidence that the diffusion resistance was exist in the system, is the copolymerization time of the systems. From **Table 4.8**, it can be obviously seen that copolymerization time of the large pore silica system (**entry 2** and **4**) was shorter than that of the small pore silica system (**entry 1** and **3**) indicating that propagation rate of system with the large pore silica was higher, due to monomer and comonomer being able to reach to the catalytic active sites more easily even located inside the pores. In addition, silica with smaller diameters could display the lower catalytic activities probably due to the higher probability of formation of bimolecular species as described by Silveria et al. [66].

Table 4.8 Catalytic activities in ethylene/1-hexene copolymerization with different supports.

Entry	Supports	Time[a] (s)	Yields (g)	Catalytic Activity[b] (kg polymer / mol Ti .h)
1	SiO_2 / (SP)	233	0.8681	1341
2	SiO_2 / (LP)	170	0.7941	1682
3	SiO_2 / (SP-Ga)	186	0.9919	1920
4	SiO_2 / (LP-Ga)	140	0.7632	1893

[a] Time when ethylene addition into the system = 0.018 mol
[b] Colymerization condition: Ti = 10 μmol, Al/Ti = 400, temperature = 70°C, 50 psi of ethylene pressure was applied

4.3.2.2 Effect of gallium modification of silica surface

To investigate an effect of gallium as modifying agent for silica support, comparisons were drawn between modified and unmodified supports on both types of silica. As seen from **Table 4.8** (**entry 2** vs **entry 4**, **entry 3** vs **entry 5**), gallium modification can increase catalytic activity in both types of silica. It has been known that adding gallium into silica surface normally increases acidic sites to the silica support [74]. These sites are required to activate metallocene catalyst to be an active species in supported system. Many inorganic supports which possess the strong Lewis acidic property, such as Al_2O_3 and $MgCl_2$ have been used as support for this purpose [75]. For silica, directly using as a support for metallocene catalysts preparation resulted in inactive catalysts formation [76]. However, in this method, MMAO took

charge of main activating agent as usual in metallocene catalyst system and gallium can assist in the activation by increase Lewis acidity in support as mentioned. Furthermore, gallium can be anchored on the surface of silica, thus lower interaction between active sites and support. The result of higher catalytic activity by gallium modification accorded with the finding of Campos et al. [77], which found that introducing gallium into supports can improve the ability of the supports to immobilize metallocene, and then enhancing the catalytic activity of the systems.

When comparing the activities of system with gallium modification on both silica types, it revealed that the small pore silica showed slightly higher catalytic activity. This was opposite to the result of activities before modifying the support. This is because the small pore silica has higher surface area than that of the large pore silica. Then, gallium modification, which mainly affected on the surface properties of support, can more efficiently influence catalytic behavior in higher surface area support than the lower surface area support. Therefore after modification, the small pore silica would give the higher activity than that of the large pore silica due to higher surface area.

4.3.3 Characterization of copolymers

The triad distribution for all copolymers investigated by ^{13}C NMR is also shown in **Table 4.9.** The triad block of comonomer (HHH) was not detected for all samples. This suggests that the good distribution of comonomer throughout the copolymer chain existed in the systems. In addition, the products of reactivity ($r_E r_H$) of some samples (**entry 3**) also showed the characteristic of random copolymers ($r_E r_H$ >1), and the rest of them showed the typical alternating copolymer character ($r_E r_H$ < 1).

Table 4.9 Properties of the obtained copolymers

Entry	Support	EEE	EEH	HEH	EHE	EHH	HHH	r_E	r_C	$r_E r_C$	% H
1	SiO_2 / (SP)	0.367	0.269	0.041	0.156	0.166	0.000	*0.605*	*1.603*	*0.969*	32.2
2	SiO_2 / (LP)	0.359	0.272	0.046	0.163	0.159	0.000	*0.583*	*1.497*	*0.873*	32.3
3	SiO_2 / (SP-Ga)	0.410	0.246	0.038	0.149	0.157	0.000	*0.685*	*1.618*	*1.108*	30.6
4	SiO_2 / (LP-Ga)	0.422	0.280	0.039	0.159	0.099	0.000	*0.724*	*1.019*	*0.737*	25.8

4.3.3.1 Effect of pore size of silica supports

It can be observed from **Table 4.9** that both pore size silicas produced copolymers with nearly the same incorporations of 1-hexene (**Entry 1** and **2**). In general, the large pore silica should supply more comonomer for propagating the copolymer chain than the small pore silica due to lower diffusion resistance within the pores. However, another factor which can influence on the incorporation of comonomers is the surface area of the supports. Regarding to surface area, the support with large surface area is expected to produce copolymers with high incorporation of comonomer as a result of more space between active sites dispersed on its surface area compared to the support with smaller surface area, as seen in **Figure 4.8**. Then, the small pore size silica with higher surface area would probably result in high comonomer incorporation with this effect. Therefore, from the result that showed a roughly equal amount of 1-hexene comonomer incorporation for two different textures of silicas indicated that both effects (pore size and surface area) have a profound impact at the same level upon the incorporation of 1-hexene in the obtained copolymers.

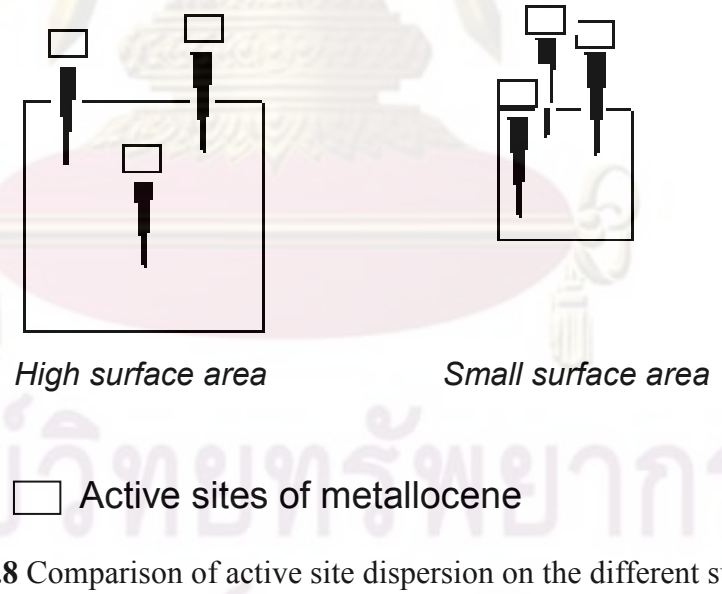

Figure 4.8 Comparison of active site dispersion on the different surface areas

4.3.3.4 Effect of gallium modification of silica surface

Comparing between **entry 1** and **3** alongside **entry 2** and **4**, we found that when modifying surface of silica support with gallium, the 1-hexene incorporations were decreased in both types of silica. This can be explained by the effect of surface

area. Since both silicas had lower surface area through modifying procedure by gallium as follow; in large pore 70.9 to 68.8 m^2/g and in small pore 216.8 to 169.7 m^2/g. Although incipient-wetness impregnation used in the modification is the easiest method of introducing a metal precursor, it results in the precipitation of small particles of the salt onto the support surface [78]. Therefore, the decrease in the surface area may be due to the partial blockage of pore by excess gallium nitrate. As seen from **Figure 4.9**, the excess substances more seriously affect the decrease in surface area of the small pore silica than the large pore silica because the small pores can be blocked by the deposit easier compared with the large pore. Then, after modification with gallium, the significant decrease in surface area occurred in the small pore silica, contrasting with in the large pore silica, which only the slight decrease occurred.

The decrease in 1-hexene incorporation in the copolymer obtained from both silicas after modification by gallium was opposite to the decrease in surface area. The significant decrease was observed for the large pore silica instead. The reason for this can be explained as seen in **Figure 4.9**. The active sites with high enough space for high 1-hexene incorporation were indicated in the figure by an empty filled square (□) while a blackened square (■) indicated the active sites with insufficient space for high 1-hexene incorporation. It can be seen that high space sites (□) in the large pore silica were decreased noticeably after modification whereas the number of the high space sites in the small pore silica remained the same. The high space sites in the small pore silica always located outside the pores, and therefore they can not be affected by the deposit of excess gallium inside the pores. On the other hand, in the large pore silica, these sites sometimes located inside the pores then the deposit on the wall of pores can hinder them from being reached by a large size molecules especially 1-hexene comonomer in copolymerization. Hence, the incorporation of 1-hexene in the large pore silica system decreased significantly after the support was modified by gallium as observed in the results.

In addition, this proposed model (**Figure 4.9**) can explain the previous results reported by our research group that sites with no or low 1-hexene incorporation rates (insufficient space site, ■) were more prevalent at short polymerization times [79]. It can be seen from the model that the said sites usually located inside the pore, so therefore at initial time of polymerization it still had an impact in polymerization. After the long period of polymerization the supports were covered by the growing

chain of polymer and then, hindered the (co)monomer to reach inside of pores, thus decreasing the impact of the sites located inside the pores in polymerization. So if the polymerization time was longer, it would found the fraction of polymer producing from sites with no or low 1-hexene incorporation rates lower. However, the important point one has to keep in mind when using this model is that the multigrain model [80] should be regarded together not the fragmentation of catalyst model. In this study, all copolymerization times were not long enough for particles to have hydraulic force pressing on them, and then, the multigrain model would be reasonable for use.

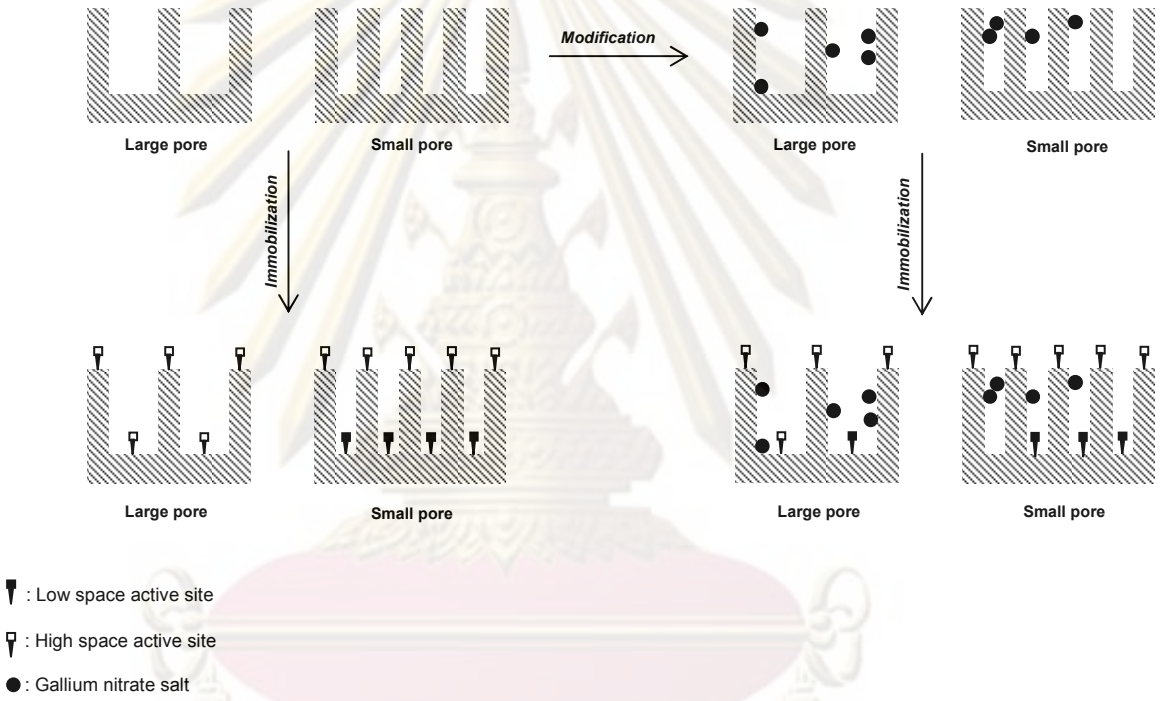

Figure 4.9 Conceptual model for impact of pore blockage on supports with different pore sizes.

The model in **Figure 4.9** also indicated that different types of catalytic sites are present in these catalysts, according to the findings of Kumkaew et al. [79] which suggested that pore sizes can influence the type of catalytic sites present in the supports. The various sites derive from different environments which mainly point to steric hindrance as seen in the model. The hindrance is not just to the monomer to attack the site but also to MMAO in forming cocatalysts-counterion fit and salvation which play a significant role in the structures and energetics of the ion pairing hence, catalytic activities and selectivities as proposed by Lanz et al. [81]. Therefore, the

alteration of selectivities by different pore sizes may be one of the reasons for the change in 1-hexene incorporations.

Figure 4.10 DSC endotherms of LLDPE synthesized with various SiO_2 supports a) SP, b) LP, c) SP-Ga and d) LP-Ga

To support that the copolymers were obtained from different catalytic sites, one simple technique that can be used for this purpose is the differential scanning calorimetry (DSC). As known that DSC endotherms were influenced by many factors such as the crystallinity and molecular weight of polymer, then being difficult to identify each peak occurring clearly. However, they could brief necessary information about characteristic of catalyst as recommended by Kumkaew et al. [79] that DSC of nascent polymer may provide information on heterogeneity of supported polymerization catalysts. From **Figure 4.10**, it can be seen that all the copolymers obtained from the supported system exhibited several DSC endoterm peak (not obviously seen in LP-Ga) indicating multiple types of catalytic sites. Another point

illustrating in **Figure 4.10** is that the DSC endoterms of copolymer obtained from Ga-modification silica system (c, d) exhibited broader peak than the unmodified one (a, b). This may be implied that silicas after modification by gallium have a greater degree of heterogeneity in catalytic sites than before modification. Therefore, it can be concluded that gallium addition into silica also change the nature of catalyst and provide more heterogeneity in catalytic sites to supported system.

4.4 Effect of method for preparation of supported catalysts *(Part 4)*

In preparation of supported catalyst, there are many important things to be concerned, for example to keep the efficiency of catalyst when it was immobilized onto the supports, to reduce the adverse effects of support in copolymerization. Therefore, a variety of methods for preparation of supported catalyst were conducted to examine their effects on the copolymerization.

4.4.1 Characteristics of support

After modifying support by tetrachlorosilane ($SiCl_4$), crystallization properties and surface properties of the support was investigated by using X-ray diffraction spectroscopy (XRD) and N_2 physisorption respectively. It was found that the support after modification still exhibited an amorphous structure as same as before modification observing from no peaks appearing on XRD pattern of the support (not shown). This means that addition of $SiCl_4$ was not changing the crystallization property of the support and $SiCl_4$ was dispersing well due to no peaks of chlorine (Cl) appearing as well. The surface area of the modified support ($SiO_2/SiCl_4$) decreased compared with the unmodified one (249 to 229 m^2/g) because of pore blockages derived from the non-reacted excess $SiCl_4$.

4.4.2 Characteristics of catalysts on the support

The finished catalyst from all 5 methods were investigated by inductive coupling plasma spectroscopy (ICP-OES) to find the amount of titanium and aluminium on the support, which is the composition of catalyst and MMAO respectively.

Table 4.11 The amount of titanium (catalyst) and aluminium (MMAO) investigated by Inductive Coupling Plasma Spectroscopy (ICP)

Run	Support	**Method**	Immobilization		Ti (%w)	Al (% w)
			Step 1	Step 2		
1	SiO_2	**C1**	Catalyst	-	0.596	0
2	$SiO_2/SiCl_4$	**A1**	MMAO	-	0	18.14
3		**A2**	MMAO	Catalyst	0.334	12.48
4		**B1**	MMAO + Catalyst	-	0.200	18.35
5		**C1**	Catalyst	-	0.586	0
6		**C2**	Catalyst	MMAO	0.192	14.30

From **Table 4.11**, it was found that by using method **C1**, which immobilized catalyst directly onto the support, the amount of catalyst in the modified support ($SiO_2/SiCl_4$) was nearly the same as in the unmodified one. It suggests that $SiCl_4$ did not help the support immobilize the amount of catalyst higher. Adding MMAO prior to catalyst (**A2**) reduced the ability of the support to hold the catalyst compared with method **C1**. Method **B1** provided the low amount of catalyst on the support. This is due to competition between catalyst and MMAO for immobilizing onto the support. When adding MMAO to the support after the catalyst had been completely immobilized onto the support (**C2**), it decreased the amount of catalyst (compared with **C1**) indicating to the leaching of catalyst by MMAO [82].

4.4.3 Catalytic activity

Catalytic activities of all the systems used the support prepared from the various methods are shown in **Table 4.12**. During copolymerization, MMAO was introduced into the system for enhancing the ability to activate the catalytic active sites. The overall ratio of MMAO to catalyst is 400 (Al/Ti). For support without catalyst (**A1**), the catalyst in liquid form will be introduced instead during copolymerization.

Table 4.12 Activity of copolymerization using catalysts from various preparation methods

Run	Support	**Method**	Immobilization		Polymer yield (g)	Activity (kg polymer / mol Ti .h)
			Step 1	Step 2		
1	SiO_2	**C1**	Catalyst	-	0.063	60
2	$SiO_2/SiCl_4$	**A1**	MMAO	-	1.638	1966
3		**A2**	MMAO	Catalyst	0.239	412
4		**B1**	MMAO + Catalyst	-	0.489	1405
5		**C1**	Catalyst	-	0.149	146
6		**C2**	Catalyst	MMAO	n.d.	0

4.4.3.1 Effect of support modification

To investigate the effect of silane ($SiCl_4$) modification to the support on activity, run 1 and run 5 will be compared. It was found that the modified support (**run 5**) gave higher activity than the unmodified one (run 1). This is because active sites on the modified support were linked with the support surface through the silane molecule which acted as a linkage (**Figure 4.9**) and consequently less interaction between them [2]. In addition, this structure favors the insertion of monomer into the reaction center due to less steric hindrance, and then enhances activity for the system.

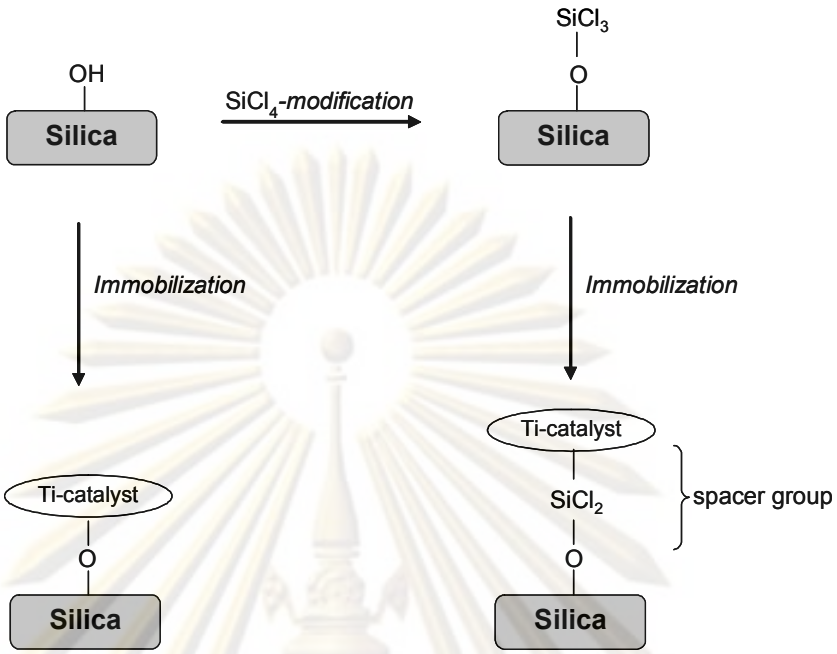

Figure 4.9 Comparison of Ti-catalyst on various supports (modified and unmodified)

4.4.3.2 Effect of catalyst phase

In this study catalyst was introduced into the system in two different phase forms: liquid phase for run 2 and solid phase as immobilized on the support for run 1, 3-5. Run 5 will be used to represent the effect of solid phase of catalyst because there was only catalyst species on the support (unmodified) whereas, in the others, catalyst was presented with MMAO. It was found that the catalyst which was immobilized (run 5) onto the support exhibited lower activity than the catalyst which was introduced into the system in liquid form (run 2). The main reasons for this should be the generation of active sites with lower propagation rates due to interactions with the support surface and the inaccessibility of MMAO to the catalyst hindering its activation [66]. For the second reason, on the other hand, the inaccessibility of the catalyst to MMAO should be the problem for run 2 which the liquid catalyst had to reach to MMAO immobilized onto the support as well. Thus, some researches indicated that this problem usually affect the catalyst supported system which MAO is the species fixed in the support. For example Ko et al [82] has found that introducing liquid catalyst into the MAO-immobilized support caused the activity even lower than introducing liquid MAO into the catalyst-immobilized support. However, the

difference between the mentioned study and this present study, beside the type of metallocene catalyst, is that the type of support. The first one used the zeolite with a highly porous structure as a support while the second use the amorphous silca as a support. Thus, with highly porous structure, the most of any species fixed in the zeolite support had to be located inside the pores, and then the rate of diffusion through the pores of the liquid species could greatly influence the activity of the system. Owing to this presumption, the system which a smaller molecule is in liquid form will raise the rate of diffusion higher than a larger one, and consequently give higher activity. Therefore, the above mentioned study is to show that the system which MAO is in liquid form would give higher activity than the system which catalyst is in liquid form due to the smaller size of MAO, as appeared in its result. However, in this study, the result was in contrast since the amorphous silica support which the most of species fixed in it is not located inside the pores like in the porous material, and then the rate of diffusion of liquid species exert a slight influence on the activity of the system. Hence, the lower activity as observes in this result mainly comes from the difficulty in generating the active sites due to the strong interaction with the support not the inaccessibility into the immobilized species.

4.4.3.3 Effect of preparation method

Supports on which both catalyst and MAO were immobilized by various preparation methods were brought into copolymerization in making comparison for effect of preparation methods (run 3, 4 and 6). It was found from **Table 4.12** that the activity of B2 catalyst was about 3 times higher than that of A2 catalyst, whereas for C2 catalyst, there was no activity. From the ICP detection (**Table 4.11**), it can be found that the titanium indicated to titanocene complex catalyst still existed on C2 catalyst, nevertheless decreasing after MAO immobilizing. Therefore, the inactive system was more likely to come from the inactive catalytic sites not the lack of catalytic sites.

The MMAO addition resulted in the catalyst leaching since MMAO would interact with the catalyst, and then reducing the interaction between the catalyst and the support whether it activate the catalyst into the active form or even just bound together without activation. Therefore, fewer catalytic sites were on C2 catalyst as proven by ICP technique. However, in this study the calculation of activity value was based on the real amount of catalyst (Ti) in the support. Thus, fewer catalytic sites

were not involved directly to the reduction of the specific activity but, nevertheless this can imply that if the leaching catalytic sites had been immobilized on the support with the weak interaction, the remained catalytic sites would have been fixed with the strong interaction with the support. These strong sites may be derived from the direct linkage between the catalyst and the bare silica surface without $SiCl_4$ coverage which was come from incomplete modification [83].

Besides strong interaction, catalyst deactivation is usually one of the problems faced when immobilized catalyst onto the support, and then it causes the activity reduction. The deactivation can break out during both support preparation and copolymerization. In **Figure 4.10**, it shows two plausible way of catalyst deactivation. **Figure 4.10 a)** is the deactivation formed when two catalyst molecule are so closed together and consequently generate the bond between them. Although this has been previously described arising more frequently in the catalytic homogeneous system [67], it also arise in the supported system if the active sites are not separated far enough, then the time taking for two adjacent active sites on the surface to diffuse to encounter distance shorter than the reciprocal of turn-over-rate, and therefore the supported catalyst decayed further [84]. Besides the adjacent two active sites that can form the deactivation species, the isolated single molecule can also form the deactivation species in case it links to the support surface by more than one bond as seen in **Figure 4.10 b)**. Another drawback of directly immobilizing catalyst onto the support is proposed by Xu et al.[85] that the oxidation state of the metal center atom (Ti) would be varied then making the catalyst deactivated. All the above reasons would therefore badly affect the activity of the catalyst prepared by method **C2** as seen in the result.

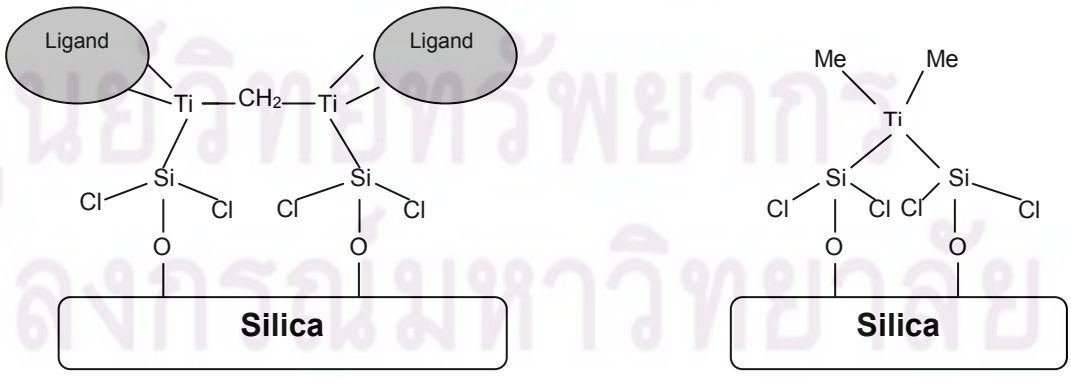

a) Bi-molecular **b) Bi-linkage**

Figure 4.10 Deactivation of catalyst on silica

A2 catalyst gave higher activity than **C2** catalyst due to the MMAO immobilized on the support beforehand. MMAO on the surface could increase the gap between the support and the catalyst then being easily accessible to monomer and also generate active sites on the surface [67], as shown in **Figure 4.9**. As known that generation of active sites is more efficient in liquid phase, hence method **A2** was superior to method **C2** due to catalyst being introduced in liquid form. However method **A2** was still inferior to method **B2** since, in method **B2** both MMAO, and catalyst were in liquid form. In method **C2** and **A2**, the generation had to be conducted when the catalyst or MMAO had been fixed to the support, and then the diffusion rate and side reactions are also influence on this. In addition, method **A2** may generate the sites that had been not active as seen in **Figure 4.11 b)**. These sites may be not activated even during copolymerization. Therefore, the activity of **A2** catalyst was lower than that of **B2** catalyst which more catalytic sites had been generated since immobilization step. One observation that the catalytic sites has been changed into the another form is the color of the finished catalyst. As observed, **B2** catalyst was grey contrasting to **A2** and **C2** catalyst with yellow color like the pristine titanocene catalyst's color.

The structure of catalyst prepared by method **B2** is difficult to predict because there were two species adsorbed in the same time. However, from the results that indicated that it was the best system giving the highest activity. Therefore, a model to represent the plausible structure will be based on the benefit of being present of two species together as seen in **Figure 4.12**. From this figure, it can be observed that catalyst having been activated still existed on the support without deactivation since it is probably stabilized by the ion of MMAO which also have been converted into the ion form during activation process, and then it enhances the activity of the system.

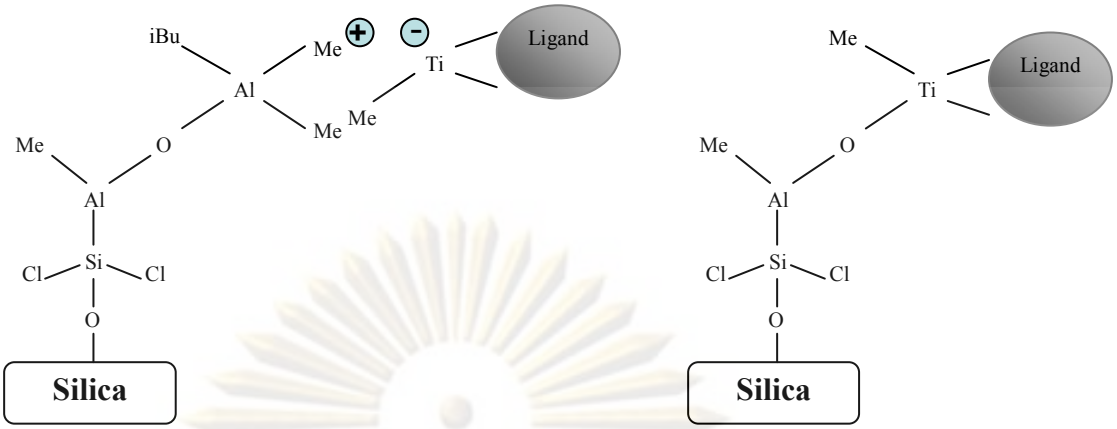

a) ion pair b) covalent bond

Figure 4.11 Linkage between silica support and catalyst through MMAO

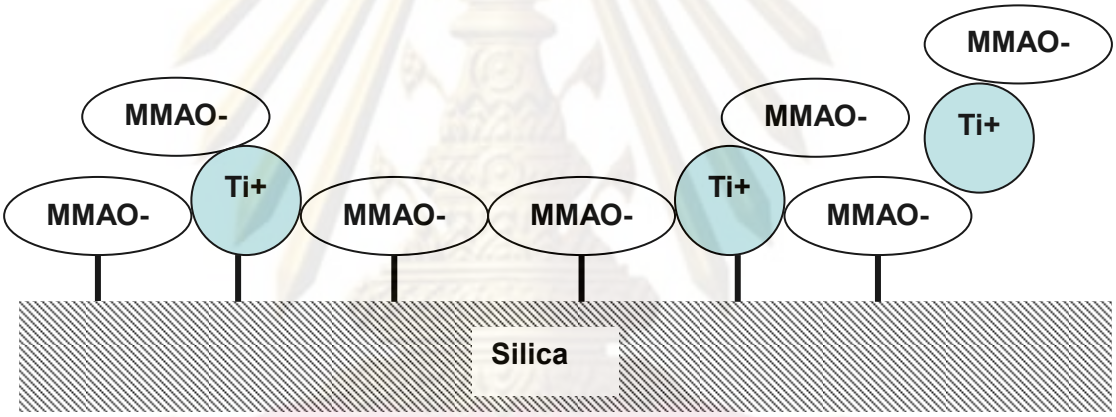

Figure 4.12 Structural model of catalyst and MMAO on the support

To prove that the amount of active sites on the support prepared by various methods will be varied, a test done by conducting copolymerization alongside each finished catalysts without adding liquid MMAO is needed. By this test, the copolymerization success was only due to the active sites having been fixed on the support. From the results in **Table 4.14**, it was found that only the catalyst prepared by method **B2** can be obtained even though the activity significantly decrease. Therefore, this can support that method **B2** provided the highest amount of active sites to the finished catalyst then enhancing the activity higher than the other methods and also proved that the generation of active sites in liquid phase is the best as been in method **B2**.

Table 4.14 Activity of copolymerization using catalysts from various preparation methods (no addition of MMAO)

Run	Support	**Method**	Immobilization		Polymer yield (g)	Activity (kg polymer / mol Ti .h)
			Step 1	Step 2		
6	$SiCl_4$	**A2**	MMAO	Catalyst	n.d.	0
7		**B2**	MMAO + Catalyst	-	0.0953	123
8		**C2**	Catalyst	MMAO	n.d.	0

4.4.4 Characteristics of polymer

4.4.4.1 Morphology

Polymers obtained from method **B2** and **A2** exhibited slightly different morphologies (**Figure 4.13**). This was due to the variation of activity making alteration to the chain propagation rates of polymers. This rate can affect hydraulic force that press on silica until it was fragmented during polymerization. The pattern of fragmentation is one of the factors that can tailor the morphology of polymer. Therefore, the variation of activity between method **B2** and **A2** may cause the difference of the fragmentation pattern in polymer and then providing their obtained polymers with different morphology. .

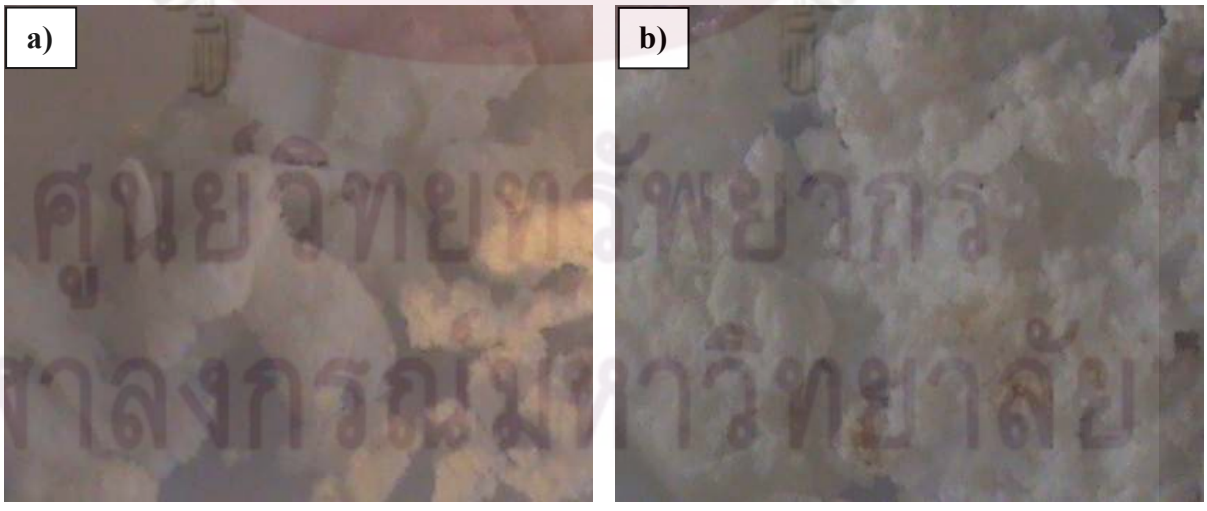

Figure 4.13 Morphologies of polymers obtained from different method a) A2 and b) B2

4.4.4.2 Polymer structure and property

It can be observed from **Table 4.15** that no 1-hexene incorporation in the polymer obtained from method **C1** for both modified and unmodified silicas. Method **C1**, as known, was to directly immobilize catalyst onto the surface, making the active sites generated too close to silica then leaving low space for monomer reaching. Therefore, it was difficult for large monomers including 1-hexene ($CH_2=CH_2CH_2CH_2CH_2CH_3$) in this case to reach to the active sites. The obtained polymer was due to composing only the small molecule of ethylene ($CH_2=CH_2$). Melting temperatures of both polymers (130.5 and 132.0 °C) also indicated to the property of high density polyethylene [1] (T_m=130-137 °C). Hence, the copolymerization of ethylene and 1-hexene with this half-metallocene/MMAO catalyst using impregnation method **C1** can not prepare LLDPE.

Table 4.15 ^{13}C-NMR and DSC analysis of polymer

Run	Support	**method**	**Triad distribution**[a]						**%H** [b]	**T_m**[c] (°C)
			EEE	*EEH*	*HEH*	*EHE*	*EHH*	*HHH*		
1	SiO_2	**C1**	*1.000*	*0*	*0*	*0*	*0*	*0*	**0**	130.5
2	$SiO_2/SiCl_4$	**A1**	*0.532*	*0.173*	*0.036*	*0.154*	*0.102*	*0.003*	**25.9**	121.3
3		**A2**	*0.556*	*0.185*	*0.024*	*0.117*	*0.116*	*0.002*	**23.5**	123.8
4		**B1**	*0.555*	*0.196*	*0.075*	*0.102*	*0.067*	*0.005*	**17.5**	122.0
5		**C1**	*1.000*	*0*	*0*	*0*	*0*	*0*	**0**	132.0

[a] Obtained from 13C-NMR
[b] 1-hexene incorporation
[c] Melting temperature

From method **A1** and **A2**, into which MMAO was introduced prior to copolymerization (**A1**) or immobilizing catalyst in order to improve surface properties, it was found that the 1-hexene incorporations of their obtained polymers were higher than the other methods. This was due to highly accessible active sites generating from being anchored to the support surface by MMAO. While method **B2** provided the obtained polymer with relatively lower 1-hexene incorporation than that of method **A1** and **A2**.

When compared with method **C1**, method **B2** was better because MMAO that was fixed together with catalyst at the same time may stabilize the active sites and

reduce interaction between them and the support then probably making these sites suitable for reacting with 1-hexene. However, MMAO may also obstruct the coordination between the active sites and 1-hexene and therefore 1-hexene incorporation of method **B2** was still lower than that of method **A1** and **A2**. Melting temperatures of method **A1**, **A2** and **B2** were 121.3, 123.8 and 122.0 °C respectively. These value indicated to the characteristic of LLDPE (Tm = 122-128 °C). Hence, LLDPE can be obtained by the preparation method **A1**, **A2** and **B2** but not **C2**. The triad distributions of LLDPE obtained from all 3 methods (**A1**, **A2** and **B2**) were similar with slightly amount of block copolymer (HHH). This indicated that the various preparations method did not affect the triad distributions in the obtained polymers.

4.5 Effect of support texture on copolymerization (Part 5)

To choose the appropriate supports for using in the system is another parameter that should be concerned as the textures of the supports can affect the system in many behaviors, ranging from the activities during polymerization to the properties of the obtained polymers. Therefore, a variety of supports were brought to use in this investigation.

4.5.1 Characteristic of support

4.5.1.1 Physical properties of supports

In this study, silicas with different textures will be used and each of them will be prepared by various methods to determine their effect on copolymerization. The specifications of all silicas used were listed in **Table 4.16**. Shapes of the silicas were also shown in **Figure 4.14**.

Table 4.16 Physical properties of supports

Type	**Spherical**	**Surface area** (m^2g-1)		**Pore diameter** (A^o)		**Pore volume** (ml g^{-1})		**Particle size** (μm)	
P-10	*Yes*	*High*	248	*Small*	172	*High*	1.50	*Large*	20
ES-70X	*Yes*	*High*	273	*Small*	225	*High*	1.54	*Large*	39
Q-50	*No*	*Low*	70.9	*Large*	368	*Low*	0.26	*Large*	5-10
NN-15	*Yes*	*High*	590-690	*Small*	-	*Low*	-	*Small*	0.015

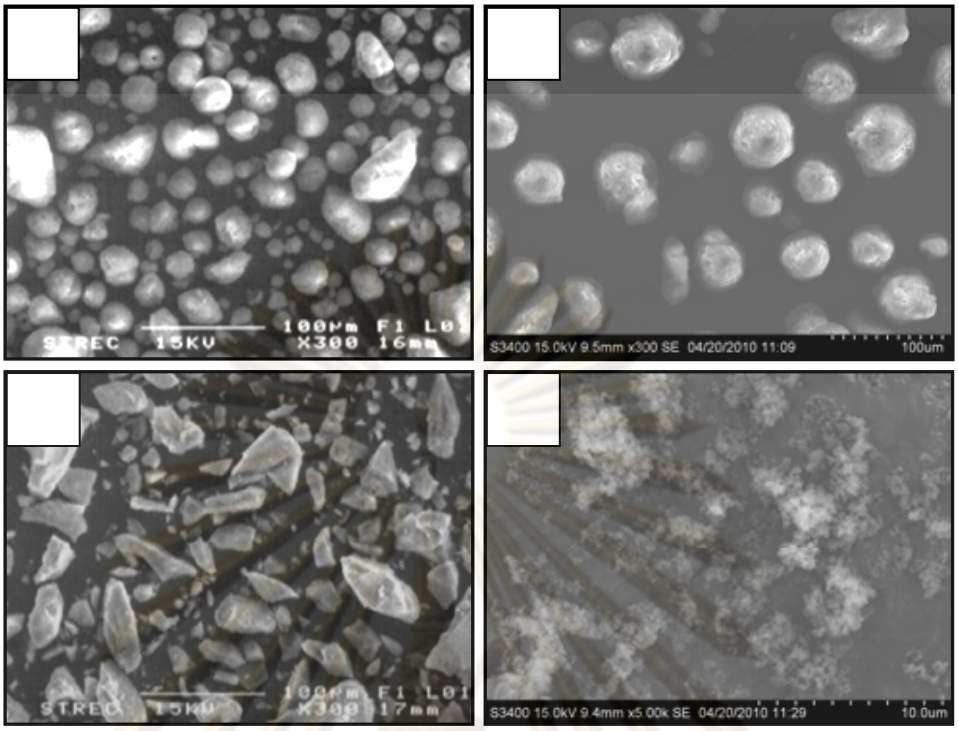

Figure 4.14 Shapes of the silicas: a) P-10, b) ES-70X, c) Q-50 and d) NN-15

4.5.2 Characteristics of catalysts on the support

The preparation methods used in this part consisted of **A2*, B2** and **C2**, whose finished catalysts have both catalyst and MMAO on them. Method **A2*** was developed from method **A2** as we have already known that the disadvantage of method **A2** was that the difficulty to achieve the active sites by letting MMAO being on the support. Therefore, in method **A2*** , after immobilizing MMAO onto the support, the excess MMAO in liquid form had still not eliminated from the system, and then instantly introduced catalyst into the system in order to offer a chance of activating catalytic sites in homogeneous liquid phase.

4.5.2.1 The amount of catalyst and/or MMAO on the supports

It can be seen from **Table 4.17** that the amount of both catalyst (%Ti) and MMAO (%AL) in silica Q-50 were the lowest among three silicas whatever preparation methods. This is probably due to the lowest surface area.

Table 4.17 The amount of titanium (catalyst) and aluminium (MMAO) investigated by Inductive Coupling Plasma Spectroscopy (ICP)

Run	SiO_2	**Method**	Immobilization		Ti (%w)	Al (% w)
			Step 1	Step 2		
7	ES-70X	**A2***	MMAO	MMAO + Catalyst	0.217	16.13
8	ES-70X	**B2**	MMAO + Catalyst	-	0.223	18.00
9	ES-70X	**C2**	Catalyst	MMAO	0.209	17.50
10	Q-50	**A2***	MMAO	MMAO + Catalyst	0.153	13.62
11	Q-50	**B2**	MMAO + Catalyst	-	0.189	15.00
12	Q-50	**C2**	Catalyst	MMAO	0.189	15.89
13	NN-15	**A2***	MMAO	MMAO + Catalyst	0.212	16.43
14	NN-15	**B2**	MMAO + Catalyst	-	0.241	19.00
15	NN-15	**C2**	Catalyst	MMAO	0.266	19.08

4.5.2.2 Interaction between catalyst and MMAO on the support

Thermal gravimetric analysis technique (TGA) was using to determine interaction among species fixed onto the supports with the aim of observing the ability of each species to survive on the support. The principal of TGA technique is to measure weight losses in a material as a function of temperature in a controlled atmosphere in this case using argon atmosphere for imitating the real reaction atmosphere. The weight losses of the supports could indicate tend of the reactions occurred on them during in both preparation steps and copolymerization.

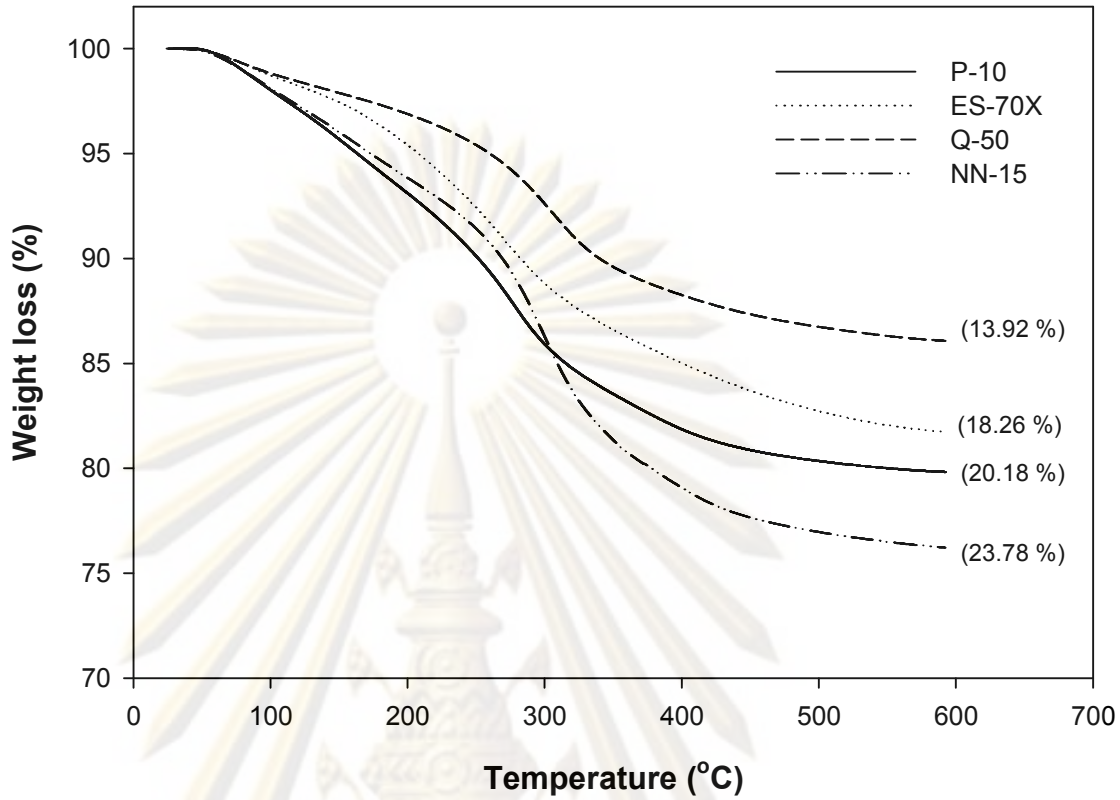

Figure 4.15 Weight losses as a function of temperature of various supported silicas prepared by method **B**

From **Figure 4.15**, which show the weigh losses as a function of temperature, it was found that the weight losses until 600 °C was correlated with the total weight of catalyst and MMAO fixed on the supports. Silica NN-15 had the highest weight loss (23.78 %) due to the highest amount of catalyst and MMAO (0.241 and 19.0 % respectively), by the same token the silica Q-50 had the lowest weight loss (13.92 %) due to the lowest amount of catalyst and MMAO (0.189 and 15.0 %). Therefore, in silica ES-70X and P-10, their weight losses were almost equal by the same reason. In addition, the weight loss patterns of these two silicas were also similar since their textures are alike then providing similar interaction.

To show the changes of weight losses obviously, the weight losses were converted into derivative form prior to plotting with temperature as seen in **Figure 4.16**. It can be observed that the highest peaks of silica ES-70X and P-10 were located closely between 272-275 °C while those of silica Q-50 and NN-15 were higher between 301-305 °C. Therefore, it can be conclude from these results that the various

textures of silicas affect interaction between the immobilized species and the supported, and then the different interactions will affect activities of the system when it is used as a supporting material in copolymerization.

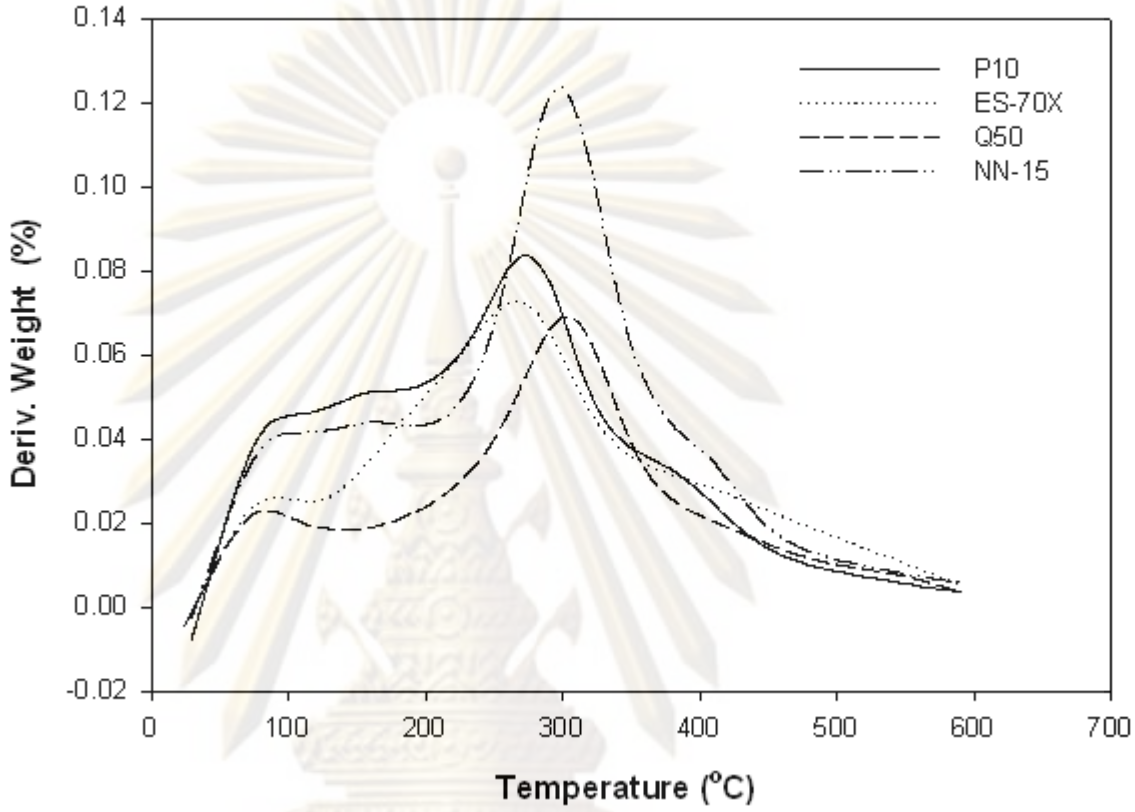

Figure 4.16 Derivative weight losses as a function of temperature of various supported silicas prepared by method **B2**

4.5.3 Characteristic activity

4.5.3.1 Effect of preparation methods

From **Table 4.18**, it can be observed that method **A2***, which leave the excess of liquid MMAO from immobilization reacting with catalyst in liquid phase, still gave a lower activity than method **B2** for silica ES-70X and NN-15 but Q-50. This is because the rest of MMAO, in liquid phase after immobilization in step 1, was not enough for activating all catalytic sites of following introduced catalysts in step 2.

However, for silica Q-50, the opposite result may be come from that the rest MMAO in step 1 was higher compared to in silica ES-70X and NN-15. Therefore, it was high enough for activating more the catalytic sites than that in silica ES-70X and NN-15. The amount of catalyst on the support shown in **Table 4.17** also agree with

this assumption as in Q-50 there was the lowest amount of catalyst on the support meaning that it was likely to present more in the liquid phase. Another point to concern is that, for silica Q-50, method **A2*** also provided a higher activity than method **B2**. This is probably due to the advantage of activating catalytic sites in liquid phase combined with the advantage of improvement the silica surface by immobilization of MMAO prior to introducing the catalyst.

Method **C2** can not achieve copolymerization for all types of silica. Therefore, the drawback of immobilizing catalysts directly onto the support even silane-modified support is on the supports no matter what textures they possess.

Table 4.18 Activity of copolymerization using different supported-catalysts from various preparation methods

Run	Support	**Method**	Immobilization		Polymer Yield (g)	Activity (kg pol. / mol Ti. h)
			Step1	Step 2		
7	ES-70X	**A2***	MMAO	MMAO + Catalyst	0.067	161
8	ES-70X	**B2**	MMAO + Catalyst	-	0.553	1327
9	ES-70X	**C2**	Catalyst	MMAO	n.a.	0
10	Q-50	**A2***	MMAO	MMAO + Catalyst	0.139	333
11	Q-50	**B2**	MMAO + Catalyst	-	0.090	216
12	Q-50	**C2**	Catalyst	MMAO	n.a.	0
13	NN-15	**A2***	MMAO	MMAO + Catalyst	0.032	77
14	NN-15	**B2**	MMAO + Catalyst	-	0.130	311
15	NN-15	**C2**	Catalyst	MMAO	n.a.	0

4.5.3.2 Effect of silica texture

Method **A2***

By using method A2*, it was found the activity of Q-50 silica was the highest followed by those of ES-70X and NN-15 respectively. One of the reasons is mentioned above that its highest activity was due to the lowest surface area providing the rest of the liquid MMAO the most after immobilization. Another reason is about a difference of pore size of supports that could affect the activity of the system. The

study conducted by Silveria et al. [86] found that the support with a smaller pore size gave higher activity than that of a larger one. This was due to the smaller pores causing more deactivation of catalyst within them. As seen in **Figure 4.17**, the smaller pore has the more negative curvature that keeps silanol groups closer then favoring the formation of hydrogen bonds and therefore, increasing the stability of silanol groups against dehydroxylation [87]. Consequently, the number of silanol groups in the smaller pore remains higher even after calcinations process (dehydroxylation). The proximity of theses groups may provide the adjacent MMAO molecules fixed on them (through $SiCl_4$) closer, and therefore promoting the generation of bimolecular species which are inactive for polymerization as described previously (**Figure 4.18**). From this reason, the small pores would give the number of inactive sites higher than that of the larger pores and then giving higher activity even the number of overall catalytic sites lower. The amount of catalyst (Ti) detected by ICP-OES can corroborate this presumption as the amount of Ti (catalytic sites) on the larger pore support (Q-50) was lower than those of the smaller pore supports (ES-70X and NN-15) but it gave higher activity. This means that the active sites existed more in the larger pore support. Hence, by using method A2*, silica Q-50 whose pores were larger than those of ES-70X and NN-15 gave the highest activity

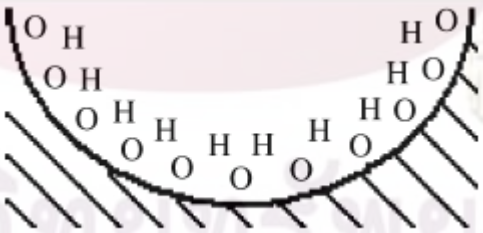

Figure 4.17 Structural model indicating the position of silanol groups in the pore [86].

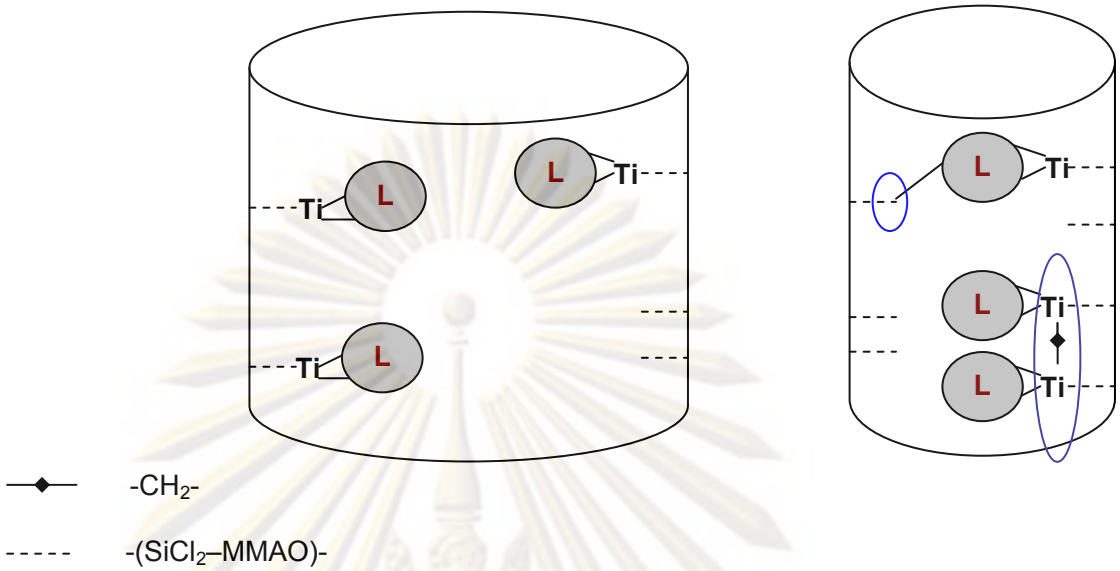

Figure 4.18 Catalyst deactivation in different pores

Method **B2**

Method **B2** was the method that two species (MMAO and catalyst) were immobilized together in the same time, and then competition between these species may occur. Therefore, a support with a high surface area that can provide better diffusion for the species on it will be appropriate. For this reason, silica ES-70X and NN-15 with the larger surface area gave the higher activity than silica Q-50.

The benefit of reduction in catalyst deactivation to silica Q-50 influenced method **B2** less than method **A2*** as a result of fact that the anion of MMAO occurred during activation step in method **B2** could prevent the deactivation much better than the capability of the large pore.

When comparing between silica ES-70X and NN-15, it was found that silica NN-15 gave lower activity despite the larger surface area. This was due to the fact that nano-size particles are likely to agglomerate, and then the active sites fixed on them become more inactive and inaccessible to the monomer during copolymerization. In addition, it was probable that the smaller particles interact with the species linked with them stronger than the larger particles, and therefore they were susceptible not to form bond with the other molecule coming to contact them including the monomer

[88]. The system, in which small particles have been dispersed all over, also has low space or short gaps between two particles thus having strong steric hindrance that decrease the polymerization rate and consequently the activity. Hence, silica NN-15 whose average particle size is in nanometer was more agglomerate and has more steric hindrance than silica ES-70X whose average particle size is in micrometer, and then gave the lower activity as seen in the result.

In addition, the determination of the interactions between species on the surface (catalyst or MMAO) and the supports was found that the temperatures at the highest derivative weight loss were adversely correlated with the activity (**Figure 4.16**). As seen, silicas P-10 and ES-70X which those temperatures were relatively low (272-275 °C) provided the higher activity than silica Q-50 and NN-15 which those temperatures were higher (301-305 °C).

This was due to the fact that species with strong interaction (high temperature at the highest derivative weight loss) like silica Q-50 and NN-15 tend not to react with the species coming after it such as monomer and comonomer in copolymerization. By the same token, species with weak interactions like P-10 and ES-70X tent to react easily with monomer and comonomer in copolymerization then enhancing activities of the system. Hence, this agrees with the results and also with the study of Bunchongturakarn et al and [63] and Wongwaiwattanakul et al. [68] which has been found that the interactions between species on the support and the support affected activities of the system.

4.5.4 Characteristic of polymer

4.5.4.1 Morphology

Polymers obtained by method **B2** from silica P-10 and ES-70X exhibited roughly similar morphologies (**Figure 4.19a)** and **b)**). This was due to the fact that the similar textures of both silicas exert an influence on the output polymers having similar morphologies. The morphology of polymer obtained from silica Q-50 (**Figure 4.19c)**) was slightly different from those of P-10 and ES-70X. There were two different shapes of polymer gathered in this polymer i.e. pellets and fibers. This was because of the large pores of silica Q-50 that could trap some active sites inside them without directly contacted to the surface. These active sites may be leached during copolymerization then reacting in liquid phase so therefore providing the polymer

whose properties like those of polymers produced by the homogeneous system. Hence, the different shapes from the heterogeneous and like-homogeneous systems were in the obtained polymer. For silica NN-15 (**Figure 4.19d)**), the obtained polymer exhibited some agglomeration as its nanosize particles were highly agglomerated and then the obtained polymer replicated the agglomeration of the support as seen in the figure.

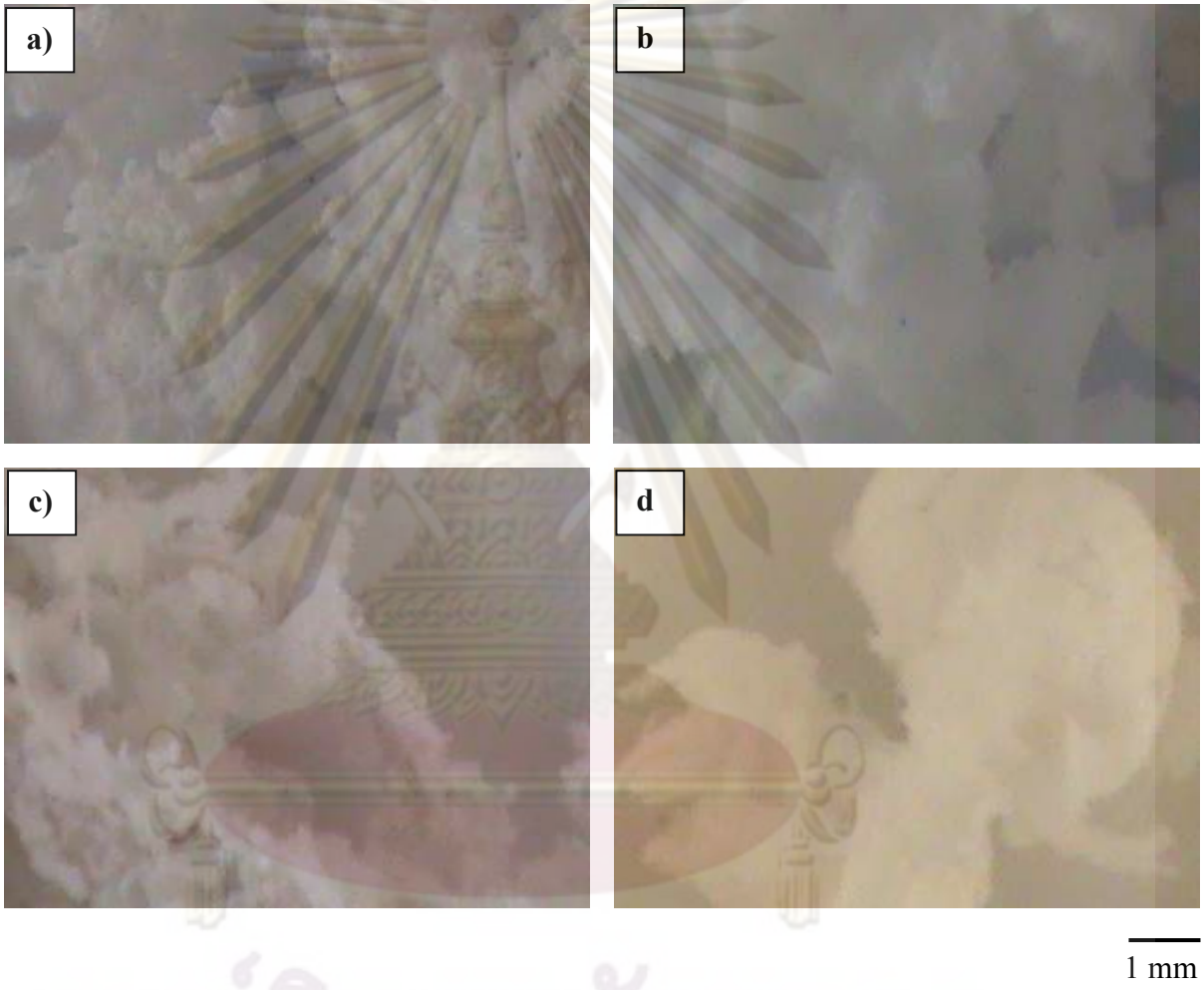

Figure 4.19 Morphologies of polymers obtained from the various silicas by method **B2** a) P-10 b) ES-70X c)Q-50 และ d) NN-15

4.5.4.2 Polymer structure and property

From **Table 4.19**, it was found that silica ES-70X had the same trend toward 1-hexene incorporation (A2 > B2) as silica P-10 due to their similar textures. However, the difference occurred in silica Q-50 which almost the same amount of

1-hexene incorporation of method A2 and B2 was observed. It was because its large pores providing 1-hexene incorporation sometimes occurred inside the pores that the various reactions inside the pores may alter the mechanism of incorporation, and then finally affected the amount of 1-hexene incorporation in the obtained polymers.

Table 4.19 ^{13}C-NMR and DSC analysis of polymers obtained from various silicas

Run	Support	**Method**	**Triad distribution**[a]						**%H** [b]	$\mathbf{T_m}$ [c]
			EEE	*EEH*	*HEH*	*EHE*	*EHH*	*HHH*		
1	ES-70X	**A2**	0.522	0.143	0.067	0.118	0.146	0.004	**26.8**	121.8
2		**B2**	0.568	0.200	0.041	0.132	0.035	0.024	**19.1**	121.1
3	Q-50	**A2**	0.525	0.233	0.051	0.120	0.064	0.006	**19.1**	118.8
4		**B2**	0.530	0.207	0.066	0.120	0.067	0.009	**19.6**	123.1
5	NN-15	**A2**	-	-	-	-	-	-	**n.d.**	
6		**B2**	0.530	0.172	0.033	0.092	0.170	0.002	**26.4**	121.2

[a] Obtained from 13C-NMR
[b] 1-hexene incorporation
[c] Melting temperature

When comparing among all the polymers obtained from all three silicas and prepared by method B2, it was found that silica NN-15 provided the highest 1-hexene incorporation as a result of having the highest surface area. Since the amount of catalyst using in all support were the same, the highest surface area of the support would provided the occupying active sites the highest space for the highest amount of 1-hexene incorporation. The triad distributions of LLDPE obtained from all 3 silicas were similar with slightly amount of block copolymer (HHH). This indicated that the various silicas with different textures did not affect the triad distributions in the obtained polymers as well as the melting temperatures of them which were not changed dramatically by the various silicas.

CHAPTER V

CONCLUSIONS & RECOMMENDATION

5.1 Conclusion

Part 1: Effect of comonomer on the half-metallocene catalytic systems

It was found that the positive comonomer effect occurred even though a very high concentration of 1-hexene that was introduced into the system. However, the microstructures of the obtained copolymer examined by ^{13}C-NMR need to be improved because the highly alternating sequence distributions of copolymer cause the loss of essential specific thermal properties.

Part 2: A Comparative study on LLDPE/ silica composites synthesized by different copolymerization systems

The heterogeneous reaction with *in situ* impregnation revealed here that it is the interesting way to synthesis LLDPE/ composites because it can be performed simply and provide a high catalytic activity. However, as a result of lower interaction between MMAO and support, some properties which were worse compared with the *ex situ* impregnation, such as thermal properties need to be improved. Comonomer contents (1-hexene incorporations) and sequence distributions of the obtained polymers (composite) from both two heterogeneous systems with various impregnation methods were nearly the same but significantly differed from that of the homogeneous system. This means that the different reaction phases have a greater influence on the microstructure of the obtained polymer than the different impregnation methods.

Part 3: Modification of supports by gallium

The higher catalytic activity of the larger pore silica was observed as a result of low internal diffusion resistance. However, after gallium modification, the small pore silica exhibited higher catalytic activity. This is because gallium modification, which mainly improves properties of surface, more efficiently influences properties on silica with higher surface area. Then, the small pore silica with higher surface can receive more improvement from gallium and raising more catalytic activities than the

large pore silica with lower surface area. Moreover, effect of surface area also caused change in 1-hexene incorporation, where a decrease in 1-hexene incorporation was evident with decreased surface area. In addition, different types of catalytic sites were observed, and then used to construct a model which helped explain the results.

Part 4: Effect of method for preparation of supported catalysts

1) For the copolymerization system of ethylene and 1-hexene with [t-BuNSiMe$_2$Flu]TiMe$_2$ as a catalyst, the best method for preparation of supported catalyst is method **B2** as a result of;

- providing the highest activity
- reducing cost by using less solvent and saving time of preparation

2) Method **C2** is not suitable for this system as a result of;

- the active sites on the supports interacting too strong with the support surface
- increasing cost with the active sites leaching during preparation step

3) Adding MMAO during copolymerization can increase the activity of system.

Part 5: Effect of support texture on copolymerization

Silica brought to be a support should have an appropriate texture to provide the system with the great activity. From the study, it can be deduced that the best support is silica ES-70X because of high surface area and suitable shape (spherical) and size (in micrometer). Moreover, silica P-10 used in the previous part, which have the similar texture with silica ES-70X can support that the appropriate texture will cause the great activity for the supported system with using [t-BuNSiMe$_2$Flu]TiMe$_2$/MMAO as catalysts especially when preparing the support by method **B2**.

5.2 Recommendations

To investigate the real oxidation states of the catalyst on the supports, the effective technique like Electron Spin Resonance (ESR) should be conducted in cooperation with this study's technique. The molecular weight of the polymers should be further investigated to have a better understating of the properties of the polymers obtained from the various method of preparation.

REFERENCES

[1] Mark, H. F. **Ethylene Polymers, LLDPE** (Vol. 2). New York: John Wiley & Sons, (2002).

[2] Severn, J. R., Chadwick, J. C., Duchateau, R., and Friederichs, N. "Bound but not gagged" - Immobilizing single-site α-olefin polymerization catalysts. **Chemical Reviews**, 105(2005), 4073-4147.

[3] Kaminsky, W., Albers, I., and Vathauer, M. New copolymers of olefins and styrene by metallocene catalysis. **Designed Monomers and Polymers**, 5(2002), 155-162.

[4] Shiono, T., Yoshida, S., Hagihara, H., and Ikeda, T. Additive effects of trialkylaluminum on propene polymerization with (t-BuNSiMe$_2$Flu)TiMe$_2$-based catalysts. **Applied Catalysis A: General**, 200(2000), 145-152.

[5] Chen, Y. X., and Marks, T. J. "Constrained geometry" dialkyl catalysts. Efficient syntheses, C-H bond activation chemistry, monomer-dimer equilibration, and α-olefin polymerization catalysis. **Organometallics**, 16(1997), 3649-3657.

[6] Kaminsky, W., Tran, P. D., and Weingarten, U. New materials by polymerisation of olefins and styrene with metallocene catalysts. **Macromolecular Symposia**, 193(2003), 1-11.

[7] Hosoda, S. Structural distribution of linear low-density polyethylenes. **Polymer Journal**, 20(1988), 383-397.

[8] Speed, C. S., Trudell, B. C., Mehta, A. K., and Stehling, F. C. Structure / property relationships in ExxpolTM polymers. In Society of Plastics Engineers, **Polyolefins VII: Seventh International Conference on Polyolefins 1991**, 46-66,(1991).

[9] Welch, M. B., Palackal, S. J., Geerts, R. L., and Fahey, D. R. Polyethylenes Produced in Phillips Slurry Loop Reactors with Metallocene Catalysts. In **MetCon '95**, Houston, TX, USA,(1995).

[10] Kashiwa, N., and Imuta, J. I. Recent progress on olefin polymerization catalysts. **Catalysis Surveys from Japan (United States)**, 1(1997), 125-142.

[11] Sinclair, K. B., and Wilson, R. B. Metallocene Catalysts: A Revolution in Olefin Polymerization. **Chemistry and Industry**, 21(1994), 857-862.

[12] Gupta, V. K., Satish, S., and Bhardwaj, I. S. Metallocene complexes of group 4 elements in the polymerization of monoolefins. **Journal of Macromolecular Science - Reviews in Macromolecular Chemistry and Physics**, C34(1994), 439-514.

[13] Naga, N., and Imanishi, Y. Copolymerization of Ethylene and Cyclopentene with Zirconocene Catalysts: Effect of Ligand Structure of Zirconocenes. **Macromolecular Chemistry and Physics**, 203(2002), 159-165.

[14] Lauher, J. W., and Hoffmann, R. Structure and chemistry of bis(cyclopentadienyl)-MLn complexes **Journal of the American Chemical Society**, 98(1976), 1729-1742.

[15] Nomura, K., Liu, J., Padmanabhan, S., and Kitiyanan, B. Nonbridged half-metallocenes containing anionic ancillary donor ligands: New promising candidates as catalysts for precise olefin polymerization. **Journal of Molecular Catalysis A: Chemical**, 267(2007), 1-29.

[16] Suhm, J., Heinemann, J., Woerner, C., Mueller, P., Stricker, F., Kressler, J., et al. Novel polyolefin materials via catalysis and reactive processing. **Macromolecular Symposia**, 129(1998), 1-28.

[17] McKnight, A. L., and Waymouth, R. M. Group 4 ansa-cyclopentadienyl-amido catalysts for olefin polymerization. **Chemical Reviews**, 98(1998), 2587-2598.

[18] Okuda, J., Schattenmann, F. J., Wocadlo, S., and Massa, W. Synthesis and characterization of zirconium complexes containing a linked amido-fluorenyl ligand. **Organometallics**, 14(1995), 789-795.

[19] Shapiro, P. J., Bunel, E., Schaefer, W. P., and Bercaw, J. E. [{(.eta.5-C_5Me_4)Me_2Si(?1-NCMe_3)}(PMe_3)Sc$H]_2$: A unique example of a single-component α-olefin polymerization catalyst. **Organometallics**, 9(1990), 867-869.

[20] Castonguay, L. A., and Rappe, A. K. Ziegler-Natta catalysis. A theoretical study of the isotactic polymerization of propylene. **Journal of the American Chemical Society**, 114(1992), 5832-5842.

[21] Kaminsky, W., and Laban, K. Metallocene catalysis. **Applied Catalysis A: General**, 222(2001), 47-61.

[22] Yang, X., Stern, C. L., and Marks, T. J. "Cation-like" homogeneous olefin polymerization catalysts based upon zirconocene alkyls and

tris(pentafluoropnenyl)borane. **Journal of the American Chemical Society**, 113(1991), 3623-3625.

[23] Chien, J. C. W., and Wang, B. P. Metallocene-Methylaluminoxane catalysts for olefin polymerization. I. Trimethylaluminum as coactivator. **Journal of Applied Polymer Science**, 26(1988), 3089-3102.

[24] Pedeutour, J. N., Radhakrishnan, K., Cramail, H., and Deffieux, A. Use of "TMA-depleted" MAO for the activation of zirconocenes in olefin polymerization. **Journal of Molecular Catalysis A: Chemical**, 185(2002), 119-125.

[25] Pedeutour, J. N., Cramail, H., and Deffieux, A. Influence of X ligand nature in the activation process of racEt$(Ind)_2ZrX_2$ by methylaluminoxane. **Journal of Molecular Catalysis A: Chemical**, 176(2001), 87-94.

[26] Cam, D., and Giannini, U. Concerning the Reaction of Zirconocene Dichloride and Methylalumoxane: Homogeneous Ziegler-Natta Catalytic System for Olefin Polymerization. **Makromolekulare Chemie-Macromolecular Chemistry and Physics**, 193(1992), 1049-1055.

[27] Soga, K., Kim, H. J., and Shiono, T. Polymerization of ethylene with homogeneous metallocene catalysts activated by common trialkylaluminiums and $Si(CH_3)_3OH$. **Makromolekulare Chemie-Rapid Communications**, 14 (1993), 765-770.

[28] Katayama, H., Shiraishi, H., Hino, T., Ogane, T., and Imai, A. The effect of aluminum compounds in the copolymerization of ethylene / α-olefins. **Macromolecular Symposia**, 97 (1995), 109-118.

[29] Steinmetz, B., Tesche, B., Przybyla, C., Zechlin, J., and Fink, G. Polypropylene growth on silica-supported metallocene catalysts: a microscopic study to explain kinetic behavior especially in early polymerization stages. **Acta Polymer**, 48 (1997), 392-399.

[30] Tait, P. J., and Monterio, M. G. Some Recent Advances in Supported Metallocene Catalysts. In **Metcon'96**, Houston, TX, USA (1996).

[31] Quijada, R., Rojas, R., Alzamora, L., Retuert, J., and Rabagliati, F. M. Study of metallocene supported on porous and nonporous silica for the polymerization of ethylene. **Catalysis letters**, 46(1997), 107-112.

[32] Chen, Y. X., Rausch, M. D., and Chein, J. C. W. Olefin terpolymerizations. I. 1,4-hexadiene. **Journal of Polymer Science Part A: Polymer Chemistry**, 33(1995), 2093-2108.

[33] Severn, J. R., and Chadwick, J. C. **Tailor-made polymers : via immobilization of alpha-olefin polymerization catalysts**. Weinheim: Wiley-VCH, (2008).

[34] Trebosc, J., Wiench, J. W., Huh, S., Lin, V. S.-Y., and Pruki, M. Solid-state MMR study of MCM-41-type mesoporous silica nanoparticles. **Journal of the American Chemical Society**, 127(2005), 3057-3068.

[35] Bartram, M. E., Michalske, T. A., Rogers Jr, J. W., and Mayer, T. M. Chemisorption of trimethylaluminum and ammonia on silica: Mechanisms for the formation of Al-N bonds and the elimination of methyl groups bonded to aluminum. **Chemistry of Materials**, 3(1991), 953-960.

[36] Scott, S., Church, T. L., Hguyen, D. H., Mader, E. A., and Moran, J. An investigation of catalyst/cocatalyst/support interactions in silica-supported olefin polymerization catalysts based on Cp^*TiMe_3. **Topics in Catalysis**, 34(2005), 109.

[37] Welborn, H. C. **Supported polymerization catalyst**. US Patent No. 4808561, (1989).

[38] Takahashi, T. **Process for producing ethylene copolymers**. US Patent No. 5026797, (1991).

[39] Razavi, A., and Debras, G. L. G. **Process for producing polyolefins and polyolefin catalyst**. US Patent No. 5719241, (1998).

[40] Gauthier, W. J., Tian, J., Rauscher, D., and Henry, S. **Polyolefin production with a high performance support for a metallocene catalyst system**. US Patent No. 2003/0236365, (2003).

[41] Jacobsen, G. B., Wauteraerts, P. L., and Spencer, L. **Supported catalyst component, supported catalyst, their preparation, and addition polymerization process**. US Patent No. 6043180, (2000).

[42] Burkhardt, T. J., Murata, M., and Brandley, W. B. **Method for making and using a supported metallocene**. US Patent No. 5240894, (1993).

[43] Spaleck, W., Krฬber, F., Winter, A., Rohrmann, J., Bachmann, B., Antberg, M., et al. The influence of aromatic substituents on the polymerization behavior of bridged zirconocene catalysts. **Organometallics**, 13(1994), 954-963.

[44] Fraajie, V., Bachmann, B., and Winter, A. EU Patent No. 780402, (1997).

[45] Dos Santos, J. H. Z., Krug, C., Da Rosa, M. B., Stedile, F. C., Dupont, J., and De Camargo Forte, M. The effect of silica dehydroxylation temperature on the activity of SiO2-supported zirconocene catalysts. **Journal of Molecular Catalysis A: Chemical**, 139(1999), 199-207.

[46] Guimaraes, R., Stedile, F. C., and Dos Santos, J. H. Z. Ethylene polymerization with catalyst systems based on supported metallocenes with varying steric hindrance. **Journal of Molecular Catalysis A: Chemical**, 206(2003), 353-362.

[47] Schrekker, H. S., Kotov, V., Preishuber-Pflugl, P., White, P., and Brookhart, M. Efficient slurry-phase homopolymerization of ethylene to branched polyethylenes using α-diimine nickel(II) catalysts covalently linked to silica supports. **Macromolecules**, 39(2006), 6341-6354.

[48] Nomura, K., Naga, N., Miki, M., Yanagi, K., and Imai, A. Synthesis of various nonbridged titanium(IV) cyclopentadienyl-aryloxy complexes of the type CpTi(OAr)X2 and their use in the catalysis of alkene polymerization. Important roles of substituents on both aryloxy and cyclopentadienyl groups. **Organometallics**, 17(1998), 2152-2154.

[49] Nomura, K., Naga, N., Miki, M., and Yanagi, K. Olefin polymerization by (cyclopentadienyl)(aryloxy)titanium(IV) complexes-cocatalyst systems. **Macromolecules**, 31(1998), 7588-7597.

[50] Tomotsu, N., Ishihara, N., Newman, T. H., and Malanga, M. T. Syndiospecific polymerization of styrene. **Journal of Molecular Catalysis A: Chemical**, 128(1998), 167-190.

[51] Al-Malaika, S., and Peng, X. Metallocene ethylene-1-octene copolymers: Effect of extrusion conditions on thermal oxidation of polymers with different comonomer content. **Polymer Degradation and Stability**, 92(2007), 2136-2149.

[52] Van Grieken, R., Carrero, A., Suarez, I., and Paredes, B. Effect of 1-hexene comonomer on polyethylene particle growth and kinetic profiles. **Macromolecular Symposia**, 259(2007), 243-252.

[53] Hong, H., Zhang, Z., Chung, T. C. M., and Lee, R. W. Synthesis of new 1-decene-based LLDPE resins and comparison with the corresponding 1-octene-

and 1-hexene-based LLDPE resins. **Journal of Polymer Science, Part A: Polymer Chemistry**, 45(2007), 639-649.

[54] Biatek, M., and Czaja, K. (Co)polymerisation behaviour of supported metallocene catalysts: Carrier effect. **Macromolecular Chemistry and Physics**, 207(2006), 1651-1660.

[55] Hagihara, H., Shiono, T., and Ikeda, T. Living polymerization of propene and 1-hexene with the [t-BuNSiMe2Flu]TiMe2/B(C6F5) 3 catalyst. **Macromolecules**, 31(1998), 3184-3188.

[56] Wannaborworn, M., and Jongsomjit, B. Ethylene/1-Octene Copolymerization over Ga-modified SiO_2-supported Zirconocene/MMAO Catalyst Using In Situ and Ex Situ Impregnation Methods. **Iranian Polymer Journal**, 18(2009), 969-979.

[57] Pothirat, T., Jongsomjit, B., and Praserthdam, P. Effect of Zr-modified SiO_2-supported metallocene/MAO catalyst on copolymerization of ethylene/1-octene. **Catalysis Letters**, 121(2008), 266-273.

[58] Intaragamjon, N., Shiono, T., Jongsomjit, B., and Praserthdam, P. Elucidation of solvent effects on the catalytic behaviors for [t-BuNSiMe$_2$Flu]TiMe$_2$ complex during ethylene/1-hexene copolymerization. **Catalysis Communications**, 7(2006), 721-727.

[59] Kawahara, N., Saito, J., Matsuo, S., Kaneko, H., Matsugi, T., Toda, Y., et al. Study on unsaturated structures of polyhexene, poly(4-methylpentene) and poly(3-methylpentene) prepared with metallocene catalysts. **Polymer**, 48(2007), 425-428.

[60] Krenstel, B. A., Kissin, Y. V., Kleiner, V. J., and Stotskaya, L. L. **Polymer and copolymer of higher α-olefins**. Munich: Hanser Publishers, (1997).

[61] Forlini, F., Fan, Z. Q., Tritto, I., Locatelli, P., and Sacchi, M. C. Metallocene-catalyzed propene/1-hexene copolymerization: Influence of amount and bulkiness of cocatalyst and of solvent polarity. **Macromolecular Chemistry and Physics**, 198(1997), 2397-2408.

[62] Jongsomjit, B., Ngamposri, S., and Praserthdam, P. Application of silica/titania mixed oxide supported zirconocene catalyst for synthesis of linear low-density polyethylene. **Industrial and Engineering Chemistry Research**, 44(2005), 9059-9063.

[63] Bunchongturakarn, S., Jongsomjit, B., and Praserthdam, P. Impact of bimodal pore MCM-41-supported zirconocene/dMMAO catalyst on copolymerization of ethylene/1-octene. **Catalysis Communications**, 9(2008), 789-795.

[64] Yu, T. C. Metallocene plastomer modification of polypropylenes. **Polymer Engineering and Science**, 41(2001), 656-671.

[65] Hung, J., Cole, A. P., and Waymouth, R. M. Control of sequence distribution of ethylene copolymers: Influence of comonomer sequence on the melting behavior of ethylene copolymers. **Macromolecules**, 36(2003), 2454-2463.

[66] Silveira, F., Alves, M. d. C. M., Stedile, F. C., Pergher, S. B., Rigacci, A., and Santos, J. H. Z. d. Effect of the silica texture on the structure of supported metallocene catalysts. **Journal of Molecular Catalysis A: Chemical**, 298(2009), 40-50.

[67] Hlatky, G. G. Heterogeneous Single-Site Catalysts for Olefin Polymerization. **Chemical Reviews**, 100(2000), 1347-1376.

[68] Wongwaiwattanakul, P., and Jongsomjit, B. Copolymerization of ethylene/1-octene via different pore sized silica-based-supported zirconocene/dMMAO catalysts. **Catalysis Communications**, 10(2008), 118-122.

[69] Che, J., Xiao, Y., Luan, B., Dong, X., and Wang, X. Surface structure, grafted chain length, and dispersion analysis of PBT prepolymer grafted nano-silica. **Journal of Material Science**, 42(2007), 4967-4975.

[70] Zakharov, V. A., Talsi, E. P., Babushkin, D. E., and Semikolenova, N. V. Structure of methylaluminoxane and the mechanism of active center formation in the zirconocene/ methylaluminoxane catalytic system. **Kinetics and catalysis** 40(1999), 836-850.

[71] Xu, J. T., Zhu, Y. B., Fan, Z. Q., and Feng, L. X. Copolymerization of propylene with various higher alpha-olefins using silica-supported **Journal of Polymer Science, Part A: Polymer Chemistry**, 39(2001), 3294-3303.

[72] Luyt, A. S., Molefi, J. A., and Krump, H. Thermal, mechanical and electrical properties of copper powder filled low-density and linear low-density polyethylene composites. **Polymer Degradation and Stability**, 91(2006), 1629-1636.

[73] Iglesia, E., Reyes, S. C., and Madon, R. J. Transport-enhanced ฮท-olefin readsorption pathways in Ru-catalyzed hydrocarbon synthesis. **Journal of Catalysis**, 129(1991), 238-256.

[74] Takahara, I., Saito, M., Inaba, M., and Murata, K. Effects of pre-treatment of a silica-supported gallium oxide catalyst with H_2 on its catalytic performance for dehydrogenation of propane. **Catalysis Letters**, 96(2004), 29-32.

[75] Finch, W. C., Gillespiy, R. D., and Hedden, D. Organometallic molecule-inorganic surface coordination and catalytic chemistry. In Situ CPMAS NMR delineation of organoactinide adsorbate structure, dynamics, and reactivity. **Journal of the American Chemical Society**, 112(1990), 6221-6232.

[76] Kaminsky, W., and Renner, F. High Melting Polypropenes by. Silica-Supported Zirconocene Catalysts. **Makromolecule Chemical Rapid Community**, 14(1993), 239-243.

[77] Campos, J. M., Lourenco, J. P., Fernandes, A., and Ribeiro, M. R. Mesoporous Ga-MCM-41: A very efficient support for the heterogenisation of metallocene catalysts. **Catalysis Communications**, 10(2008), 71-73.

[78] Hegedus, L. L. **Catalyst Design, Progress and Perspectives**. New York: John Wiley & Sons, (1987).

[79] Kumkaew, P., Wu, L., Praserthdam, P., and Wanke, S. E. Rates and product properties of polyethylene produced by copolymerization of 1-hexene and ethylene in the gas phase with $(n\text{-}BuCp)_2ZrCl_2$ on supports with different pore sizes. **Polymer**, 44(2003), 4791-4803.

[80] Laurence, R. L., and Chiovetta, M. G. **Heat and Mass Transfer During Olefin Polymerization from the Gas Phase**. Munich: Hanser, (1983).

[81] Lanza, G., Fragala`, I. L., and Marks, T. J. Energetic, structural, and dynamic aspects of ethylene polymerization mediated by homogeneous single-site "constrained geometry catalysts" in the presence of cocatalyst and solvation: An investigation at the ab initio quantum chemical level. **Organometallics**, 21(2002), 5594-5612.

[82] Ko, Y. S., and Woo, S. I. Generation of active site confined inside supercage of NaY zeolite on a nano-scale and its ethylene polymerization. **European Polymer Journal**, 39(2003), 1553-1557.

[83] Garcia, M., van Zyl, W. E., ten Cate, M. G. J., Stouwdam, J. W., Verweij, H., Pimplapure, M. S., et al. Novel Preparation of Hybrid Polypropylene/Silica Nanocomposites in a Slurry-Phase Polymerization Reactor. **Industrial & Engineering Chemistry Research**, 42(2003), 3750-3757.

[84] Chien, J. C. W. Supported metallocene polymerization catalysis. **Topics in Catalysis**, 7(1999), 23-36.

[85] Xu, J., Zhao, J., Fan, Z., and Feng, L. ESR study on SiO_2-supported half-titanocene catalyst for syndiospecific polymerization of styrene. **Macromolecular Rapid Communications**, 18(1997), 875.

[86] Silveira, F., Pires, G. P., Petry, C. F., Pozebon, D., Stedile, F. C., Santos, J. H. Z. d., et al. Effect of the silica texture on grafting metallocene catalysts. **Journal of Molecular Catalysis A: Chemical**, 265(2007), 167-176.

[87] Iler, R. K. **The Chemistry of Silica**. New York: Wiley Interscience Publication, John Wiley & Sons, USA, . (1979).

[88] Chaichana, E., Jongsomjit, B., and Praserthdam, P. Effect of nano-SiO_2 particle size on the formation of LLDPE/SiO_2 nanocomposite synthesized via the in situ polymerization with metallocene catalyst. **Chemical Engineering Science** 62(2007), 899 - 905.

APPENDICES

APPENDIX A
(NUCLEAR MAGNETIC RESONANCE)

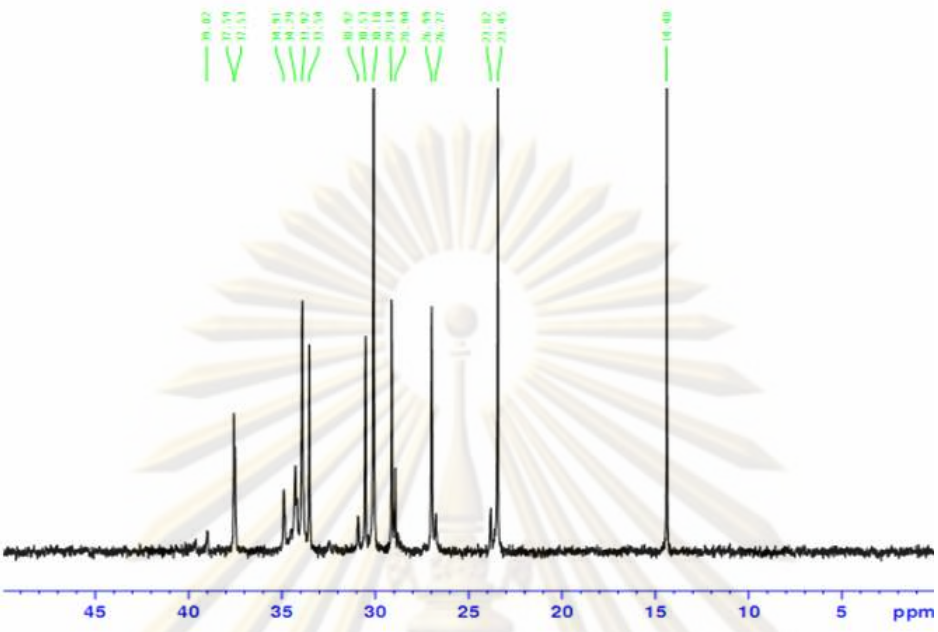

Figure A-1 ^{13}C NMR spectrum of ethylene/1-hexene copolymer at ratio 1:2

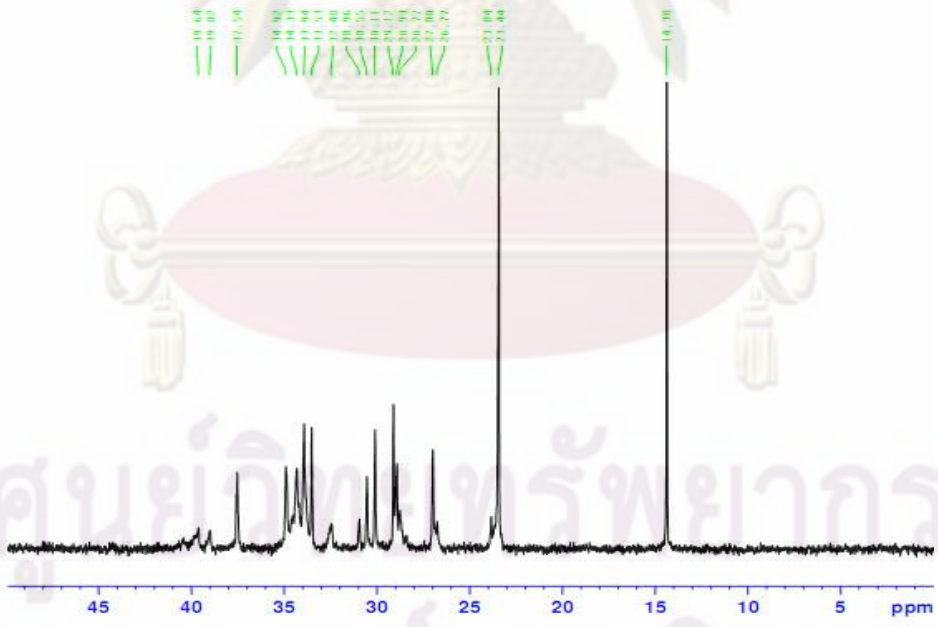

Figure A-2 ^{13}C NMR spectrum of ethylene/1-hexene copolymer at ratio 1:1

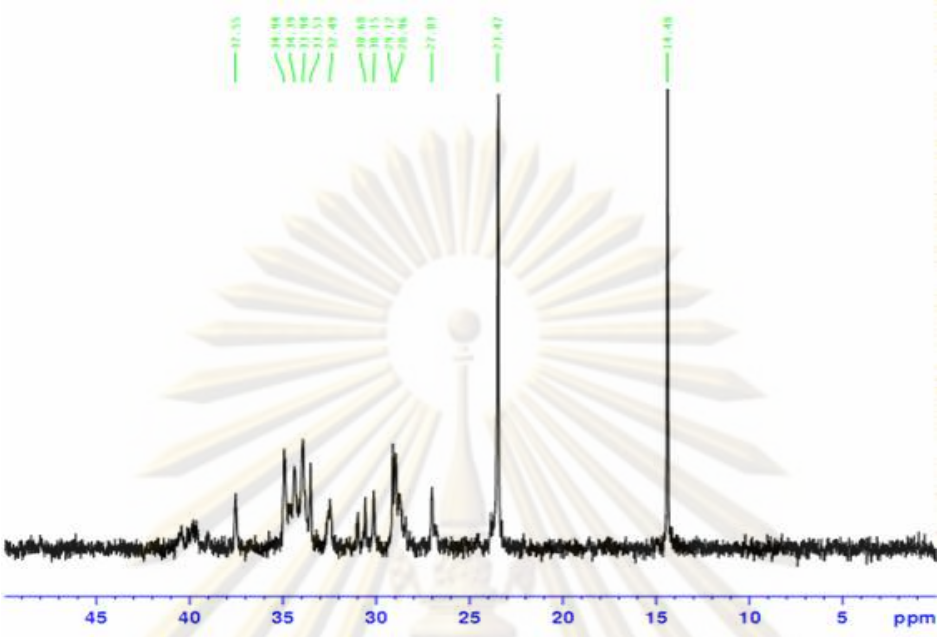

Figure A-3 ^{13}C NMR spectrum of ethylene/1-hexene copolymer at ratio 2:1

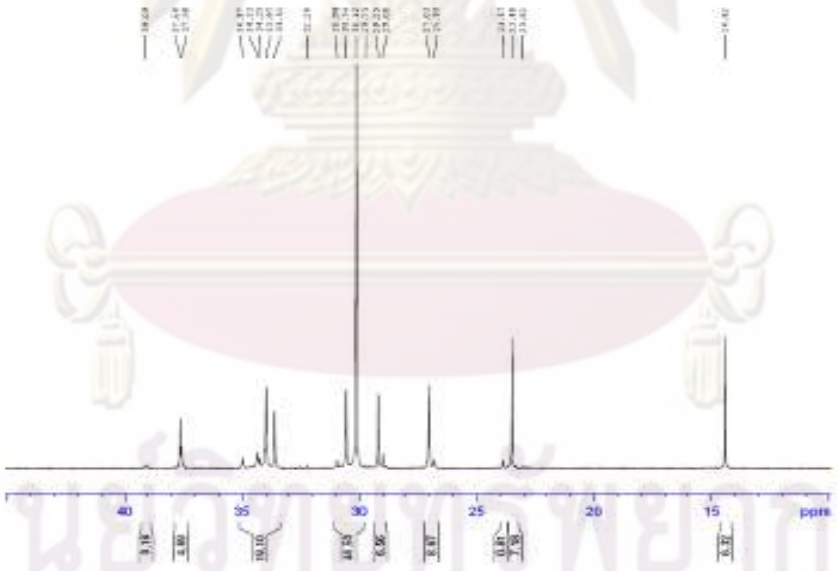

Figure A-4 ^{13}C NMR spectrum of ethylene/1-hexene copolymer obtained from the homogeneous system

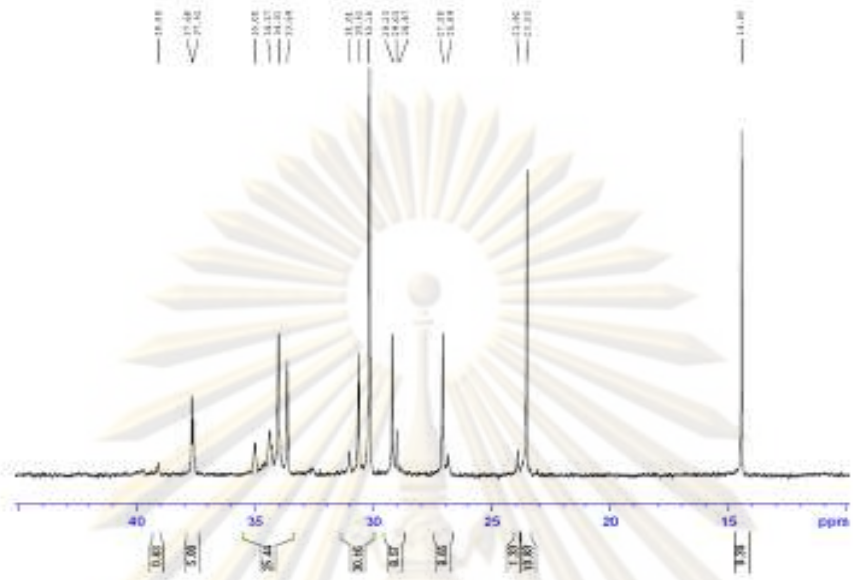

Figure A-5 ^{13}C NMR spectrum of ethylene/1-hexene copolymer obtained from the heterogeneous system with SiO_2-*S* support

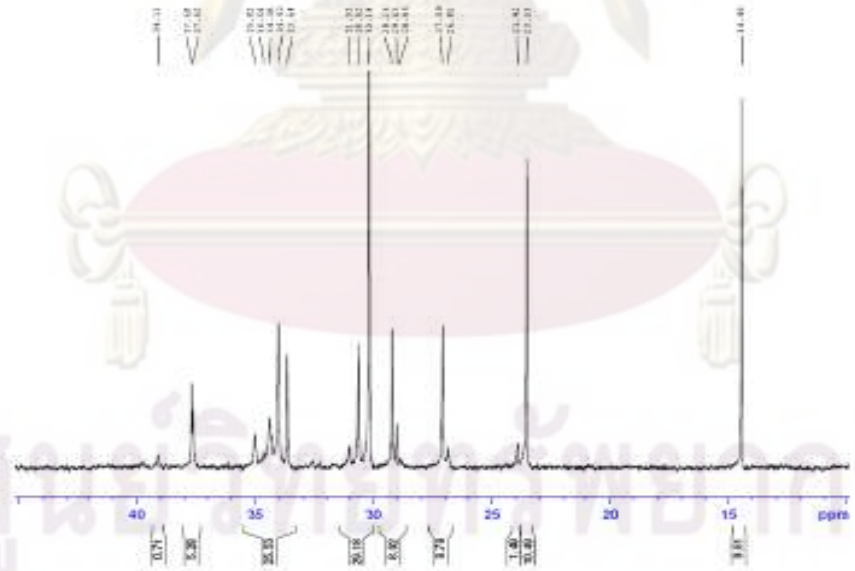

Figure A-6 ^{13}C NMR spectrum of ethylene/1-hexene copolymer obtained from the heterogeneous system with SiO_2-*L* support

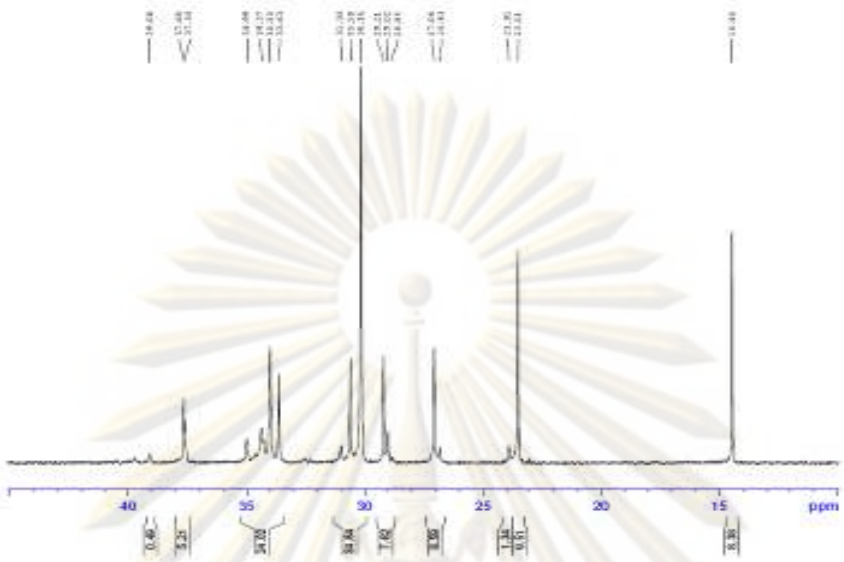

Figure A-7 ^{13}C NMR spectrum of ethylene/1-hexene copolymer obtained from the heterogeneous system with SiO_2-Ga-*S* support

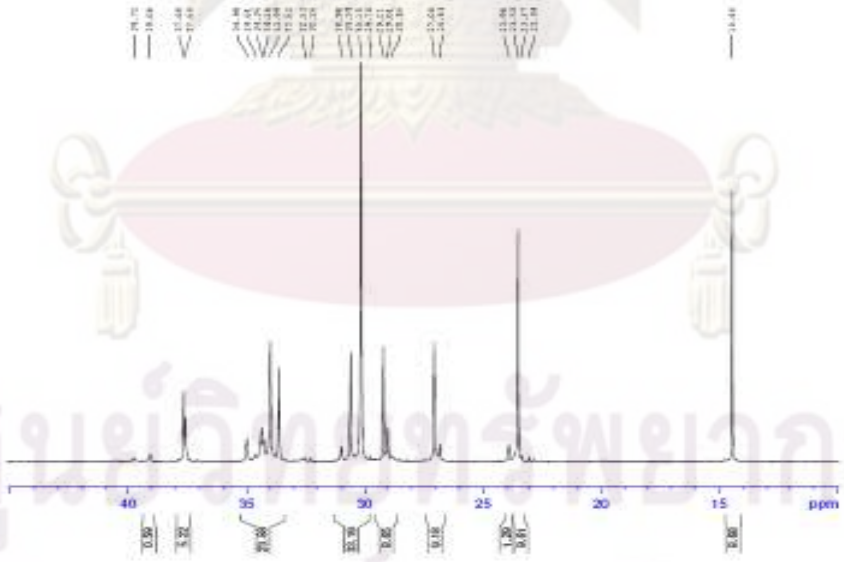

Figure A-8 ^{13}C NMR spectrum of ethylene/1-hexene copolymer obtained from the heterogeneous system with SiO_2-Ga-*S* support

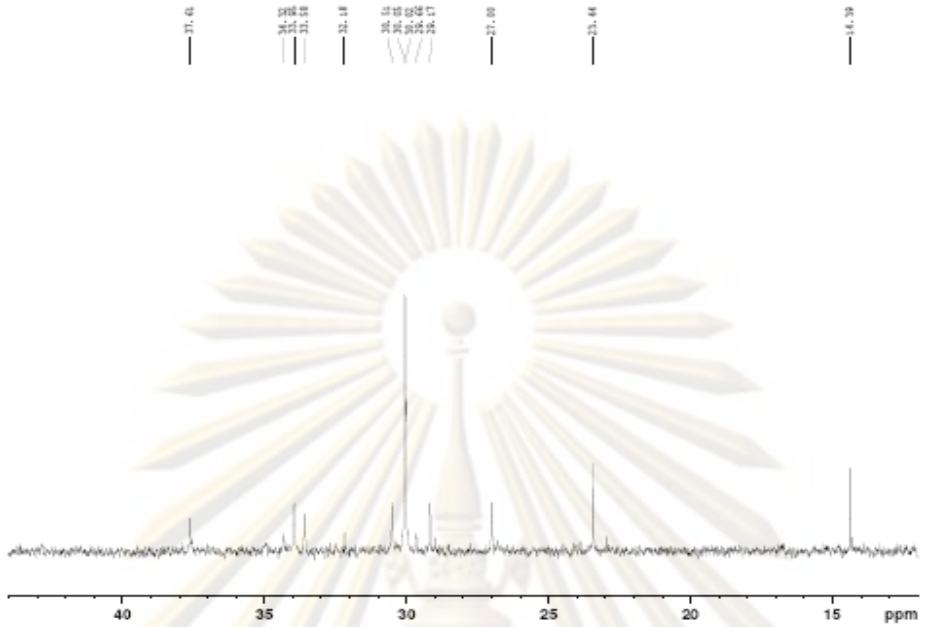

Figure A-9 ^{13}C NMR spectrum of ethylene/1-hexene copolymer obtained from silica ES-70X prepared by method **A2**

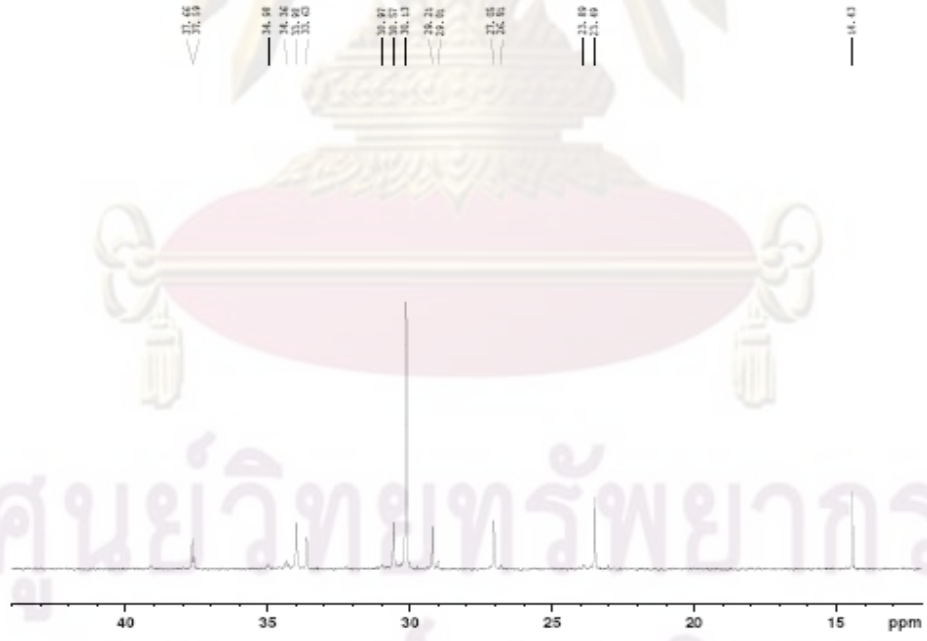

Figure A-10 ^{13}C NMR spectrum of ethylene/1-hexene copolymer obtained from silica ES-70X prepared by method **B2**

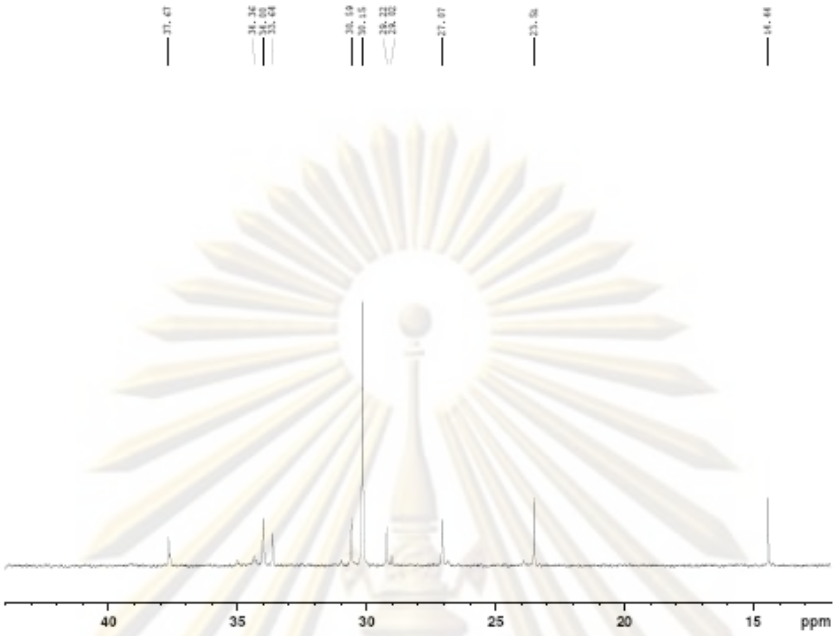

Figure A-11 ^{13}C NMR spectrum of ethylene/1-hexene copolymer obtained from silica Q-50 prepared by method **A2**

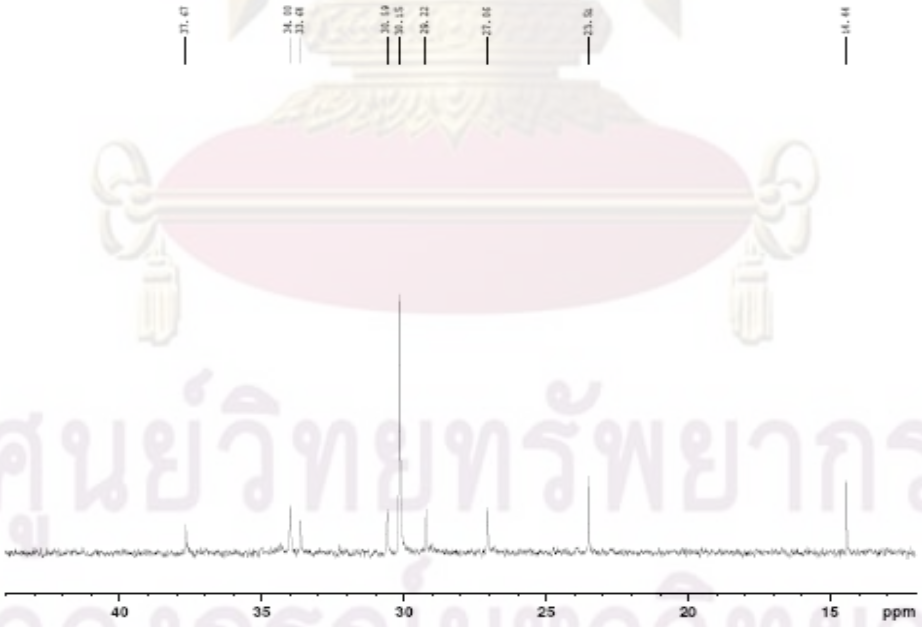

Figure A-12 ^{13}C NMR spectrum of ethylene/1-hexene copolymer obtained from silica NN-15 prepared by method **B2**

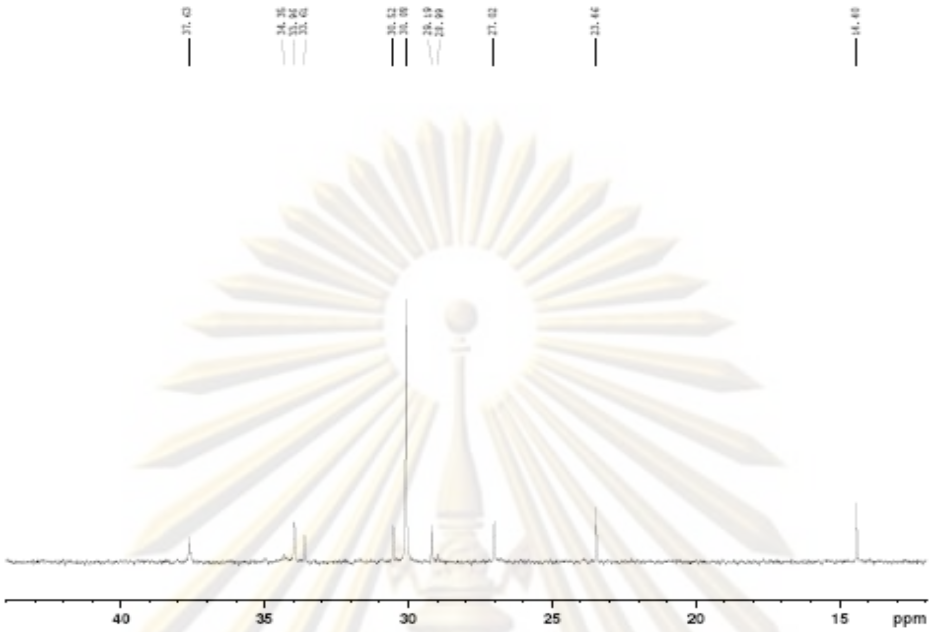

Figure A-13 ^{13}C NMR spectrum of ethylene/1-hexene copolymer obtained from silica P-10 prepared by method **A1**

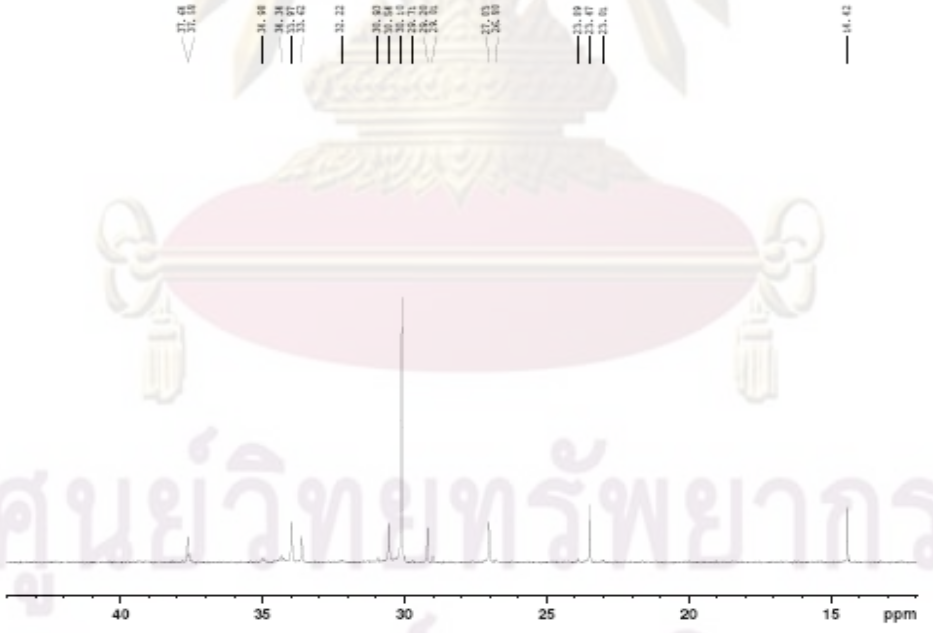

Figure A-14 ^{13}C NMR spectrum of ethylene/1-hexene copolymer obtained from silica P-10 prepared by method **A2**

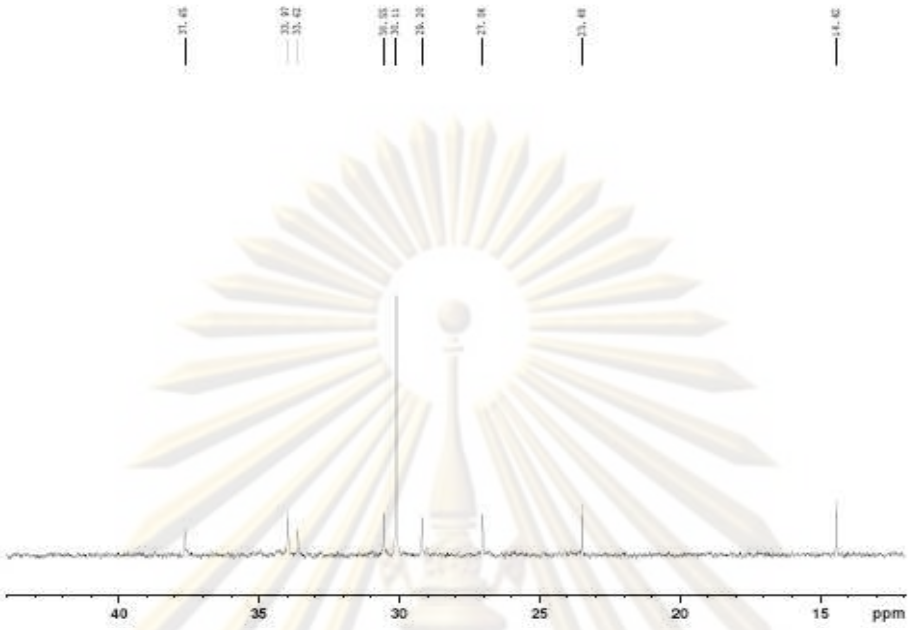

Figure A-15 ^{13}C NMR spectrum of ethylene/1-hexene copolymer obtained from silica P-10 prepared by method **B2**

APPENDIX B
(CALCULATION OF POLYMER PROPERTIES)

Calculation of polymer microstructure

Polymer microstructure and also triad distribution of monomer can be calculated according to the Galland *et al.* [1996] in the list of reference. The detail of calculation for ethylene/α-olefin copolymer was interpreted as follow.

Etthylene/1-hexene copolymer

The integral area of ^{13}C-NMR spectrum in the specify range are listed.

T_A	=	39.5 - 42	ppm
T_B	=	38.1	ppm
T_C	=	33 - 36	ppm
T_D	=	28.5 - 31	ppm
T_E	=	26.5 - 27.5	ppm
T_F	=	24 - 25	ppm
T_G	=	23.4	ppm
T_H	=	14.1	ppm

Triad distribution was calculated as the followed formula.

k[HHH]	=	$2T_A - T_C + 2TF + TE$
k[EHH]	=	$2T_C - 2TG - 4TF - 2TE - 2TA$
k[EHE]	=	T_B
k[EEE]	=	$0.5T_D - 0.5T_G - 0.25T_E$
k[HEE]	=	T_E
k[HEH]	=	T_F

All copolymer was calculated for the relative comonomer reactivity (r_E for ethylene and r_C for the comonomer) and monomer insertion by using the general formula below.

$$r_E = 2[EE]/([EC]X) \qquad r_C = 2[CC]X/[EC]$$

where r_E = ethylene reactivity ratio

r_C = comonomer (α -olefin) reactivity ratio

[EE] = [EEE] + 0.5[CEE]

[EC] = [CEC] + 0.5[CEE] + [ECE] + 0.5[ECC]

[CC] = [CCC] + 0.5[ECC]

X = [E]/[C] in the feed = concentration of ethylene (mol/L) / concentration of comonomer (mol/L) in the feed.

%E = [EEE] + [EEC] + [CEC]

%C = [CCC] + [CCE] + [ECE]

APPENDIX C
(DIFFERENTIAL SCANNING CALORIMETER)

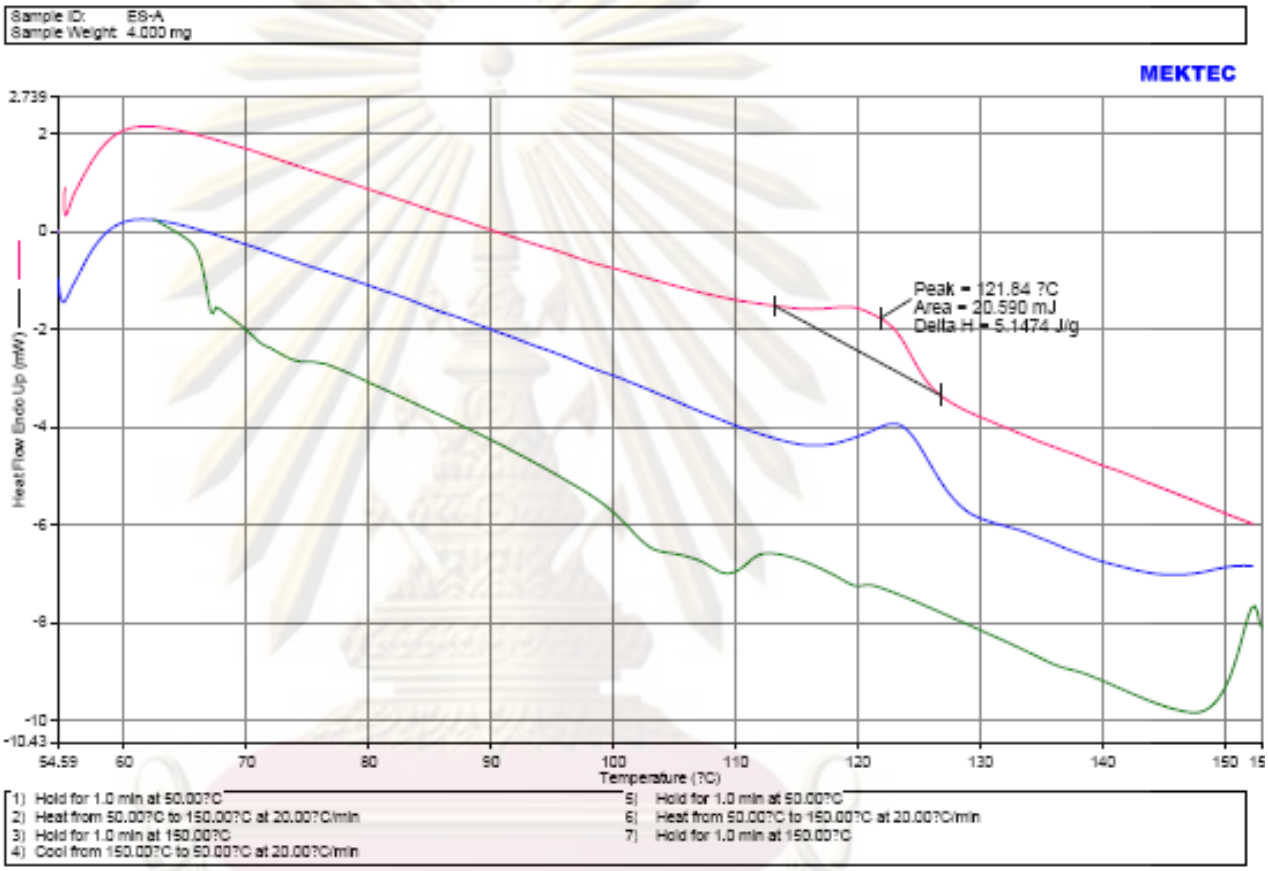

Figure C-1 DSC curve of ethylene/1-hexene copolymer obtained from silica ES-70X prepared by method A2

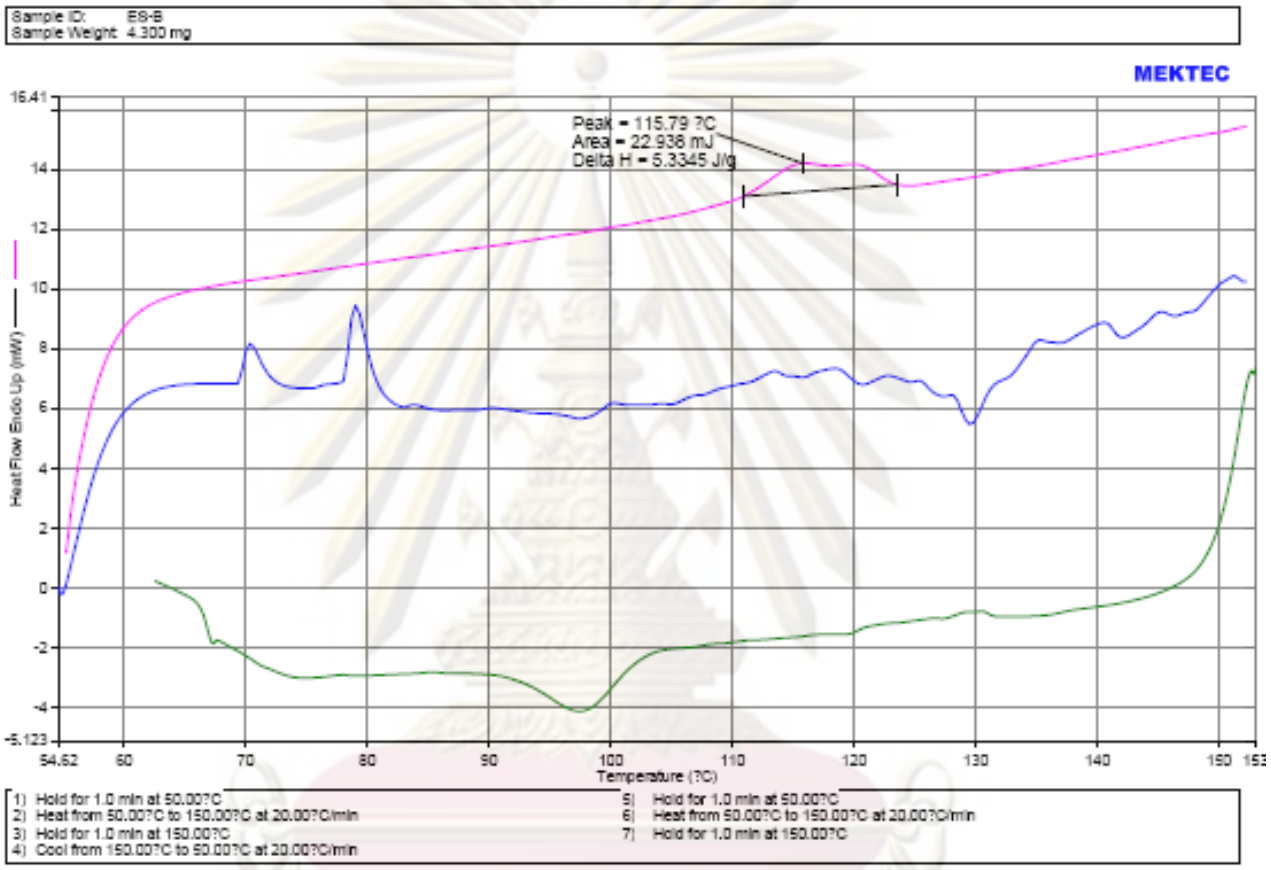

Figure C-2 DSC curve of ethylene/1-hexene copolymer obtained from silica ES-70X prepared by method B2

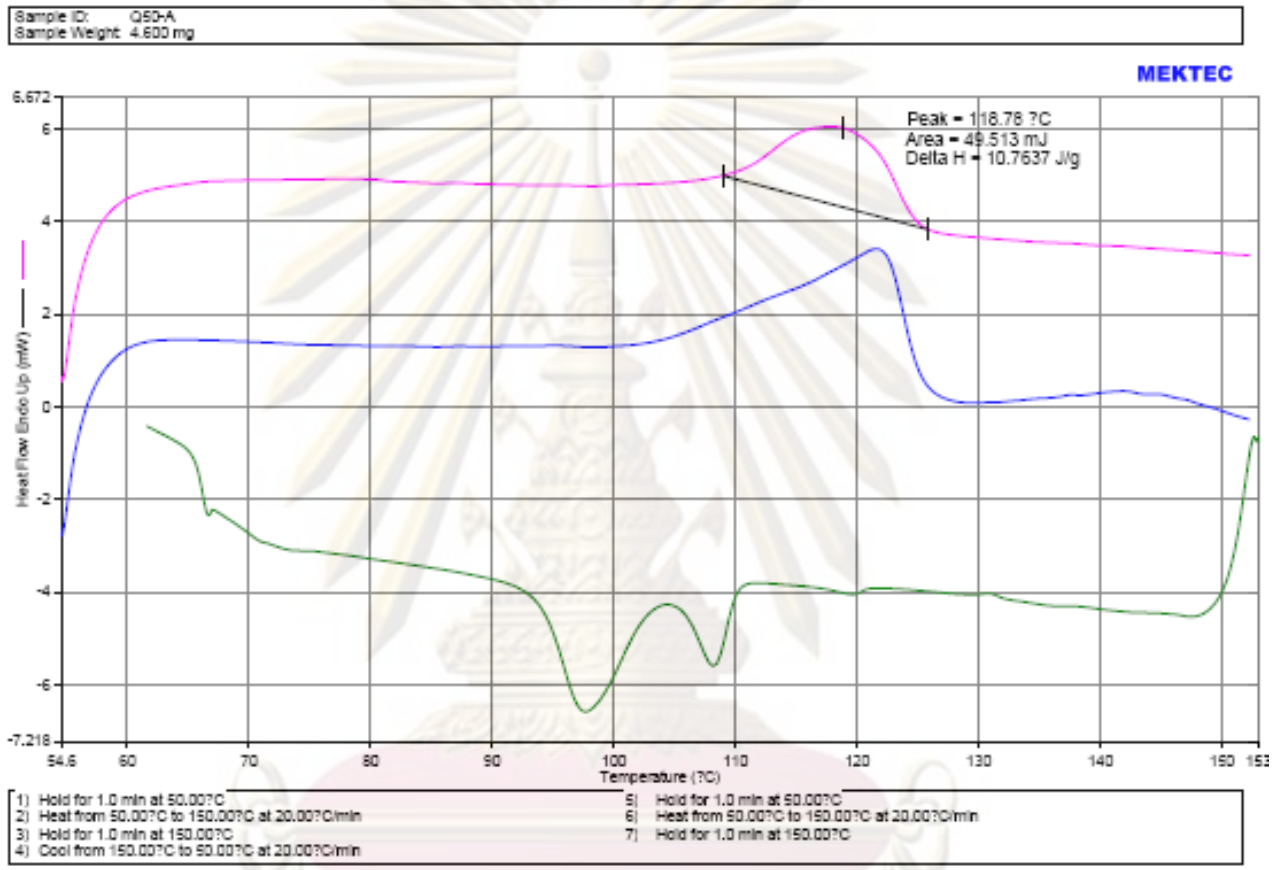

Figure C-3 DSC curve of ethylene/1-hexene copolymer obtained from silica Q-50 prepared by method A2

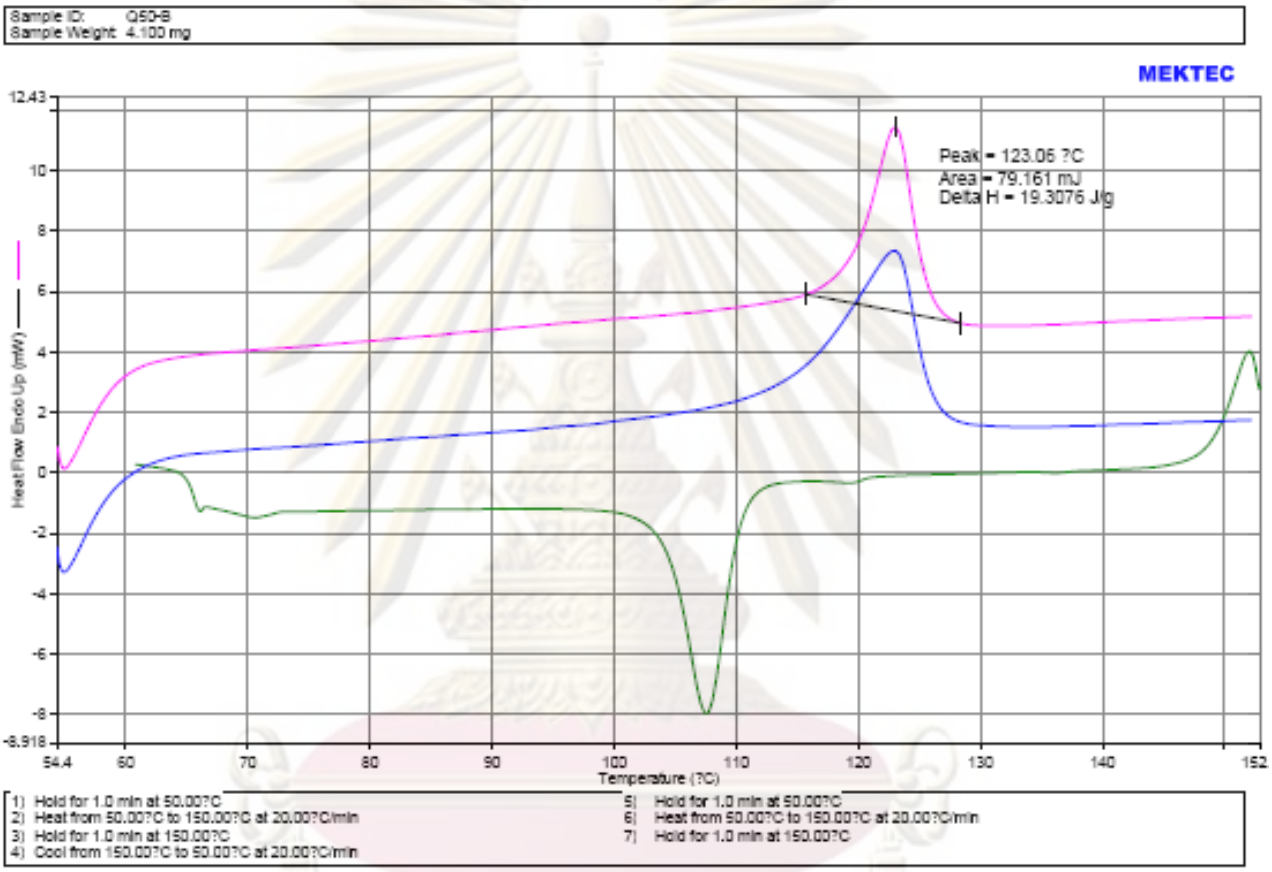

Figure C-4 DSC curve of ethylene/1-hexene copolymer obtained from silica Q-50 prepared by method B2

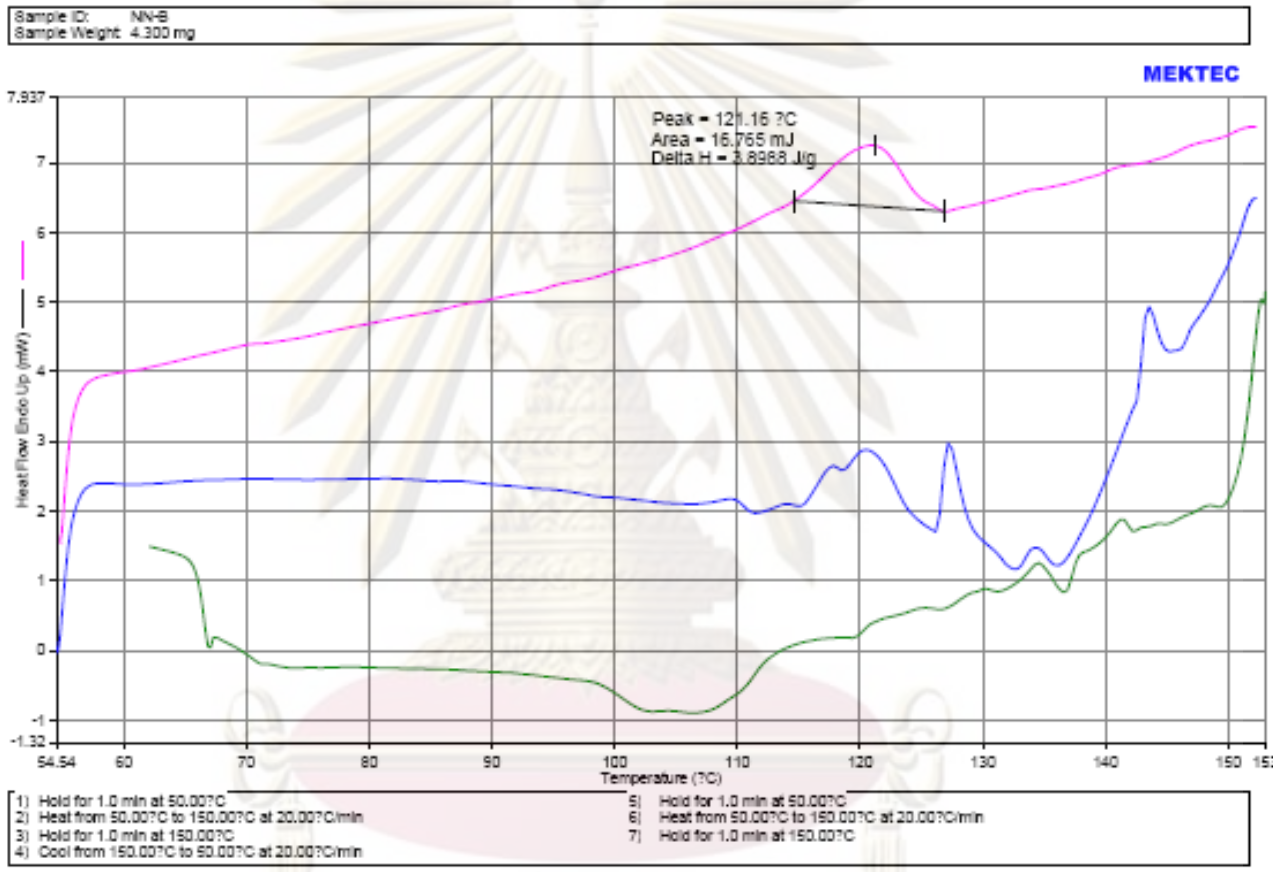

Figure C-5 DSC curve of ethylene/1-hexene copolymer obtained from silica NN-15 prepared by method B2

VITAE

Mister Ekrachan Chaichan was born on March 5, 1980 in Samutsakorn, Thailand. He received the Bachelor's Degree of Science from the Department of Chemistry, Faculty of Science, Silpakorn University in March 1999, he continued his Doctoral study at Chulalongkorn University in October, 2006.